Journal of the
OPTICAL SOCIETY *of* AMERICA

VOLUME 36, NUMBER 4 APRIL, 1946

Unity in Diversity

MUCH of the recent progress in optics has resulted from bringing together in one organization the designers and the users of optical equipment. So long as the user is dependent upon the skill of the designer, and the designer is dependent on the user for suggesting new and better instruments to design, it is obviously desirable to keep the gulf between the two as narrow as possible. For this reason the Optical Society of America has avoided segregation of its membership into groups; the color analysts, the instrument designers, the spectrographers, and various other special groups all meet together. When the program of a meeting is being planned, group interests are recognized by providing symposia on special topics, by organizing informal group conferences, and in many other ways. The Society thus attempts to emphasize unity in diversity.

The Directors of the Optical Society feel that by following such a procedure they are carrying out the basic principles stated at the time of the incorporation of the Society: "to increase and diffuse the knowledge of optics, to promote the common interests of investigators of optical problems, and to encourage cooperation among them."

There will always be more users of optical equipment than designers of such equipment. For many years the users of color measuring devices constituted the largest group in the Optical Society, but during recent years their numbers have been exceeded by the users of spectrographic equipment. Eventually spectrography may grow to the point where it will justify a separate national organization, comparable in importance to the other classical divisions of science, and supporting its own journal. In the meantime spectrographic equipment and techniques seem destined to undergo many additional improvements and refinements resulting from the use of new optical materials, new methods of optical design, new light sources, new photoelectric cells, new techniques of photometry, and so on. So long as this is the case, spectrographers can benefit by association with other workers in the fields of optics. In fact, much will be lost when the various groups now constituting the Optical Society have grown to such size that it will no longer be practicable for them to meet together, since the cross fertilization of one field by another will then be greatly reduced.

The arguments advanced above should not prevent the organization of smaller groups along geographical lines. A case in point is the Rochester Section of the O.S.A., which is a completely autonomous local group whose aims and purposes are identical with those of the national society. The local group benefits from the prestige that results from affiliation with the national organization, and by having available the pages of this journal in which to record for the archives its principal activities and the names of its officers. The Society benefits through the further extension of its aims and purposes and through the increased circulation of its journal.

Many societies require membership in the national organization as a qualification for membership in a local section. The Board of

BOSTON UNIVERSITY
COLLEGE OF LIBERAL ARTS
LIBRARY

Directors of the Optical Society feels that this is an unnecessary and unwise restriction. Thus, though the Rochester Section contains a substantial number of O.S.A. members, it is nearly double the size that it would be if membership were restricted to members of the national society. The Board of Directors believes that any local group having the same aims and purposes as the national society will inevitably contain enough O.S.A. members to maintain the spirit, aims, and purposes of the society.

The fact that a local group accepts the aims and purposes of the O.S.A. does not require that all of these aims and purposes be pushed with equal vigor. The local group in Rochester may well concern itself primarily with lens design and photography, since these are of primary interest in the community. In other communities the chief interest may be in spectrography or color or communications. The formal organization of such regional groups depends on the initiative of those interested in them.

Representatives of any such group having optical interests are invited to petition the Optical Society for formal recognition as a local group, and to use the office of its Secretary for liaison with other local groups. Should the activities of local groups make undue demands on the time of the Secretary, recommendation will be made to the Board of Directors that provision be made for a new officer entitled "Secretary for Local Sections." His responsibilities would involve keeping each local section informed regarding other local sections, aiding in securing speakers, and in other possible ways assisting the local sections in carrying out their functions.

It should thus be possible to combine the advantages of local groups with those of a unified national organization. Accordingly local groups interested in optics are invited to investigate the desirability of requesting affiliation with the Optical Society of America.

GEORGE R. HARRISON
President

Adolph Lomb Medal Notice

THE Adolph Lomb Medal Committee of the Optical Society of America is engaged in selecting a nominee for this award, which is made "to a person under thirty (30) years of age who shall have made a noteworthy contribution to optics" [J. Opt. Soc. Am. (June, 1940)]. The choice this year is made more difficult by wartime restrictions and the lack of publication on optical developments of the past several years. To help the committee avoid making a glaring omission, persons desiring to recommend possible candidates for this award are asked to communicate their suggestions, together with supporting information, to some member of the Committee, preferably the chairman, *BEFORE JUNE 1, 1946.* Members of the Committee are:

SELIG HECHT, *Columbia University, New York, New York*
ELMER HUTCHISSON, *Case School of Applied Science, Cleveland, Ohio*
W. F. MEGGERS, *National Bureau of Standards, Washington, D. C.*
GEORGE S. MONK, *University of Chicago, Chicago, Illinois*
BRIAN O'BRIEN, *University of Rochester, Rochester, New York*
Chairman: MARY E. WARGA, *University of Pittsburgh, Pittsburgh, Pennsylvania.*

Spectral Intensity Measurements with Photo-Tubes and the Oscillograph*

G. H. DIEKE, H. Y. LOH, AND H. M. CROSSWHITE
Johns Hopkins University, Baltimore, Maryland

(Received February 18, 1946)

WHEN intensity measurements of spectrum lines are performed, the process of measuring takes a definite finite time. The results of the measurements are averages over the period of measurement. If the interest is in constant intensity ratios, the time it takes to make the measurements is of little consequence. A relatively long time then may be advantageous because it averages out erratic fluctuations due either to the light source itself or to the process of measuring. If, however, a knowledge of short period changes is desired, the method of measurement must be capable of giving meaningful results within the required time. How short the response of the measuring device has to be depends on the particular results required. If one wants to follow, for instance, a high frequency discharge, it may be necessary to make measurements within a period of a millionth of a second or less.

Photographic intensity measurements require exposure times of seconds or minutes, and the results cannot give any information about changes of shorter duration. Photoelectric tubes with ordinary meters are limited by the period of the meter, which is usually of the order of magnitude of one second. For many problems this is an adequate speed, and the combination of photo-tube and recording microammeter provides a very effective means for registering changes in light intensity of a moderate rate of change.

Most spectroscopic light sources are run with alternating current, and in order to understand what is going on, it is necessary to make measurements which are of a duration short compared to the length of one cycle. The length of a cycle may be 1/60 of a second for an ordinary a.c. discharge to a microsecond or less for high frequency condenser discharges. The only measuring instrument with a short enough response is the cathode-ray oscillograph. Because of their high sensitivity and the ease with which they can be used, multiplier photo-tubes are particularly suited for use with the oscillograph. For these reasons we have explored the results that can be obtained when the output of a photo-multiplier tube is fed into a cathode-ray oscillograph. The general procedure and some typical results are described in this paper.

We can expect significant results that cannot be obtained otherwise from the study of electrical discharges which are operated under rapidly changing non-stationary conditions. However, a great deal of information can also be obtained about the shortcomings of light sources, like the d.c. arc, which are supposed to operate under stationary conditions.

EXPERIMENTAL PROCEDURE

The spectrograph used in most cases was one with a 21-foot grating in a Wadsworth mounting. Its facilities for the use with photo-tubes have been described previously.[1,2] The output of a photo-tube, (931A or *IP*28), which is placed on a definite spectrum line, is fed into a resistance R and the voltage developed across the resistance applied to the proper terminals of the oscillograph (Fig. 1). For reasonably strong lines the sensitivity is ample.

The power supply for the multiplier photo-tubes must be entirely free from any short period fluctuations. This is not always easily achieved when the power is obtained from rectified and filtered alternating current, although such a supply may be entirely adequate for ordinary purposes. For this reason we have usually used

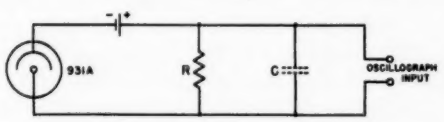

FIG. 1. Schematic circuit diagram.

* Results of work on a project sponsored by the Office of Production Research and Development of the War Production Board.

[1] G. H. Dieke and H. M. Crosswhite, J. Opt. Soc. Am. **35**, 471–480 (1945).
[2] Report of the O.P.R.D. No. *W*-193.

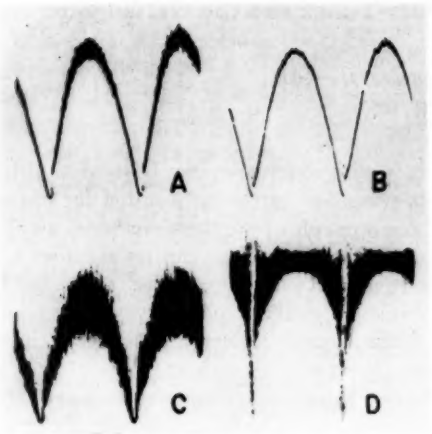

FIG. 2. Test of photo-multiplier tubes with the oscillograph. A, good tube; B, same at high attenuation; C, poor tube; D, defective tube.

dry batteries with 90–110 volts for each dynode and 180 volts for the plate voltage. As the current drain is very small, the batteries practically last their shelf life.

An important question is how fast the system can respond to variations in the light intensity. A limit is imposed on this by the transit time of the electrons in the photo-tube, which according to Zworykin[3] is of the order of magnitude 10^{-8} second. So far we have not encountered any phenomena requiring quite this speed.

For practical purposes the most important consideration is whether the circuit which feeds the signal into the oscillograph can handle high enough frequencies. The frequency response of the oscillograph, its amplifier and attenuator circuits must, of course, also be considered. The ability of a circuit to handle high frequencies is determined by its time constant RC, where in our case R is the resultant of the input resistance shunted by the input impedance of the oscillograph and any leakage that might occur. C is the sum of the input capacity of the oscillograph and the distributed capacity of the input circuit. From this it is apparent that in order to obtain the fastest response it is necessary to keep both C and R as low as possible. When care is taken that the distributed capacity of the circuit is negligible, which can be achieved by short and properly designed leads, C is entirely the input capacity of the oscillograph, which is of the order of magnitude $3 \cdot 10^{-11}$ farad. The ordinary commercial oscillograph does not handle frequencies higher than one megacycle. To achieve a time constant of 10^{-6} second, we should have $R < 30{,}000$ ohms. With a photo-current of 100 microamperes a voltage difference of 3 volts is produced, which is more than ample for full scale deflection. Actually as small an input resistance should be used as will give sufficient sensitivity in order to be able to operate the oscillograph at full gain. For usually, the attenuators built into the oscillograph suppress the higher frequencies.

If full use is to be made of the potentialities of the photo-multiplier tubes, we need a time constant of the order of magnitude 10^{-8} second and an oscillograph of the type DuMont 248 which can handle such high frequencies. With an input capacity of $4 \cdot 10^{-11}$ farad, R must be smaller than 250 ohms, which requires an instantaneous photo-current of 400 μA to give one-inch deflection. However, because of the limitations of the amplifier, frequencies of 100 megacycles cannot quite be reached. If the signal is applied directly to the plates of the cathode-ray tube, $C = 1.5 \cdot 10^{-11}$ farad and $R = 660$ ohms for a time constant of 10^{-8} sec. One milliampere instantaneous photo-current will produce a voltage difference of 0.67 volt, which would produce a deflection of less than one millimeter on the oscillograph screen. While photo-currents of 1 mA or more should be avoided under ordinary circumstances, we are only interested in pulses of very short duration, and for such very short periods instantaneous currents of considerably higher magnitude can be tolerated. We see from this that under favorable circumstances we can get to intervals of about 10^{-7} sec., which is by a factor ten short of the full resolving power of the multiplier tubes. There is no difficulty at all to obtain a resolving power of one microsecond. So far we have encountered no phenomena of duration shorter than one microsecond. The reserve resolving power will then insure that pulses of this duration will be rendered without distortion. If the full resolving power of 10^{-8} of the multiplier tubes is to be used, a special amplifier must be constructed which can handle such high frequencies.

[3] V. K. Zworykin, Proc. I.R.E. **24**, 351 (1936).

It is obvious that the preceding considerations can give only the order of magnitude of the time resolving power. Pulses of short duration require a time constant considerably smaller than the pulse duration in order to be reproduced without noticeable distortion.

At the short time intervals with which we are dealing, the accidental fluctuations in the photo-current are another source of errors that limits the resolving power of the circuit. Under ideal circumstances the accidental fluctuations in the output are determined only by the statistical fluctuations in the photo-current, which are

$$\langle d_t^2\rangle_{Av} = nt,$$

where n is the average number of electrons per second, t the length of the time interval, and $\langle d_t^2\rangle_{Av}$ the average square of the fluctuations. The relative fluctuations can be expressed by

$$R_t = \frac{\langle (d_t^2)^{\frac{1}{2}}\rangle_{Av}}{nt} = \frac{1}{(nt)^{\frac{1}{2}}}.$$

One ampere is equivalent to 6.25×10^{18} electrons per second. If we have a photo-current of 100 μA and a multiplication factor of about 200,000, we have a photo-current of about $3 \cdot 10^9$ electrons per second. We have therefore

$$n = 3 \cdot 10^9.$$

For a time interval of one microsecond we have $(nt)^{\frac{1}{2}} = 55$ and $R_t = 2$ percent. If we want to go to the maximum attainable resolution of 10^{-8} sec., we get fluctuations in the current of 20 percent. These are the fluctuations which cannot be avoided even if all circumstances are perfect. There may be considerably larger fluctuations in imperfect tubes or when there is current leakage.

The preceding considerations give the magnitude of the fluctuations to be expected with ideal tubes, where the fluctuations are only the unavoidable statistical fluctuations in the photo-current. Some of the actual tubes come very close to these conditions. However, there are many individual tubes which because of leakage or traces of gas or possibly other causes show much larger fluctuations. Such tubes are unsuitable for this kind of work and also for the measurement of very weak intensities, where the fluctuations in the dark current may conceal the signal. The tubes can very easily be tested with the oscillograph. Figure 2 shows three tubes tested with a constant signal and the resistance R adjusted so as to give the same deflection. A is a good tube, C is poor, and D is a tube which shows quite an abnormal behavior, probably due to some traces of gas. This latter tube had also shown anomalies when used in a regular measuring circuit, but they were apparent there only after more extended use.

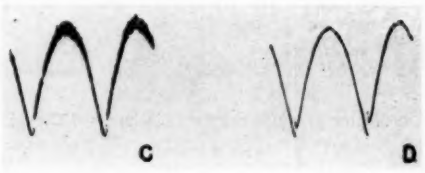

FIG. 3. Intensity diagrams: C, short time constant; D, longer time constant, all other things equal.

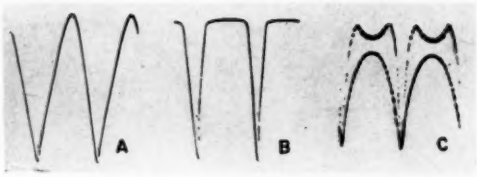

FIG. 4. A, intensity curve under proper conditions; B, iR too high; C, insufficient power supply.

The time interval t which determines the magnitude of the fluctuations is, as far as the order of magnitude is concerned, equal to the time constant of the combined input circuit of the cathode-ray tube. If high frequency response is not necessary, the arbitrary fluctuations can be cut down by paralleling the input resistance by a capacity so that the time constant of the circuit is not much shorter than the period of the phenomena to be observed. The exact value often is a compromise and depends on how the suppression of details due to the suppression of the higher harmonics of the trace compares to the gain in details due to the suppression of the fluctuations. Figure 3 shows the effect of such an increase in the time constant.

The commercial oscillographs respond only to the a.c. components in the photo-currents. If a d.c. component or low frequency a.c. component is present, one of two ways is open. The signal can be applied directly to the plate with a loss in

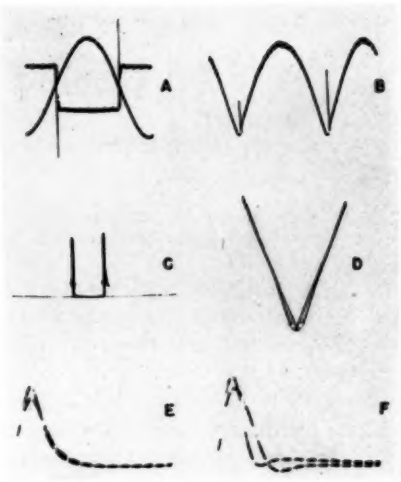

FIG. 5. Low pressure mercury discharge, A–E 60 cycles, F 800 cycles.

A, voltage and current;
B, intensity of 5461 line;
C, intensity against voltage;
D, intensity against current;
E–F, initial intensity bursts. Markers one microsecond.

sensitivity. The use of most of the controls of the instrument is then also lost. Another way is by interrupting the signal fast enough so that the resulting pulsating currents can be handled by the a.c. amplifiers of the oscillograph. The interruption can be accomplished by interrupting the light beam by a rapidly rotating sector. An even simpler way of doing this is by placing an electronic switch in the output of the photo-tube which makes and breaks the connections to the oscillograph. In this way it is possible to observe the output of two different photo-tubes simultaneously on the screen. When the first tube is switched on, the second one is switched off, and *vice versa*, and the switching rate can be adjusted so that two continuous traces appear on the screen. Examples of this are Figs. 4C, 5A, and 9. Electronic switches of this type can be obtained commercially. They are, however, not suitable for high frequencies.

In order that the cathode-ray deflection be proportional to the instantaneous light intensity, it is necessary that the plate voltage is high enough or the load resistance low enough that the voltage drop across the resistor is not so large as to leave too low a voltage drop across the photo-tube. Figure 4 shows what happens in such a case. 4A is a normal intensity diagram of a 60-cycle mercury discharge; 4B is obtained when the resistor R is too large or the plate voltage too small. For too large intensities the photo-current is then independent of the intensity. Figure 4C shows what can happen with a defective voltage supply for two tubes. When the battery is unable to furnish the combined plate currents, the photo-current for one of the tubes may actually drop with an increase in intensity.

APPLICATIONS

The combination of multiplier photo-tube and cathode oscillograph can be used for the study of any light phenomena. The high sensitivity of the device makes it possible to reach phenomena which hitherto were inaccessible to such an analysis. Thus, weak light phenomena can be studied with comparative ease. The light may be weak because the source itself is inherently weak or because we want to isolate a single spectrum line in a spectrograph of high dispersion, or because we are perhaps interested in the variations over the source and want to take only a small localized part of the light at a time. We are

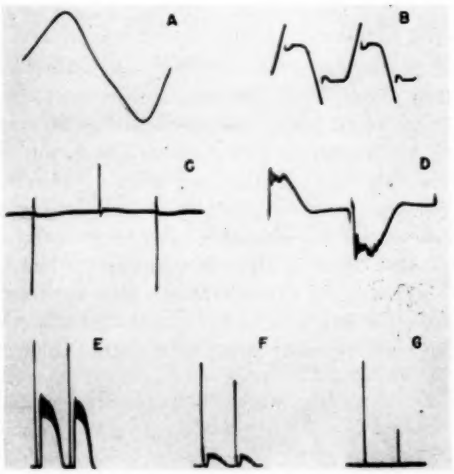

FIG. 6. Low pressure mercury discharge, 800 cycles.

A, voltage of generator;
B, voltage across tube;
C, current;
D, current, higher Y-gain;
E, intensity of 2537 line;
F, intensity of 4358 line;
G, intensity of 3984 line.

giving below some typical applications which illustrate the versatility and the usefulness of the method.

Discharge Tubes

The phenomena in some of the commonly used light sources like arcs and sparks result from a number of very complex fundamental processes occurring at the same time. The same fundamental processes can be studied in a much simplified form in some gas discharges at reduced pressure. Figures 5–6 give the results obtained with a low pressure capillary mercury discharge. Here the photoelectric data supplement the electrical characteristics of the discharge. Figure 5A shows simultaneously the voltage across the tube and the current through the tube when the discharge is operated by ordinary 60-cycle alternating current.

Figure 5B gives the light intensity as function of time for the 5461 line. As is to be expected, the light intensity has roughly the same shape as the tube current if the latter were put through a full wave rectifier. The overshooting of the voltage at the beginning of each half-cycle is to be noted, followed by a breakdown and a sharp current surge. This is analogous to the usual spark breakdown and is accompanied by a sharp surge in light intensity. This intensity surge, unresolved in Fig. 5B, is shown on an extended scale in Fig. 5E. The half-width is of the order of magnitude of one microsecond.

Instead of obtaining the intensity as function of time, as in Fig. 5B it may sometimes be desirable to obtain it as function of the tube voltage (Fig. 5C) or as function of the tube current (Fig. 5D). In both these figures the part due to the initial surge has been suppressed. Figure 5D shows again that the intensity of the light emitted is approximately proportional to the tube current. The doubling at low currents is due to the fact that the temperature of the vapor and, therefore, its pressure is slightly higher near the end of a half-cycle than near the beginning.

Figures 6 and 5F show the same tube operated at the same r.m.s. current with nothing but the frequency of the current changed from 60 to 800 cycles. Figure 6A shows the voltage delivered by the generator, which is very nearly sinusoidal. Figure 6B is the voltage across the tube, and 6C and 6D the current through it. It is seen that the discharge characteristics have changed considerably. The initial surges in the current are very much accentuated, and the discharge has no time to develop fully the main part. Figures 6E–G show the intensity diagram for three different mercury lines. Compared with the 60-cycle discharge (Fig. 5B) they all show the initial surge very much accentuated compared to the main part. This is least apparent in the 2537 line (Fig. 6E) which has the lowest excitation (4.9 volts). In the green line (Fig. 6F, excitation 7.7 volts) the surge is much more prominent. Figure 6G shows the line 3984 of ionized mercury (excitation 15.2 volts). The whole intensity is here exclusively concentrated in the initial surges. Figure 5F gives a detailed picture of the surges at 800 cycles. Their duration is not significantly different from the duration at 60 cycles, but there is a slight change in the exact shape of the two half cycles.

A comparison of Figs. 5 and 6 gives a simple explanation of the well-known fact that high frequency discharges yield predominantly the spark spectrum even though the applied voltage may be perfectly sinusoidal. The concentration

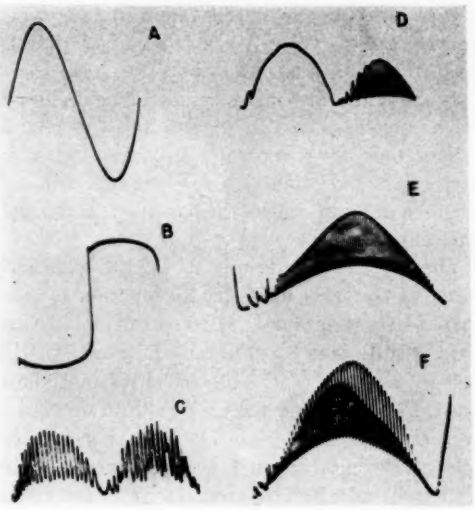

FIG. 7. Low pressure mercury discharges.

A, current;
B, voltage;
C, intensity;
D–F, intensity, different tube.

of the light in the initial burst favors, as the figures show, very much the lines of high excitation, i.e., the spark lines.

It should be emphasized that the behavior of a discharge illustrated in Figs. 5 and 6 is characteristic only for a mercury discharge under the particular conditions. Other discharges with only small changes in the conditions may yield a very different picture.

The very legitimate question arises whether a study of the light intensity as function of time, particularly that of individual spectrum lines, can yield results which cannot be obtained just as well by a study of the electrical characteristics alone. For an answer to this question, we turn to Fig. 7. Figures 7A and 7B show current and voltage through another low pressure mercury discharge tube.* They represent about what should be expected of this type of tube with no remarkable features. Figure 7C shows the intensity curve in the positive column and reveals oscillations which are completely masked in the tube current and voltage curves. Such oscillations, often greatly modified, are almost universally found in all discharges, and are frequently also revealed in the electrical characteristics. They seem to have aroused hitherto no or very little attention. They will be discussed more fully in a forthcoming paper. Figures 7D–E show similar oscillations in the light intensity in another tube.

At fairly low frequencies the a.c. discharge approximates a sequence of stationary d.c. discharges. The typical features of the stationary discharge like cathode-dark space, negative glow, positive column, etc., cannot be observed because the change of polarity and current is too rapid to be observed directly. By observing the intensity diagrams as function of the distance from the electrodes, the properties of the stationary discharge can be deduced very easily, and unless very accurate quantitative data are required, with infinitely less labor than by the usual method of varying gradually current and voltage of a stationary d.c. discharge. Figure 7D shows the asymmetry in the two half-cycles of light coming from the vicinity of one electrode. The conclusion is, therefore, that a great deal of information can be obtained from a detailed study of the intensity curves that cannot be obtained from the electrical characteristics.

The question whether a study of the time characteristics of individual spectrum lines may reveal information not obtainable from the total light is answered by Figs. 6E–G, which show that different lines may have quite different time characteristics.

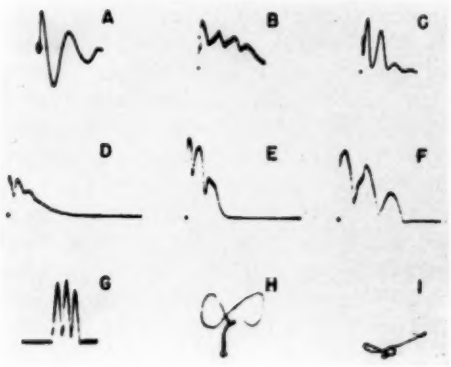

FIG. 8. Iron spark in air.

A, current 3560 c.p.s.;
B, intensity of Fe I line;
C, intensity of Fe II line;
D–G, intensity of Fe I line at frequencies 7130, 5040, 2520, 1780 c.p.s.;
H, intensity against current, Fe I line;
I, intensity against current, Fe II line.

Sparks

The difference between different spectrum lines is also shown in Fig. 8, in which iron lines of an ordinary spark in air are analyzed. Figure 8A represents the current through the spark gap with the circuit constants so adjusted that the frequency of the discharge is about 3560 c.p.s. Figures 8B and 8C give the intensity diagram of an arc and spark line, respectively, under otherwise identical conditions. The differences are striking. While the current through the spark goes through zero, the arc line intensity remains fairly high. This is due to the fact that, although no new excitation can occur, the recombination of ions furnishes a large enough number of excited atoms. This is quite different for a spark (Fe II) line where the intensity goes very nearly

* We are very much obliged for this tube to Dr. H. C. Rentschler of the Westinghouse Bloomfield Research Laboratories. It has cold electrodes, and is filled with argon under 4-mm pressure. It contains also mercury vapor of low pressure, as the operating temperature of the tube is only slightly above room temperature.

to zero with the exciting current. The Fe II lines are emitted by the positive iron ion. In order to obtain excited ions, capable of emitting this Fe II line by recombination, the presence of a large number of double ionized iron atoms would be required. The absence of the Fe III spectrum in sparks of this type suggests that such ions are not present in appreciable amounts.

That the residual intensity of Fe I lines when there is no excitation is due to recombination is also shown by Figs. 8D–G which shows the same Fe I line in sparks of the same type except that the frequency of the discharge is changed. The values are 7130, 5040, 2520, 1780 c.p.s., respectively. (Figure 8G is on a different time scale.) The figures show that the longer the time between successive excitation periods, the more chance the ions have to disappear and the lower the residual intensities at the currentless moment are. From a quantitative study of such records, valuable data can be obtained about the rate of recombination of ions. Figures 8H and 8I, where intensity is plotted against current, tell the same story. However, in the interpretation of such diagrams, particular care is required unless precautions have been taken which insure that there are no differences in the two circuits involved which might introduce a phase difference.

Study of d.c. arcs

While a d.c. arc under ideal conditions should be stationary, that is, have constant voltage, current, and light output, it is well known that in actual cases these conditions are usually not fulfilled. A study of the arc during small time intervals will give valuable clues as to what causes these irregularities. Figures 9A–B compare the fluctuations in the light output (top) with the fluctuations in the current or voltage. Upward deflections mean lower values. We see that there is a correlation in this case between disturbances in the voltage, current, and intensity. At a disturbance the voltage rises while current and intensity drop. Figure 9C shows the intensities of two iron lines in a fluctuating arc, and reveals

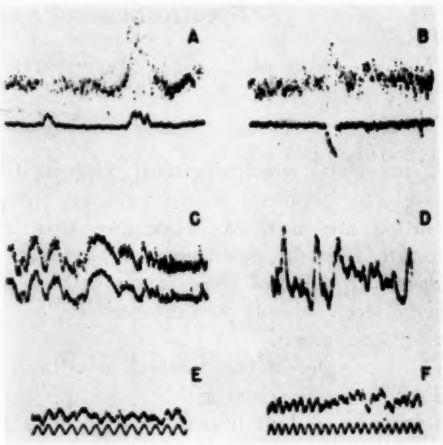

FIG. 9. D.c. arc, iron electrodes.

A, variation in current (below) and intensity;
B, variation in voltage (below) and intensity;
C, intensity variation of two different iron lines;
D, same, both curves superimposed;
E–F, rectified and partly filtered d.c.-a.c. ripple about 6 percent. Current (below) and intensity.

that both have identical fluctuations. Figure 9D shows this perhaps even better, as the two curves have been shifted up and down so as to coincide. The fact that the curves of both lines appear as one trace shows that both lines behave in the same fashion. A device which would measure instantaneous values of the relative intensities of the two lines would be, therefore, free from fluctuations.

It has often been maintained that an arc made to run at constant current would give constant intensity, and a great deal of ingenuity has been spent on devices to regulate the arc current, which have all more or less failed. There are good and well-known theoretical reasons for this. Figures 9E and 9F provide an empirical demonstration that stationary arc current does not necessarily mean constant intensity. The bottom trace shows the current, which is in this case rectified and filtered a.c. which provides d.c. current with about a 6 percent 60-cycle a.c. ripple. The top traces show the light intensity. While the current is absolutely regular, the intensity shows pronounced irregularities.

Spectrochemical Analysis with the Oscillograph*

G. H. Dieke and H. M. Crosswhite
Johns Hopkins University, Baltimore, Maryland

(Received February 18, 1946)

In industrial spectrochemical analysis there are often problems where speed and ease of operation are of more importance than high accuracy. In such cases a very simple procedure leads to a method of analysis where the results can be seen almost instantaneously on the oscillograph screen.

The principles of this method have been explained in the previous article. The application can perhaps be best illustrated with an actual example.

Suppose we want to analyze steel samples for copper, manganese, and chromium. A suitable line of each element is selected and also an iron line which serves as reference line. A separate photo-tube is installed to receive each line. The output of each tube is alternately connected to the oscillograph through a rotating switch (see circuit diagram, Fig. 1). In this particular case the switch allowed each line to be connected for 1/25 second during every 1/5 second interval. The time base of the oscillograph is synchronized with the rotating switch so that the repeated traces of each line always fall in the same horizontal interval on the screen. The height is proportional to the intensity and, therefore, an indication of the concentration of the particular constituent. A condenser is inserted in order to increase the time constant of the circuit, which will eliminate the influence of short period fluctuations.

Figure 2 shows photographs of patterns for four different steel samples. The presence of manganese and copper in the electrolytic iron sample (2*A*) is less than might be judged from the height of the traces. These deflections are largely due to background light. For all samples, no attempts were made to select the lines so that self-reversal and other causes would not influence the results. Nevertheless, all four samples have quite distinctive patterns which would permit at least an immediate identification of the type of steel.

If the light source shows strong fluctuations, the whole pattern may fluctuate up and down on the screen, but in first approximation holding

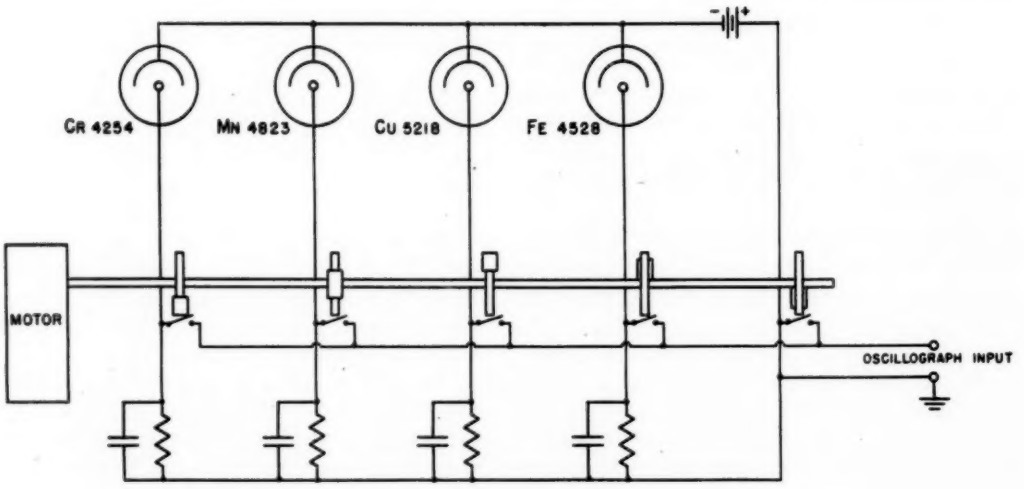

Fig. 1.

* Results of work on a project sponsored by the Office of Production Research and Development of the War Production Board.

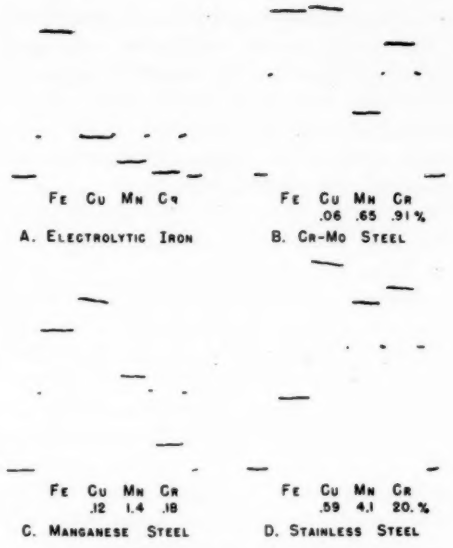

FIG. 2. Steel analysis with oscillograph.

the relative position of the traces. All traces should, therefore, always be evaluated in terms of the iron deflection. Nevertheless, when strong fluctuations occur the observation of the pattern may not be easy. A somewhat modified procedure will improve this situation considerably.

Instead of using the time base of the oscillograph, the iron line is put on the horizontal (X) axis. The other lines are put on the vertical (Y) axis of the oscillograph. This is shown in the circuit diagram Fig. 3. The voltages are applied here directly to the plates of the cathode-ray tube, and in order to make large deflections possible, an auxiliary voltage V_2 is applied which displaces the zero point into one corner of the screen.

The results are shown in Fig. 4 for the same samples as Fig. 2. However, the iron line is also used on the Y axis to give a reference point, and one of the positions is grounded to give a zero. (One of these two is superfluous.) The rotating switch is used in the same way as in the former example. We are now getting the intensities plotted as vertical deflections against the horizontal deflection of the iron reference line. If the light source remains constant, each element will produce a point, and all points will lie on a vertical line. If the source fluctuates, every point will move along a straight line going through the origin. The slope of this straight line will then measure the intensity of the spectrum line and therefore the concentration of the element. A.c. light sources can, therefore, be used for this method, while they would be ordinarily impossible with the method of Fig. 1.

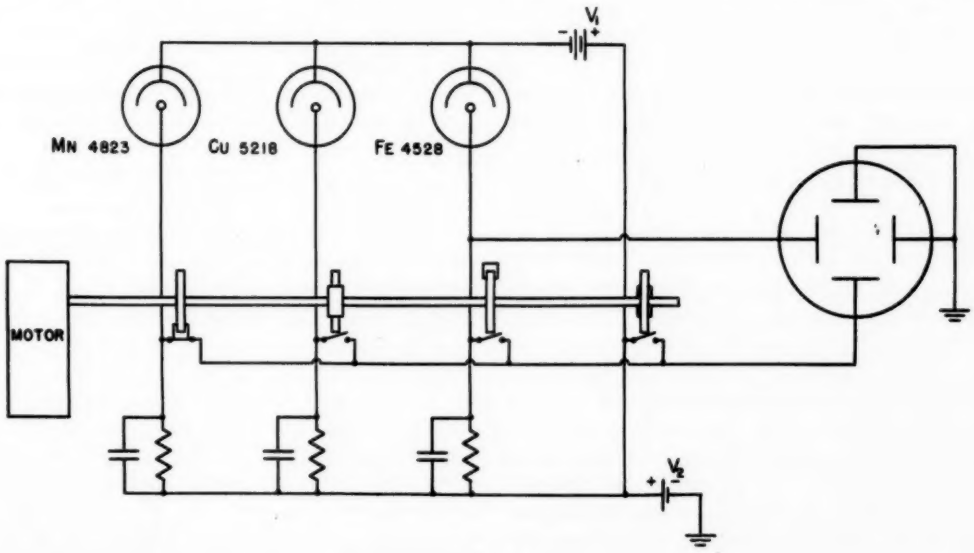

FIG. 3.

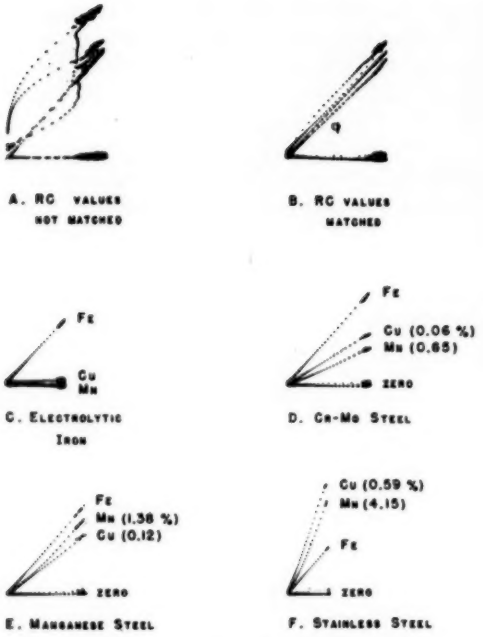

FIG. 4. Steel analysis with cathode-ray tube

In order not to run into any difficulties, it is, however, necessary to have the time constants of all tube circuits matched. In all cases of Fig. 4, the screen was photographed with the light on the photo-tube which produced the heavy parts on the right side of each diagram. Then the light was shut off and the camera lens left open while the condensers discharged. If the time constants are matched, the condensers discharge at the same rate and we get straight dotted lines connecting the original deflections with the origin. We see, however (Fig. 4*A*), that the pattern is very irregular and therefore unsuitable if the time constants are not matched. These irregularities immediately disappear when the circuit constants are adjusted (Fig. 4*B*).

The pattern is quite easily read quantitatively if a suitable transparent scale is attached to the screen. In order to avoid flickering which occurs if the switching rate is fairly low, a screen of long persistence should be used. We estimate that we can read the intensities to about 5 percent accuracy, which compares with the accuracy of the photographic plate. The fact that some of the points do not appear very sharp is due to the peculiarities of the particular cathode-ray tube, which shows considerable astigmatism. (Horizontal lines do not appear sharp for the same setting of the focus control as vertical lines.) In order to bring out the dots connecting the original spots to the origin, the pictures had to be considerably overexposed.

The screen patterns must of course be calibrated with standard samples in the same way as in any other method.

The advantage of this scheme over the first one is based on the fact that although a light source may strongly fluctuate and, therefore, the intensities of individual lines may vary considerably with time, the ratios of two lines nevertheless may remain quite constant. This is not necessarily so, and the previous paper gives several examples where this is not the case. However, if the lines have similar excitation conditions, the ratio will remain constant. This may be tested experimentally by allowing the variations to be quite large. This is illustrated by Fig. 5, which is obtained with an a.c. discharge in mercury vapor. The voltages in this case are applied through a condenser and the zero point is in the middle. Figure 5*A* represents a superposition of the diagrams for two line pairs with different intensity ratios. In all cases straight lines are obtained, which shows that the intensity ratios remain fixed through the full cycle. Figure 5*B* shows three line pairs and also the coordinate axes. These are obtained by placing alternately a zero potential on each pair of deflection plates. The slope of the lines is a measure for the relative intensities.

The question of whether this method of analysis with the cathode-ray oscillograph has any advantages over other photographic or photoelectric methods can be answered definitely only when it has been tried out under industrial routine conditions. However, even now some obvious applications suggest themselves.

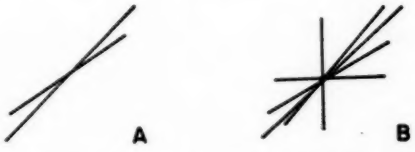

FIG. 5. Intensity ratios of mercury lines throughout full cycle of an a.c. discharge.

If a complete analysis is required for many constituents, the pattern on the screen becomes too complicated to be easily interpreted. This is not an unsurmountable obstacle, as electric pulses with characteristic shapes can be added to the trace of each element to make its identification easy. We feel, however, that its greatest usefulness will be for cases when only a few elements are of importance, and particularly when only a semi-quantitative analysis is required, as is the case for many trace elements.

In such cases a very simple spectrograph is often quite sufficient. The installation of the tubes presents no particular difficulties. The price of an oscillograph is about the same as that of a good microammeter, and will, therefore, not increase the cost of the installation if it is used instead of the meter. We have used only commercial oscillographs which have many features that are not needed for this particular application. Oscillographs specially designed for this problem would be both cheaper and more serviceable.

The use of the oscillograph opens up therefore possibilities for inexpensive special purpose instruments which would permit very rapid analyses for particularly important elements. The low cost of such instruments would make it possible to use different ones for each purpose.

From the preceding remarks it is evident that, wherever an instrument like a "steeloscope" is used, the oscillograph can be used just as easily and with more accurate results. Moreover it is not restricted to the visible, and its results are objective. As far as our experience goes, we believe that an arc will be a more suitable light source for this kind of work than the spark. Naturally when segregation plays an important role in the sample it suffers from the same disadvantages as all short period instruments.

JOURNAL OF THE OPTICAL SOCIETY OF AMERICA VOLUME 36, NUMBER 4 APRIL, 1946

Recording Infra-Red Analyzers for Butadiene and Styrene Plant Streams*

N. WRIGHT AND L. W. HERSCHER
The Dow Chemical Company, Midland, Michigan

A simple compact instrument is described which analyzes various organic mixtures by automatic measurement of absorption of infra-red radiation. Optically the instrument consists of a double beam system employing a single source of radiation, a split lens or mirror, a sample cell and various filters through which one or both beams may pass, and two electrically opposed detectors upon which the beams are focused. Selectivity of wave-length is provided by the filters and by detectors having selectively absorbing radiation receivers. The detectors are two opposed arms of an a.c. excited bolometer made of fine nickel wire embedded in a selectively absorbing medium. A vacuum tube amplifier working on the bolometer output actuates a potentiometer-recorder which automatically restores the bridge balance and in the same operation records the analysis of the sample. Successful operation of these instruments on continuous analysis of plant streams of butadiene-butene gas mixtures and of styrene-ethylbenzene liquid mixtures is detailed. One unit has been in service for over three years automatically controlling a distillation process.

ANALYSIS of mixtures of organic compounds by means of the infra-red spectrograph has become well established in recent years. In its present stage of development the infra-red spectrograph functions quite reliably in laboratories but is hardly rugged enough for installation in the usual industrial chemical plant. Nevertheless there is an urgent demand in many plants for very rapid or continuous analysis of certain streams of organic mixtures for the purpose of process control. To fill this need a simple and rugged infra-red instrument for continuous analysis has been developed which operates well

* Paper presented at the 30th annual meeting of the Optical Society of America, New York, New York, October 18–20, 1945.

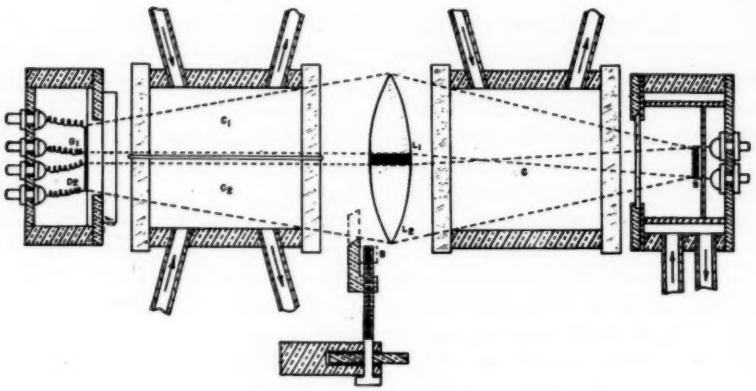

FIG. 1. Schematic diagram of the apparatus.

under plant conditions. The instrument is somewhat limited in the capacity to discriminate between components of complex mixtures since it relies upon the selective transmission of filters and upon the selective absorption of the detecting elements rather than upon dispersion of the spectrum as does a spectrograph. Despite this limitation analyzers of this type have proved successful on several plant streams of different kinds, and in one case a unit has served satisfactorily as an automatic controller of a plant process.

The principle of the analyzer[1] can be inferred from Fig. 1 which is a schematic diagram of the optical system. Infra-red radiation from a single source S is split into two beams by the half-lenses L_1 and L_2 which form images of the source on the two bolometer elements D_1 and D_2. These elements are the opposed arms of a Wheatstone bridge, hence the balancing of the radiation beams (by means of the adjustable stop B) removes the effect of variations of the source. Both beams pass through cell C, but each passes through a separate compartment (C_1 or C_2) of a double cell. If desired, a split concave mirror, mounted behind the source in a somewhat larger source housing, may be used instead of the half-lenses.

Three methods of analysis involving different mechanisms are possible with this apparatus. Method I applies to a mixture of two components, one of which simply absorbs a greater portion of the total radiation from the source than the other. The sample is placed in cell C_1, and the other cells may be left empty. Black (unselective) receivers may be used on the bolometers but, as will be explained later, selective receivers may be used to advantage. After the beams have been balanced with a standard sample in the cell, the introduction of any subsequent sample having different proportions of the components unbalances the system and produces a reading on the recorder or indicating device. An improvement in the accuracy of this method can be made by maintaining a standard sample of average constitution in the other compartment C_2 of the double cell.

Method II makes use of selectively absorbing materials as radiation receivers in contact with the bolometer elements, a principle employed by Pfund.[2-4] This renders the instrument sensitive to a particular constituent of a multi-component mixture. The medium in contact with the bolometer elements should have strong absorption bands coinciding with distinctive bands of the component to be determined but should not have strong bands matching those of the other constituents. Here as in Method I the sample occupies compartment C_1, and the other cells remain empty. Again, however, the use of a permanent standard sample in compartment C_2 improves the stability of the apparatus.

[1] N. Wright, U. S. Patent No. 2,386,831, Oct. 16, 1945 (Dow Chemical Company).

[2] A. H. Pfund, Science **90**, 326 (1939).

[3] A. H. Pfund and C. L. Gemmill, Bull. Johns Hopkins Hospital **67**, No. 1, 61 (1940).

[4] A. H. Pfund, U. S. Patent No. 2,212,211, August 20, 1940.

Method III, similar to that of Schmick,[5] consists of placing in one beam, e.g., in cell C_1, a pure specimen of the component for which the analysis is to be made. The unknown sample now occupies cell C, cell C_2 remains empty, and the radiation receivers may be black. Again, however, selective receivers may be used to advantage. The mechanism becomes evident if one considers the effect of increasing the concentration in the sample of the component under analysis. Little or no loss in intensity is experienced by the beam which passes through C_1 since the wave-lengths affected by the component under analysis are exactly those removed by absorption in C_1. The other beam, on the contrary, is weakened by increased absorption of these wave-lengths and a reading of the indicator results.

DESCRIPTION OF THE APPARATUS

The source of radiation is an electrically heated nichrome coil flattened into a rectangle, 9 mm×20 mm, and mounted in a water cooled housing (Fig. 2). It is usually maintained at about 800°C, requiring 40 watts. A window of quartz (1 mm thick, long wave-length transmission limit 4.7μ) or of AgCl (2 mm thick, long wave-length limit >24μ) seals the housing. Supporting the housing is a solid block of Bakelite which provides thermal insulation between the source and the base plate of the instrument.

The lenses are of rocksalt (long wave-length transmission limit 16μ) or of AgCl. The surfaces

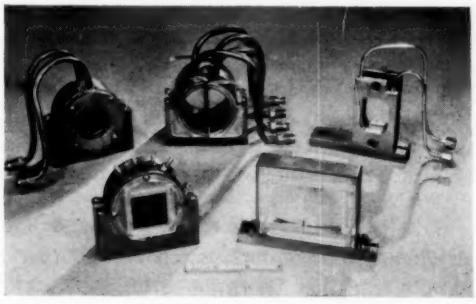

FIG. 2. Various parts of the instrument. Left to right: source, bolometer, split gas cell, split lens, cell for liquid sample.

[5] H. Schmick, U. S. Patent No. 1,758,088, May 13, 1930.

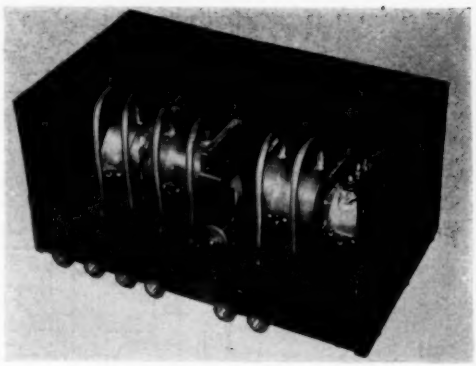

FIG. 3. Gas analyzer (over-all dimensions, 12″×7″×6″).

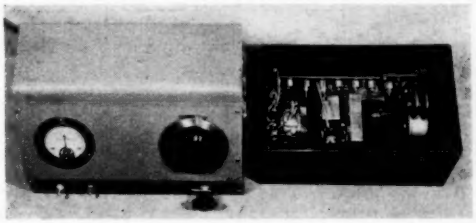

FIG. 4. Analyzer for liquid samples. At left: amplifier and hand-operated potentiometers.

are spherical, double-convex in the case of rocksalt and plano-convex in the case of AgCl, and in both cases the focal length is 5 cm. Each is the half of a circular lens originally 5 cm in diameter. Figure 2 shows the lens mount. Shown also in Fig. 2 are the cells and cell mountings for gases and liquids. Windows are of LiF (5 mm thick, long wave-length transmission limit 6μ), rocksalt, or AgCl.

The bolometer elements consist of two 240-ohm coils of Ni wire (0.0015 inch diameter) embedded in a plastic film approximately 0.075 mm thick. The coils are in the form of flat rectangular areas, 10×20 mm, of uniformly spaced windings balanced to within 0.1 ohm. They are placed side by side, 3 mm apart, within a strip of the film which is mounted in the brass housing shown in Fig. 2. In this case the block supporting the housing is of brass to provide good thermal contact with the $\frac{1}{4}$″ iron base plate, a feature which aids in eliminating drift caused by temperature inequalities. Windows of LiF or of AgCl, depending on the wave-length range

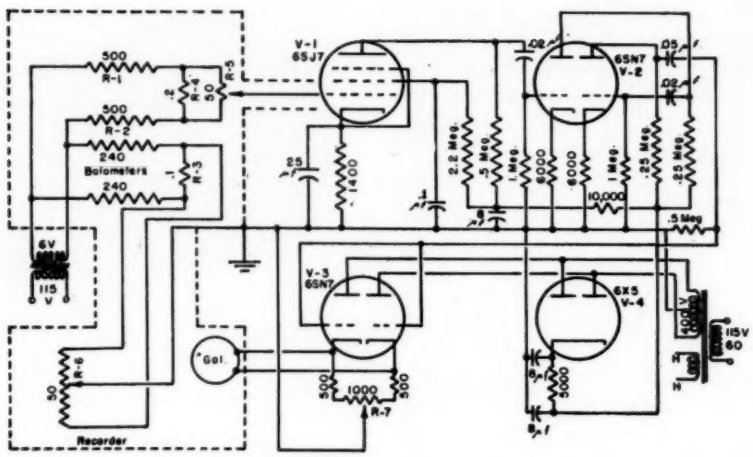

FIG. 5. Circuit diagram of amplifier and recorder.

required, seal the housing. Figures 3 and 4 are photographs of assembled analyzers for gases and liquids, respectively.

The bolometer arms are connected in a bridge (Fig. 5) which is activated by 6 volts a.c. (60 cycle) supplied by a constant-voltage transformer. Resistances R-1 and R-2, each 500 ohms, which complete the bridge are of manganin wire. Variable resistances R-5 and R-6 are wire-wound potentiometers, R-6 being usually the slide wire of a recording potentiometer (such as the Leeds-Northrup micromax) in which it serves to indicate the analysis by its setting. R-5 serves as a zero adjuster which is usually hand operated. Shunting these slide-wires are the resistances R-3 and R-4, 0.1 ohm and 0.2 ohm, respectively. It will be observed that a full-scale movement of either slide-wire has the effect of moving the resistance of the corresponding shunt from one arm of the bridge to the other. A full-scale deflection of the indicator thus corresponds to a temperature difference of 0.14°C between the bolometer arms.

The potential difference developed between the two slide-wire contactors when the bridge is unbalanced is applied to the amplifier as shown in Fig. 5. A phase-discriminating rectifier tube V-3 converts the output to d.c. which is applied to the galvanometer of the automatic potentiometer, the polarity being determined by the direction of unbalance in the bolometer. The automatic potentiometer adjusts the indicating slide-wire (R-6) so as to maintain the bolometer bridge in balance (i.e., at null output) at all times during operation, a procedure that renders the analysis independent of amplifier characteristics and of bridge-voltage fluctuations. The over-all time of response of the bolometer-recorder system is about 20 seconds.

ANALYSIS OF TOTAL BUTENES IN BUTADIENE GAS

For this analysis a mechanism which can be described as intermediate between Methods I and II has been applied. The sample occupies cell C_1 at atmospheric pressure, while cells C_2 and C remain empty (or C_2 may contain a permanent standard). The radiation is limited effectively to the range 1 to 4.7μ by operating the source at 800°C (maximum at 2.7μ) and equipping the housing with a quartz window.

In this spectral range butadiene has a single region of strong selective absorption, centering at 3.27μ, which is due to the stretch vibration of the C−H bond of the $=\overset{|}{C}-H$ group. Each of the butenes (butene-1, *cis*- and *trans*-butene-2, and isobutene) has absorption in the 3.27μ region but in addition has a second very strong band centering at 3.4μ, which is due to the saturated groups $-CH_2-$ and $-CH_3$. The analysis for butenes therefore depends upon a measurement of the absorption at 3.4μ.

Because of the greater total of energy absorbed by butenes as compared with butadiene in the range 1–4.7μ, Method I, employing black receivers, can be used. However, the selectively absorbing receiver used, in this case ethyl cellulose film in contact with the bolometer arms, provides two advantages: It insures total absorption at 3.4μ (where ethyl cellulose has a strong absorption band), and, by transmitting a portion of the ineffective radiation of other wave-lengths, it permits the receivers to operate at a lower temperature. This results in a more stable functioning of the bolometer. Because of the considerable general absorption of this type of receiver the method does not accurately qualify under II.

To illustrate the mechanism of this analysis, let it be assumed that a sample of the butadiene-butene mixture is placed in cell C_1 and that the two radiation beams striking the bolometer arms have then been balanced by adjustment of the stop B (Fig. 1). If now the sample is replaced by a new sample with a larger concentration of butenes, the transmitted radiation of wave-length 3.4μ decreases in intensity, detector D_1 cools, and the recording potentiometer indicates the change in analysis as the slide wire R-6 automatically adjusts to the new position required to balance the bolometer bridge.

Calibration is carried out in the following manner: With the source turned off, the recording pen is brought to the center of the scale by means of the zero adjuster slide wire R. The source is then turned on and a known sample containing approximately the average concentration of butenes encountered in the stream to be analyzed is placed in the cell. The radiation beams are then balanced by adjusting the stop B so as to bring the pointer again to the center of the scale. Without further adjustment of the apparatus other standard mixtures covering the required range of concentrations are then used to complete the calibration. Figure 6 shows a typical calibration curve for total butenes in butadiene. The butene mixture used was characteristic of the particular plant stream involved (approximately 75 percent butene-1, 15 percent isobutene, 5 percent butene-2, 5 percent butanes).

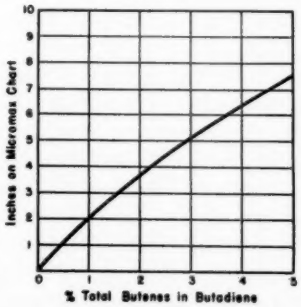

FIG. 6. Calibration curve for analysis of total content of butenes in butadiene gas.

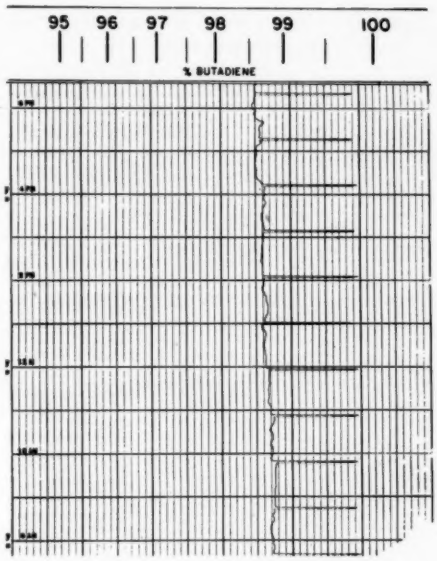

FIG. 7. Section of chart recorded by plant-installed infra-red gas analyzer continuously determining the total butene impurity in a stream of butadiene. Standardized automatically at 45-minute intervals (disregard time scale at left).

The accuracy of the analysis in the range 97 to 100 percent butadiene is within ± 0.05 percent of total sample. However, to achieve this accuracy the apparatus must be standardized with a known sample sufficiently often, and the proportions of the individual butenes must not be allowed to vary too widely. Changes in barometric pressure, hence in sample pressure, are adequately corrected for by the frequent use of a standard sample which is also introduced at atmospheric pressure. Tests made to establish this showed that for each inch Hg pressure increase the butene content as read on the analyzer

was increased by only 1.7 percent of the difference between butene content of the sample and that of the standard. Since this difference seldom amounts to more than 1 percent (of total sample), a barometric change of 1 inch Hg produces an error of only 0.017 percent (of total sample) in the analysis. Furthermore, changes in the proportions of the individual butenes present have a rather small effect on the analysis as is illustrated by the following example: With the apparatus calibrated using the above-mentioned butene mixture introduction of a synthetic sample containing 97.57 percent butadiene and 2.43 percent *trans*-butene-2 gave a reading of 2.17 percent as total butenes. Error from this source was negligible in the plant stream involved.

The performance of the apparatus as a continuous recording analyzer is illustrated in Fig. 7 showing a section of chart recorded by a unit installed in a plant. In this case the instrument is automatically standardized at 45-minute intervals by the introduction of a standard sample into the sample cell. Automatic valves cut off the flow of the regular sample and admit the standard gas. Slide-wire *R*-5 (the zero-adjuster) is automatically adjusted (by a mechanism in the recorder originally intended for battery standardization) so as to give the correct analysis of the standard. The accuracy of the instrument is indicated by the smallness of the displacements in the trace after each standardization.

ANALYSIS OF BUTADIENE IN A MIXTURE OF BUTENES

Method III is used for this analysis with the exception that the radiation receivers are partially transparent at wave-lengths shorter than 3μ instead of being black throughout the spectrum. This is accomplished by using films of ethyl cellulose (or rubber hydrochloride) coated with a mixture of ester type resins in contact with the bolometer arms. Since butadiene absorption bands in the region from 5 to 8μ are effective in this analysis the source and cell windows are of AgCl or NaCl. One of the double cell compartments (C_1, Fig. 1), 5 cm long, contains pure butadiene at atmospheric pressure which serves as a filter and provides the selectivity as earlier explained. The gas flows at atmospheric pressure through C which is also 5 cm long.

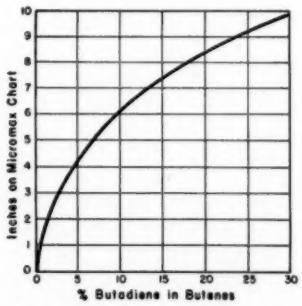

FIG. 8. Calibration curve for analysis of small amounts of butadiene in a mixture of butenes.

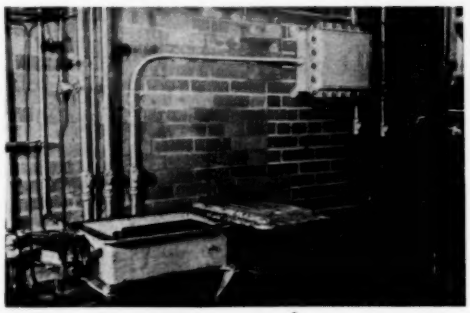

FIG. 9. Plant installation of infra-red gas analyzer for butadiene-butene mixtures mounted in explosion-proof housing. At upper right is explosion-proof housing containing amplifier.

The sensitivity of the analysis is indicated by the calibration curve (Fig. 8) which was obtained in the same manner as in the preceding case, using a mixture of the same proportions of the individual butenes. Accuracy well within 0.5 percent of total sample has been achieved with a plant-installed unit, a photograph of which appears as Fig. 9. The stability of the apparatus is demonstrated in Fig. 10 by a recording lasting $6\frac{1}{2}$ hours, during which a standard sample flowed through the cell. In ordinary practice the effects of barometric changes are again made negligible by periodic introduction of a standard (Fig. 11). An idea of the magnitude of error caused by changes in the proportions of the individual butenes can be gained from the following example: After calibrating the analyzer using the usual butene mixture a synthetic sample containing 7.9 percent butadiene in butene-1 pro-

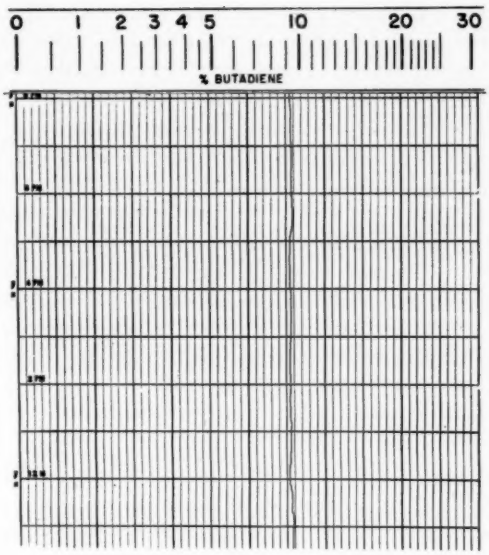

FIG. 10. Section of chart showing stability of infra-red gas analyzer during 6½-hour run on standard gas (disregard time scale).

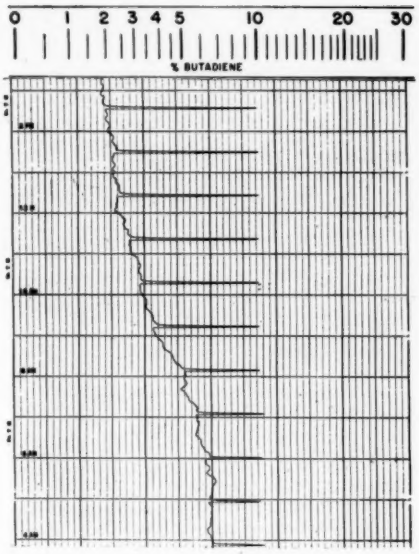

FIG. 11. Section of chart recorded by plant-installed gas analyzer continuously determining the butadiene content in a stream of butenes. Standardized automatically at 45-minute intervals (disregard time scale).

duced a reading of 5.9 percent butadiene. Variation of the plant mixture in this respect is ordinarily small enough to constitute a minor source of error. Figure 11 shows a typical strip of recording produced by an analyzer on a plant stream. Here also the instrument is automatically standardized at 45-minute intervals, and the accuracy is demonstrated by the smallness of the corrections required.

ANALYSIS OF ETHYL BENZENE IN LIQUID STYRENE MONOMER

The mechanism of this analysis is in every respect identical with that involved in the case of total butenes in butadiene. As in the case of butenes the ethyl benzene molecule has a strong absorption band centering at 3.4μ (due to the ethyl group) as well as a band centering at 3.28μ (due to C−H of the benzene ring). Corresponding with butadiene the styrene molecule has but one strong band centering at 3.28μ. In the present case the sample stream consists of liquid mono-styrene which flows through a cell corresponding to C_1 (Fig. 1) designed for a liquid layer 0.3 mm thick (Figs. 2 and 4). Figure 12 shows a typical calibration curve. The accuracy is within 0.1 percent of total sample in the range 98 to 100 percent styrene. Standardization is required at intervals of 2 to 4 hours. No temperature control of the sample or of the standard is required other than bringing both to room temperature. A typical example of continuously recorded analysis of a plant stream is shown in Fig. 13 which covers the period near the end of a batch distillation.

AUTOMATIC CONTROL

From the standpoint of instrumentation, it is a very short step from continuous recording of

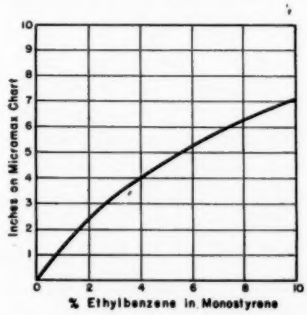

FIG. 12. Calibration curve for analysis of ethyl benzene in liquid styrene monomer.

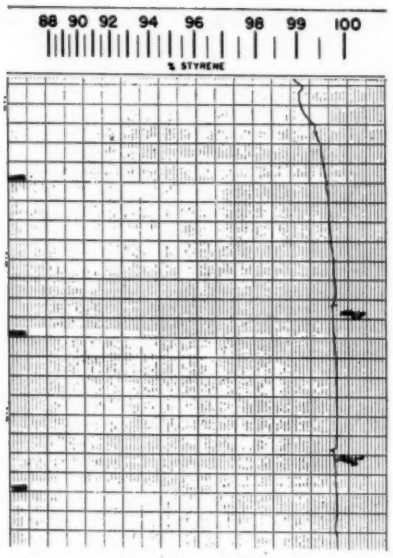

FIG. 13. Section of chart recorded during 12 hours by plant-installed infra-red analyzer continuously determining ethyl benzene impurity in liquid styrene monomer.

analysis to automatic control of a process. Many commercial pen-type recorders are equipped with control mechanisms for automatically adjusting valves, rheostats, etc., in accordance with the analysis being recorded. For more than three years an infra-red analyzer of the type described above has been in satisfactory service controlling the operation of a distillation column used for azeotropic separation of butadiene from a mixture of butenes. The gas sample (butadiene-butene mixture) is drawn from the column at a selected plate and allowed to flow continuously through the analyzer cell. The analyzer-recorder system automatically controls the adjustment of the feed-valve to the still and secures proper operating conditions by holding the butadiene concentration of the sample stream at a prescribed value (about 75 percent).

CONCLUSION

The simple infra-red analyzer described in this report is capable of handling a variety of plant streams, continuously recording the analysis or automatically controlling processes. Eight of these instruments are now in service in plants of this company, and it is expected that applications will become widespread as the apparatus becomes available commercially.*

* Instruments of this type are now being manufactured by Baird Associates, Cambridge, Massachusetts.

JOURNAL OF THE OPTICAL SOCIETY OF AMERICA VOLUME 36, NUMBER 4 APRIL, 1946

Photographic Granularity and Graininess†,*

II. The Effects of Variations in Instrumental and Analytical Techniques

LOYD A. JONES AND GEORGE C. HIGGINS
Kodak Research Laboratories, Eastman Kodak Company, Rochester, New York

(Received February 5, 1946)

Several proposals for measuring the granularity of developed silver images, in purely objective terms, have appeared in the literature. These can be classified into two general groups, namely: those which base the evaluation of granularity upon the variations in the transmittance of relatively small elements of the developed image and those which use variations in density. In this paper one method representing each of the two classes is examined in some detail, especially with respect to the dependence of the granularity value upon the size of the scanning aperture which is used in obtaining basic data on the variations in transmittance or density. The experimental results indicate clearly that values of granularity, determined on the basis of the assumption that the distribution of transmittance values is represented by the Gaussian equation, are not independent of the size of the scanning aperture. Moreover, the frequency of occurrence of transmittance variations departs markedly from the Gaussian law when relatively small scanning apertures are used. Values of granularity based upon the variations in density, assuming a Gaussian distribution of these variations, also depend upon the size of the scanning apertures used. While the frequency of occurrence of density variations corresponds approximately to the Gaussian law for some scanning aperture sizes, the departure from Gaussian distribution is very marked in the case of small scanning apertures. With the photographic materials used in this work, no scanning aperture size was found which gave granularity-*versus*-density functions similar in shape to the graininess-density function. Some alternative methods of analyzing the basic data are discussed briefly. None of these show promise of yielding a satisfactory solution of this problem which, in our opinion, demands that the granularity-density function derived from objective functions shall be identical in shape to that of the graininess function. Finally, some preliminary discussion of certain visual aspects of the general problem is given. It is assumed that some definite and unique relationship should exist between the size of the scanning aperture used in the objective evaluation of granularity and the *effective* size of the light-sensitive elements of the eye. Some semiquantitative data are presented which illustrate, in a general way at least, the distribution of illuminance on the retinal mosaic when the granular photographic image is viewed at the blending distance. These indicate that the number of visual field elements imaged on a single visual receptor (foveal cone) is small, usually of the order of 3 or 4, and seldom exceeding 8 or 10, even though the photographic materials used in this work varied over a wide range with respect to the coarseness of granular structure.

I. INTRODUCTION

IN a previous communication[1] we have reported the results of graininess and granularity measurements made on a group of photographic materials differing widely with respect to granular structure. The graininess measurements were made by a psychophysical method which gives a direct evaluation of the visual appearance of the spatial inhomogeneities which occur in developed silver deposits. The granularity measurements were made by five methods which have been proposed for the evaluation, in purely objective terms, of these spatial inhomogeneities.

None of the objective methods gave granularity-density functions in agreement with the graininess-density functions. Moreover, it was found that the *ratio* of graininess to granularity was not the same function of density for different materials. Each of these objective methods ranked the photographic materials roughly in the same order as the graininess measurements, but no method gave exactly the same order as that based upon the graininess values, and in some cases the differences in order were very marked. These results indicate that the various objective methods studied measured some, but not all, of the factors controlling graininess.

It seems desirable, therefore, to make a further study of the fundamental principles underlying

† Communication No. 1065 from the Kodak Research Laboratories.

* The first paper in a series from these Laboratories appeared in the July, 1945 issue of the *Journal of the Optical Society of America* under the title "The Relationship between Granularity and Graininess of Developed Photographic Materials." This should be considered as the subtitle of the first (I) member of this series appearing under the general title "Photographic Granularity and Graininess."

[1] L. A. Jones and G. C. Higgins, "The relationship between the granularity and graininess of developed photographic materials," J. Opt. Soc. Am. **35**, 435 (1945).

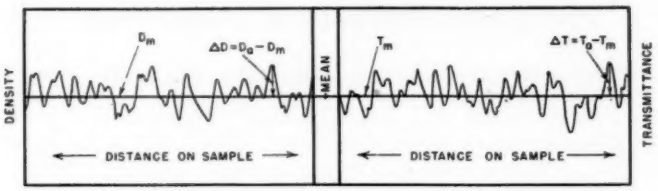

FIG. 1. Sample microphotometer record.

the objective evaluation of the granular structure of developed photographic images, that is, the property that is commonly designated as granularity. This characteristic of photographic materials is of great importance, since in many cases it determines certain qualities of the final photographic reproduction. It is hoped that such an investigation may lead to some modification in the technique of making and interpreting granularity measurements which will yield values more nearly in accord with the visual appearance (that is, graininess) of developed silver images, and which will be valid indications of the graininess of prints made therefrom on photosensitive materials of known granular structures.

Three of the granularity methods studied in our previous communication,[1] namely, the van Kreveld, the Goetz-Gould, and the Selwyn methods, resemble each other in some respects. Thus, they all evaluate granularity in terms of transmittance or density variations among a large number of relatively small surface elements. Although the terms in which these variations are measured are dependent upon the method used, the conclusion is reached in all cases that the frequency of occurrence of these variations can be expressed moderately well by the Gaussian distribution function. Granularity is then defined as follows:

By van Kreveld.—

$$VK = \text{average } (T_{a1} - T_{a2}), \tag{1}$$

where T_{a1} = the transmittance of area, $a1$, and T_{a2} = the transmittance of an immediately adjacent and equal area, $a2$.

By Goetz and Gould.—

$$GG = 1000\sigma_{tg} \cdot \sqrt{2}, \tag{2}$$

where σ_{tg} = the standard deviation of the relative transmittance variations, $\Delta T/T_m$, obtained as a characteristic of a Gaussian distribution function, $\Delta T = T_a - T_m$, T_a = the transmittance of a small surface element of area, a, and T_m = the mean transmittance of a large number, n, of T_a's.

By Selwyn.—

$$S = \sigma_{dg}(2a)^{\frac{1}{2}}, \tag{3}$$

where σ_{dg} = the standard deviation of density variations, ΔD, obtained as a characteristic of a Gaussian distribution function, $\Delta D = D_a - D_m$, where D_a = the density of a small surface element of area, a, and D_m = the mean density of a large number, n, of D_a's.

Although these three methods of measuring granularity are similar, the values obtained by one method cannot be used to predict with certainty the values obtainable by either of the other methods. To discover the reason why these methods do not give granularity values that agree with each other or with graininess, it will be necessary not only to examine the details of the experimental technique (the optical and physical characteristics of the microphotometer and the associated recording devices) used in obtaining the basic data, but also to analyze the treatment to which these data are subjected in finding a numerical value for granularity.

II. STATISTICAL CONSIDERATIONS

Before the presentation of new data, the mathematical principles involved in obtaining granularity values will be reviewed briefly to clarify the basic concepts underlying these measurements and to establish a terminology for use in the subsequent discussion.

We shall first illustrate graphically the nature of the fundamental data upon which the evaluation of granularity is based. While individual methods may differ in the actual techniques by which the amount of light transmitted by small areas of the granular structure is measured, the curve in Fig. 1 represents in a general way the

manner in which the transmittance and density fluctuations are recorded. The ordinates of this microphotometer record represent either transmittance or density, and the abscissas represent the linear distance on the sample traversed by the scanning aperture. It is evident that measurements in terms of transmittance can be converted to densities, and *vice versa*, by the well-known relation,

$$\text{Density} = \log_{10} 1/\text{transmittance}.$$

The solid horizontal line gives the *mean* density or transmittance of all of the measured D_a's or T_a's. Since each ordinate of the microphotometer record gives the transmittance or density of an area, a, of the silver deposit, a large number of values of ΔT and ΔD may be obtained by reading the departures of the record from the line representing the mean value. This record then represents the basic data which must now be treated by suitable statistical methods in order to obtain an evaluation of granularity.

Goetz and Gould[2] have reported that the statistical distribution of transmittance fluctuations over the surface of an exposed and developed photographic material is essentially Gaussian. Selwyn[3] made a study of the statistical distribution of density fluctuations and reported that for practical purposes this distribution is

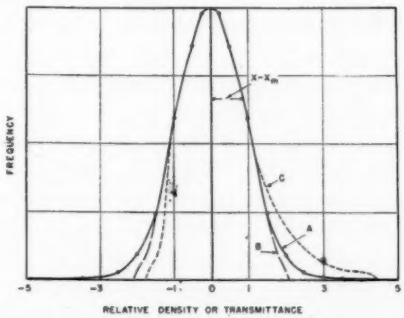

FIG. 2. Hypothetical distribution functions. Curve A, Gaussian; B, symmetrical with finite limits; C, asymmetrical with finite limits.

[2] A. Goetz and W. O. Gould, "The objective quantitative determination of the graininess of photographic emulsions," J. Soc. Mot. Pict. Eng. **29**, 510 (1937); A. Goetz, W. O. Gould, and A. Dember, "The objective measurement of the graininess of photographic emulsions," J. Soc. Mot. Pict. Eng. **34**, 279 (1940).

[3] E. W. H. Selwyn, "Experiments on the nature of graininess," Phot. J. **79**, 513 (1939).

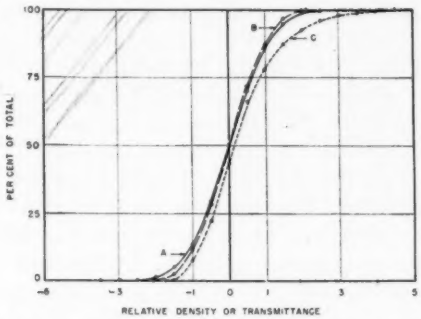

FIG. 3. Hypothetical data showing Fig. 2 plotted as cumulative frequency functions.

also essentially Gaussian. As pointed out, these authors define granularity in terms of sigma, the standard deviation of the measured values from the mean. They then determine the value of sigma by a statistical analysis of the microphotometer record based upon the properties of the Gaussian distribution function. A Gaussian* distribution function is plotted as the solid curve, A, in Fig. 2. The equation of this curve is

$$y = A \exp\left[-(x-x_m)^2/2\sigma^2\right], \qquad (4)$$

where y is the frequency of occurrence of the deviations $(x-x_m)$. The standard deviation, σ, is defined by the equation,

$$\sigma = \left[\sum (x-x_m)^2/n\right]^{\frac{1}{2}}, \qquad (5)$$

where n is the number of observations. This function is symmetrical with respect to the vertical line through x_m, and the abscissa values extend from $-\infty$ to $+\infty$.

For some purposes it is convenient to express the Gaussian distribution function (Curve A, Fig. 2) as a cumulative frequency curve. This curve, which is known as an ogive, is plotted as the solid curve, A, in Fig. 3. The equation of this curve is

$$y = 1/(\sigma(2\pi)^{\frac{1}{2}}) \int_{-\infty}^{x} \exp\left[-(x-x_m)^2/2\sigma^2\right] dx, \qquad (6)$$

where y is the percent of the total number of fluctuations $(x-x_m)$ having a value equal to or less than that of x.

* Perhaps the more modern terminology employs the word "normal" in reference to the distribution represented by Eq. (4). However in the literature of photographic granularity the term "Gaussian" has been most frequently used. We shall follow this precedent.

The cumulative frequency data may be plotted on arithmetic probability paper, as shown by the solid line, *A*, in Fig. 4. This coordinate paper has a non-linear ordinate scale which is so chosen that all Gaussian distributions are represented by straight lines. The reciprocal of the slope of each line is equal to the standard deviation, σ, for that distribution. Therefore the value of σ, and of granularity, can be obtained from the microphotometer record (Fig. 1) by plotting the cumulative frequency data on probability paper.

The Gaussian distribution was developed originally as a means of representing the most probable distribution of errors in the experimental measurement of physical dimensions. The application of this distribution function to many other problems has proved exceedingly useful. While in many cases the Gaussian function fits the experimentally measured variations over only a part of the range of fluctuations, the function can still be used to characterize the distribution if the agreement covers the range in which interest is centered. Curves *B* and *C* in Fig. 2 are hypothetical examples of two distributions which follow the Gaussian law over only a portion of the total range. Curve *B* represents the common case where the distribution has finite limits, while Curve *C* represents the case where the distribution not only has finite limits but also is not symmetrical with respect to the vertical line through x_m. The type of distribution represented by Curve *C* is common to size-frequency distributions such as grain size in undeveloped photographic emulsions.

The distributions represented by Curves *B* and *C* in Fig. 2 are plotted as cumulative frequency curves in Figs. 3 and 4. The variation of these distributions from Gaussian is shown very clearly when these data are plotted on arithmetic probability paper, as in Fig. 4. The curves are no longer straight lines except over a limited region, and the nature of these departures from the straight line is an indication of the properties of the distributions. This is a convenient method of showing graphically that portion of any distribution which is Gaussian. The reciprocal of the slope of the straight portion is the value of σ_{dg} (or σ_{tg}) for the Gaussian distribution represented by this section of the curve. It is clear that the value

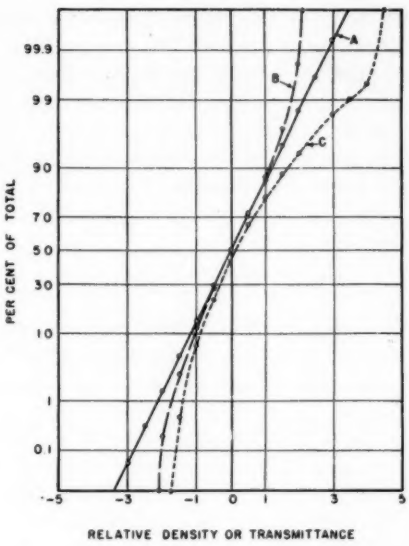

FIG. 4. Cumulative frequency functions from Fig. 3 plotted on arithmetic probability paper.

of σ_{dg} obtained in this manner can give no information as to the nature of the distribution in those regions where the fluctuations are not represented by a Gaussian distribution. While the three distributions plotted in Fig. 2 all have the same value of σ_{dg} (or σ_{tg}) as determined from the slope of the straight portion of the curves in Fig. 4, it is evident that the three values of σ_{dc} (or σ_{tc}) computed by Eq. (5) may not be equal to each other. As will be seen later it is necessary to deal with some cases where the frequency distribution of density (or transmittance) does not conform to the Gaussian law. Therefore it is essential that a clear distinction be made between sigma obtained by computing a value, which will be designated as σ_{dc}, by using Eq. (5), and the other value σ_{dg} which is the standard deviation of the density readings derived from the cumulative frequency curve obtained by mechanical integration of the density values. For a frequency distribution conforming to the Gaussian law, values of σ_{dg} and σ_{dc} are identical. When the Gaussian law is not obeyed, σ_{dg} (or σ_{tg}) characterizes uniquely only that range of densities (or transmittances) which does follow the Gaussian distribution.

III. THE RELATIONSHIP BETWEEN TRANSMITTANCE AND DENSITY FLUCTUATIONS

Goetz and Gould[2] state, "As density is related to the transparency by $D=\log 1/T$, the measurement of the *relative* transparency fluctuations, $\Delta T/T$ corresponds in good approximation to the *absolute* density fluctuations which, according to Fechner's law, is the true representation of the visual impression of the observer caused by graininess." It seems desirable to examine the accuracy of this approximation in detail.

Using the relation $D=\log_{10} 1/T$, we may write

$$D_a-D_m=\log_{10} 1/T_a-\log_{10} 1/T_m$$
$$=-\log_{10} T_a/T_m. \quad (7)$$

The symbols have the same meaning as those in Eqs. (2) and (3). Since $\Delta D=D_a-D_m$, and $\Delta T=T_a-T_m$, Eq. (7) may now be written

$$\Delta D=-\log_{10}[1+(T_a-T_m)/T_m]$$
$$=-\log_{10}(1+\Delta T/T_m). \quad (7a)$$

Equation (7a), expanded by the standard Maclaurin's series for $\log_e(1+x)$, becomes

$$\Delta D=-0.4343\left[\Delta T/T_m-(\Delta T/T_m)^2/2+\frac{(\Delta T/T_m)^3}{3}-\frac{(\Delta T/T_m)^4}{4}\cdots\right]. \quad (8)$$

It is clear from Eq. (8) that the value of the relative transmittance fluctuation, $\Delta T/T_m$, is a good approximation to that of the absolute density fluctuation, ΔD, only as long as ΔT is small compared to T_m, in which case the higher powers of $\Delta T/T_m$ can be neglected. Whether this condition is satisfied or not in making granularity measurements depends upon the scanning area used, the nature of the photographic material being examined, and the density of the deposit. While quantitative data on the accuracy of this approximation will be given in a later section, it should be noted that for the same density on different materials the values of $\Delta T/T_m$, and consequently the accuracy of the Goetz-Gould approximation, will vary even though the scanning area remains constant.

IV. THE SCOPE OF THIS INVESTIGATION

Since it is undesirable to attempt to deal in one communication with all the factors that influence the value of granularity, the treatment following is limited to a few of the more important ones. The data presented at this time pertain to the following aspects of granularity measurements:

A. The dependence of granularity upon the area, a, of the scanning aperture.

B. The dependence of the frequency distribution of transmittance and density variations upon the area, a, of the scanning aperture.

C. The relation between granularity as evaluated in terms of transmittance variations and as evaluated in terms of density variations.

D. The necessity for adjusting the technique of making granularity measurements and the method employed for the interpretation thereof, with due regard for the characteristics of the human visual mechanism and its mode of functioning, if there are to be significant correlations between the values of granularity and graininess.

The scope of this treatment is limited also to two objective methods for the evaluation of granularity, namely, those attributable to Goetz and Gould, and to Selwyn. The former was chosen as typical of those methods which evaluate granularity in terms of *transmittance* variations, while the latter is representative of those techniques which express granularity in terms of *density* variations.

The scope is limited further by making all granularity measurements with scanning apertures of fixed shape, namely, a circular area. We wish to emphasize that for the present at least we are endeavoring to establish a significant correlation between granularity and graininess. Granularity values derived from the use of a circular scanning aperture will probably yield the most direct correlation with the visual appearance of the granular structure, that is, graininess. This follows because the sensitive elements of the retina are approximately circular in cross section. Although the foveal cones are so closely packed that they tend to become hexagonal in cross section, this departure from a circular shape is probably too small to be of any appreciable importance. However, for some purposes for which granularity measurements may be made, a scanning aperture of some other shape may be desirable. Thus, if granularity measurements are to be applied in such fields as spectroscopy or the

photographic recording and reproduction of sound, it may be desirable to use a scanning aperture having the form of a long narrow slit in measuring the variations in transmittance or density.

While we have made some determinations of the dependence of granularity upon the shape of the scanning aperture, the area, a, being fixed, it seems unnecessary to present these in detail. An analysis of this situation leads so obviously to the conclusion that the value of granularity must, at least under certain conditions, depend upon the shape of the scanning aperture that experimental evidence seems unnecessary. This conclusion is justified by a consideration of the schematic diagram of a hypothetical granular structure shown in Fig. 5. The rectangular aperture or slit at A has a length ten times its width. Its area is the same as that of the circular scanning aperture represented at B. Let it be assumed that the granularity pattern is moving in the direction indicated by the arrow. It is evident that when a silver grain, or perhaps a group of grains, having a size and shape similar to that of the scanning aperture, B, moves to the right, the transmittance (measured through B) will be reduced to a very low value, thus giving rise to a large density or transmittance variation. The same grain or group of grains moving past the rectangular slit, A, will at no time decrease the transmittance to much less than 50 percent of its maximum value. Thus, when the granular structure is relatively coarse compared to the size of the scanning aperture,

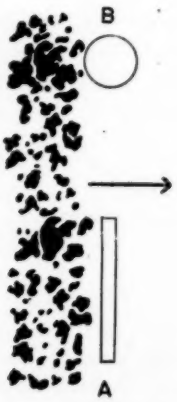

FIG. 5. Two configurations of equal area apertures compared to a hypothetical granular structure.

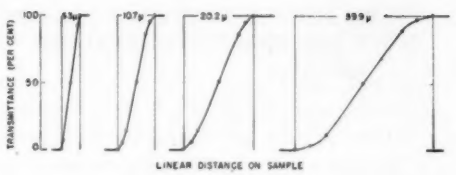

FIG. 6. Microphotometer traces of a straight edge as made with various diameter scanning apertures. The points represent theoretical computed values.

the shape factor will become of great importance in the determination of magnitude of density or transmittance variations. Our experimental results confirm this conclusion.

V. EXPERIMENTAL PROCEDURE

The recording microphotometer used in this work was described in detail in the previous paper.[1] A slight modification was made in this instrument to permit the use of a series of circular apertures (at G in Fig. 3 of the previous paper) which determine the effective size of the scanning spot on the sample being measured. The diameter of each aperture was measured with a microscope having a micrometer in the ocular, and the effective diameter when projected back on the sample by the microscope objective* was then computed using the magnification as measured with a stage micrometer. The effective diameters on the sample varied from 5.3 to 311μ. These computed values were then checked experimentally by scanning a knife edge with the microphotometer when each of these apertures was being used. The microphotometer traces made with the first four of these apertures, together with the computed curves, are shown in Fig. 6. The abscissas represent linear distance on the sample and the ordinates represent transmittance. The computed curves were obtained by calculating the value of transmittance for each position of the knife edge as it passed across the circular aperture. The calculated and experimental curves are in complete agreement.

With small scanning apertures and samples of high granularity, the effect of the lag of the recording galvanometer of the microphotometer on the record obtained can be very large. For a given speed ratio between sample and record,

* 8-mm coated objective, NA 0.50.

TABLE I. Photographic materials.

No.	Material	Abb.	Dev.	T_D
1	Kodak Aerographic Tri-X Panchromatic Film	Tri-X	D-19	8 min.
2	Kodak Aeromap Super-XX Film	Super-XX	D-19	8 min.
3	Kodak Panatomic-X Panchromatic Film	Pan-X	D-76	12 min.
4	Eastman Fine Grain Panchromatic Duplicating Negative Film	FG Neg.	D-76	6 min.

several combinations of sample and recording film speeds can be used. An experimental check was made to determine the effect of galvanometer lag by making repeated traces over the same area on a sample at the same speed ratio, but with different sample speeds. As the sample speed was decreased, the fluctuations increased in amplitude and frequency until a speed was reached below which all traces matched each other. Sections of two such traces are shown in Fig. 7. All microphotometer traces used to obtain data were made with a sample speed one step slower than that necessary to obtain traces which matched perfectly when superimposed on each other. The maximum deflection of the recording galvanometer was kept approximately constant for all records by means of an Ayrton shunt.

Two amplifiers, as mentioned in our previous paper, were used, one giving a response linear with respect to transmittance for obtaining the basic data concerning the magnitude of transmittance variations, and the other having a response linear with respect to density for obtaining the basic data for evaluating granularity in terms of density variations.

The microphotometer traces obtained are similar to those shown in Fig. 1. The integrator previously described[1] was then used to obtain from these traces the cumulative frequency curves similar to those shown in Fig. 3. The cumulative frequency data were then plotted on arithmetic probability paper, as shown in Fig. 4, and values of σ_{tg} and σ_{dg} were then determined as the reciprocals of the slopes of the straight-line portions of these curves.

Four photographic materials differing widely with respect to granular structure were chosen. The commercial designation of these materials is given in the second column of Table I, and in the third column are listed the abbreviations which will be used in referring to these products. In the fourth column are given the formula numbers** of the developing solutions used in making the samples, and in the last column are shown the development times. All of the exposed samples were developed in a sensitometric developing machine[4] with the solutions held at a temperature of 20°C.

VI. EXPERIMENTAL RESULTS

The Goetz-Gould Method

Goetz and Gould have defined granularity by Eq. (2). The granularities of uniformly exposed and developed photographic deposits on Super-XX, Pan-X, and FG Neg. materials were determined by the Goetz-Gould method, using a series of scanning apertures differing in diameter, ϕ, as indicated in the first column of Table II. The values of σ_{tg} derived from the cumulative frequency curves when plotted on probability paper are shown in the second column of Table II. The values of granularity, GG, are shown in the third column of Table II and in the last column is given the product, $GG \cdot a^{\frac{1}{2}}$. Each measurement was repeated at least three times. Granularity values for the larger scanning apertures could not be obtained in the case of Pan-X and FG Neg. materials because of the exceedingly small transmittance fluctuations occurring when these large apertures were used.

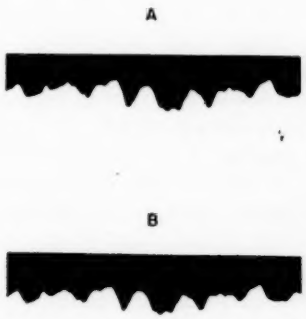

FIG. 7. Microphotometer traces made at different sample speeds: A, 0.17 mm/min.; B, 0.08 mm/min.

** The constitution of these developers may be found by consulting the published literature of the Eastman Kodak Company.

[4] L. A. Jones, M. E. Russell, and H. R. Beacham, "A developing machine for sensitometric work," J. Soc. Mot. Pict. Eng. **28**, 73 (1937).

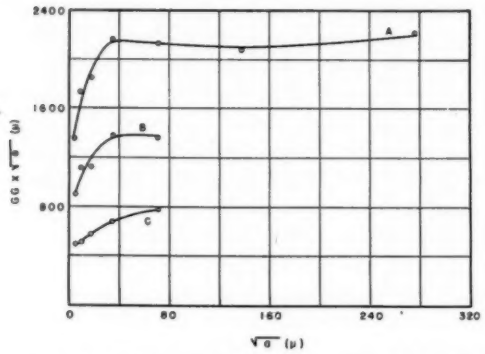

FIG. 8. The variation of $GG \cdot a^{\frac{1}{2}}$ with $a^{\frac{1}{2}}$. Sample *A*, Super-XX; *B*, Pan-X; *C*, FG Neg.

According to Goetz and Gould, the product, $GG \cdot a^{\frac{1}{2}}$, should be constant for all measurements on the same deposit with scanning apertures differing in size. In Fig. 8 the values of $GG \cdot a^{\frac{1}{2}}$ are plotted as ordinates against $a^{\frac{1}{2}}$ as abscissa. These curves are not straight lines, as predicted by theory. These data show that the relation $GG = GG_1 \cdot (a_1)^{\frac{1}{2}}/a^{\frac{1}{2}}$, as suggested by Goetz and Gould, cannot be used to compute the values of granularity that would be obtained with an aperture having an area, a, from those obtained with a different aperture of area, a_1. When the cumulative frequency data obtained by integration, from the granularity traces, are plotted on arithmetic probability paper, the curves will be straight lines if the distribution (frequency of occurrence) of the transmittance fluctuations is Gaussian. These data as obtained with the scanning apertures of various diameters are plotted on probability paper in Figs. 9–11. For those measurements made with apertures having diameters greater than 20.2μ, the curves are essentially straight lines within the limits of experimental error. The curves derived from measurements with apertures having diameters equal to or less than 20.2μ on Super-XX and Pan-X show definite curvature, indicating considerable departure from the Gaussian distribution. Likewise, in the case of FG Neg. the curves (Fig. 11) for apertures 10.7μ and less show pronounced departure from the straight-line condition. The smaller the aperture and the coarser the grain of the sample, the greater is the curvature of these lines. It should be noted that the curves are drawn only between ordinate values of 1 percent and 99 percent, and, since in all cases the fluctuations are between finite limits, every curve must depart from a straight line at its extremities.

The Selwyn Method

Selwyn has defined granularity in terms of Eq. (3). Because it seems probable that granularity based upon variations in density, rather than upon variations in transmittance, will yield more significant and useful correlations with graininess, a more detailed study has been made of the properties of granularity as defined by Selwyn. Measurements were made with the scanning apertures of various diameters, as indicated in Column 1 of Tables III and IV on ten deposits differing in density as indicated in Column 2 on the Super-XX and FG Neg. materials. Each measurement was repeated at least three times. The values of the standard deviation, σ_{dg}, are given in Column 3, and of granularity, S, in Column 4 of Tables III and IV.

Granularity, S, is plotted against the $\sqrt{a}$ in Figs. 12 and 13, the former giving the results for the FG Neg. material and the latter for Super-XX. Each curve refers to a developed silver image of the densities as indicated. These curves are not straight lines as predicted by theory. The data

TABLE II. Goetz-Gould granularity *versus* size of scanning aperture.

ϕ μ	σ_{dg}	GG	$GG \cdot (a)^{\frac{1}{2}}$
	Super-XX, $D = 0.43$		
5.3	0.203	287	1349
10.7	.129	182	1729
20.2	.073	103	1844
39.9	.043	61	2159
79.8	.021	30	2121
156.9	.011	15	2085
311.2	.006	8	2208
	Pan-X, $D = 0.40$		
5.3	0.135	191	898
10.7	.082	116	1102
20.2	.044	62	1110
39.9	.028	39	1381
79.8	.013	19	1343
	FG Neg., $D = 0.44$		
5.3	0.073	103	484
10.7	.037	53	504
20.2	.023	32	573
39.9	.013	19	673
79.8	.008	11	778

are in general qualitative agreement with the results reported by Selwyn[3] for the sizes of circular apertures which he employed (32 to 198μ in diameter).

The cumulative frequency data for measurements with the scanning apertures of different sizes on a silver deposit having a diffuse density of 0.28, on the Super-XX material, are plotted on probability paper in Fig. 14. These curves are straight lines within the limits of experimental error for apertures having diameters greater than 20.2μ and depart definitely from the straight-line condition for measurements with apertures having diameters equal to or less than 20.2μ.

The cumulative frequency data for the measurements with the 39.9μ-diameter aperture on the deposits of different density, on the FG Neg. material, are plotted on probability paper in Fig. 15. These curves are straight lines within the limits of experimental error for all samples except the one of the lowest density (0.07). As in the case of curves for transmittance fluctuations, these are only plotted between the ordinate values of 1 percent and 99 percent, and, since in every case the fluctuations are between finite limits, each curve must depart from the straight line at the extremities.

To show graphically the relation between granularity and density, and the dependency of the relationship upon the size of the scanning aperture, the data in Tables III and IV have been replotted in Fig. 16, the ordinates being granularity and the abscissas density. In the upper part of the figure the data pertaining to Super-XX are shown, and it will be noted that the shape of the granularity-density function depends markedly upon the size of the scanning aperture. The data pertaining to the FG Neg. material are shown in the lower part of the figure. While the dependence of shape on size of scanning aperture does not appear as marked, in this case it should be noted that the total change in granularity with density is much less in the case of this fine-grain material than in the case of the coarser-grain material, Super-XX. For the larger apertures, these curves all tend to show an increase in granularity with increasing density, as is predicted by theory. On the other hand, with the smaller apertures the granularity goes through a maximum and then decreases with increasing density.

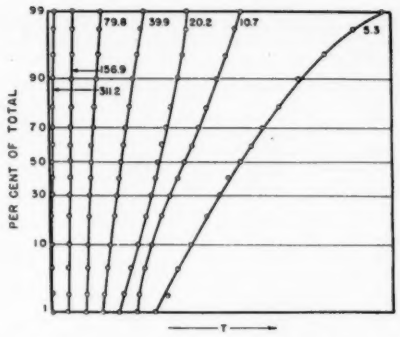

FIG. 9. Cumulative frequency curves for Super-XX obtained with various diameter (μ) scanning apertures.

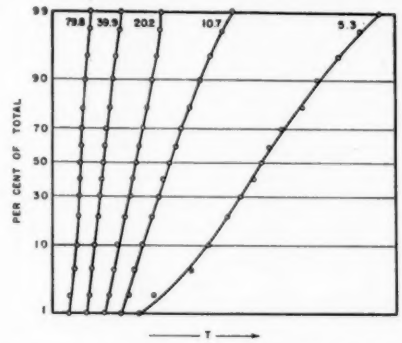

FIG. 10. Cumulative frequency curves for Pan-X obtained with scanning apertures of various diameters.

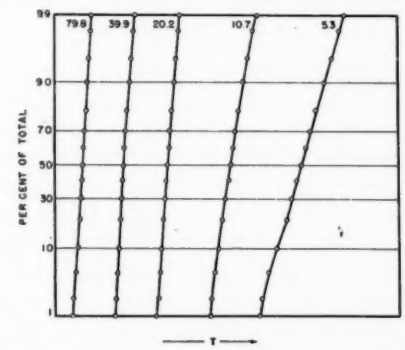

FIG. 11. Cumulative frequency curves for FG Neg. obtained with scanning apertures of various diameters.

The Distribution of Density Fluctuations

It is clear from Fig. 14 that for small scanning apertures the frequency of occurrence of

TABLE III. Selwyn granularity *versus* size of scanning aperture. Fine Grain Panchromatic Duplicating Negative Film.

ϕ μ	Density	σ_{dg}	$\sigma_{dg}\cdot(2a)^{\frac{1}{2}}$ (density microns)
5.3	0.07	0.028	0.19
5.3	0.15	.033	.22
5.3	0.23	.038	.25
10.7	0.07	.015	.20
10.7	0.15	.018	.24
10.7	0.23	.023	.31
10.7	0.44	.025	.34
10.7	0.66	.029	.39
10.7	0.79	.039	.52
10.7	1.00	.024	.32
20.2	0.07	.008	.20
20.2	0.15	.011	.28
20.2	0.23	.013	.33
20.2	0.44	.018	.46
20.2	0.66	.020	.51
20.2	0.79	.024	.61
20.2	1.00	.022	.56
20.2	1.26	.028	.71
20.2	1.44	.021	.53
20.2	1.60	.020	51
39.9	0.07	.004	.20
39.9	0.15	.006	.30
39.9	0.23	.007	.35
39.9	0.44	.009	.45
39.9	0.66	.009	.45
39.9	0.79	.009	.45
39.9	1.00	.009	.45
39.9	1.26	.012	.60
39.9	1.44	.012	.60
39.9	1.60	.013	.65

density does not correspond to the Gaussian distribution. Because of the finite size of the slit used in the automatic integrating device and because there is some unavoidable flare light present in this instrument, the toe and shoulder of the cumulative frequency curves are not determined accurately. As a result it is difficult to obtain from the machine-integrated data very reliable curve shapes at the extremities of the cumulative frequency curves. These regions are not of great importance in determining granularity by the Selwyn method if the slope of the straight-line part of the cumulative frequency curve, on probability paper, is to be taken as a measure of the standard deviation of density variations. However, these portions of the ogive are very important in determining the exact shape of the density-frequency distribution curve. Moreover, the range of densities which can be measured by automatic integration is limited to those densities for which the response of the microphotometer is linear with respect to density.

To obtain additional information on the frequency of occurrence of density values for scanning apertures differing in size, a series of measurements was made on a developed silver image on Tri-X Aero Film having a diffuse density of 0.42. A series of six scanning apertures having diameters varying from 5.3μ to 156.9μ was used.

The following procedure was used in making and evaluating the microphotometer traces in order to reduce the experimental errors to a minimum. The microphotometer was calibrated in terms of specular density before and after each trace was run. The densities were then measured by placing the trace (similar to that in Fig. 1) over a piece of coordinate paper on which the calibration for that particular run had been indicated, and reading the density at intervals along the trace corresponding to the diameter of the scanning aperture. In this way any nonlinearity of the microdensitometer was eliminated and larger density fluctuations could be measured than was possible with the automatic integrator. Densities as high as 1.3 were found with the smallest aperture and were repeatable to ± 0.001 with the larger apertures. In all cases the traces were repeated at different sample speeds until those for the two slowest were alike (Fig. 7), and the trace to be analyzed was then made at the slower of these two speeds. The speed ratio was adjusted so that for any scanning aperture the distance on the trace corresponding to the diameter of the scanning aperture was approximately 5 mm.

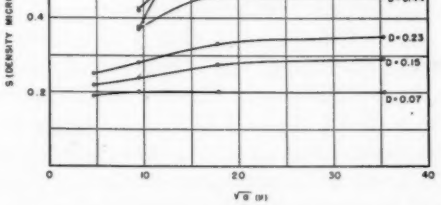

FIG. 12. Granularity, S, as a function of $a^{\frac{1}{2}}$. Each curve is for a different density on FG Neg.

Approximately 200 density readings were taken on each trace. These data were then plotted as cumulative frequency curves which are shown in Fig. 17. The ordinate gives the percentage of the total number of density values which are equal to, or less than, that indicated by the corresponding abscissa. The relative frequency of occurrence of any density value was determined by measuring the slope of the ogive at the point having that value of density as abscissa. The frequency distribution curves for the densities were then obtained by plotting these slopes as a function of density. The resultant curves are shown in Figs. 18–20. The abscissas represent density and the ordinates the relative frequency of occurrence of density values. These curves were obtained in this manner rather than by the direct computation from the density readings because the ogive, being an integral of the frequency distribution curve, reduces the scatter of points by averaging out the variations introduced by experimental errors. Since the ogive is the integral of the frequency curve, the slope of the ogive gives the frequency curve by geometrical differentiation.

The coordinate scales in Figs. 18–20 are not identical, having been adjusted so that the shape of the density-frequency curve obtained with each of the several apertures can be seen most clearly. It is obvious that the use of the smaller apertures yields frequency distribution curves which are not represented by the Gaussian distribution function since they depart widely from the symmetrical condition. For larger apertures, the curves become more symmetrical and approach the general shape of that of the Gaussian distribution. It is interesting to note that with the smallest aperture ($\phi = 5.3\mu$) 3.8 percent of the total density values are less than 0.05 and 3.1 percent are greater than 1.30. This scanning aperture was so small in comparison to the size of the largest developed grains or clumps

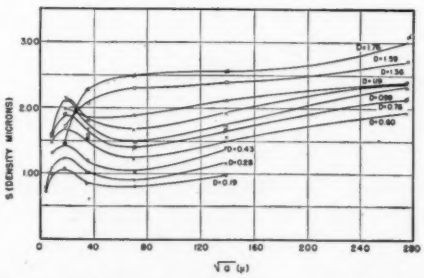

FIG. 13. Granularity, S, as a function of $a^{\frac{1}{2}}$. Each curve is for a different density on Super-XX.

TABLE IV. Selwyn granularity *versus* size of scanning aperture. Aeromap Super-XX Film.

ϕ μ	Density	σ_{dg}	$\sigma_{dg} \cdot (2a)^{\frac{1}{2}}$ (density microns)
5.3	0.19	0.111	0.73
5.3	0.28	.122	0.80
10.7	0.19	.073	0.98
10.7	0.28	.083	1.11
10.7	0.43	.104	1.40
10.7	0.60	.109	1.46
10.7	0.76	.117	1.57
10.7	0.99	.114	1.53
20.2	0.19	.041	1.04
20.2	0.28	.050	1.27
20.2	0.43	.058	1.47
20.2	0.60	.064	1.62
20.2	0.76	.075	1.90
20.2	0.99	.086	2.18
20.2	1.19	.082	2.08
20.2	1.36	.079	2.00
20.2	1.59	.068	1.72
20.2	1.76	.057	1.44
39.9	0.19	.017	0.85
39.9	0.28	.020	1.00
39.9	0.43	.022	1.10
39.9	0.60	.029	1.45
39.9	0.76	.030	1.50
39.9	0.99	.031	1.55
39.9	1.19	.036	1.80
39.9	1.36	.033	1.75
39.9	1.59	.042	2.10
39.9	1.76	.046	2.30
79.8	0.19	.008	0.80
79.8	0.28	.009	0.90
79.8	0.43	.010	1.00
79.8	0.60	.014	1.40
79.8	0.76	.014	1.40
79.8	0.99	.014	1.40
79.8	1.19	.017	1.70
79.8	1.36	.019	1.90
79.8	1.59	.023	2.30
79.8	1.76	.025	2.50
156.9	0.19	.005	0.98
156.9	0.28	.006	1.18
156.9	0.43	.008	1.57
156.9	0.60	.007	1.38
156.9	0.76	.008	1.57
156.9	0.99	.008	1.57
156.9	1.19	.012	2.36
156.9	1.36	.011	2.16
156.9	1.59	.012	2.36
156.9	1.76	.012	2.36
311.2	0.60	.005	1.96
311.2	0.99	.006	2.34
311.2	1.19	.006	2.34
311.2	1.36	.006	2.34
311.2	1.59	.007	2.73
311.2	1.76	.008	3.12

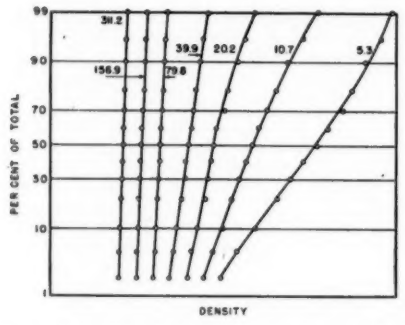

FIG. 14. Cumulative frequency curves for a single density on Super-XX obtained with scanning apertures of various diameters.

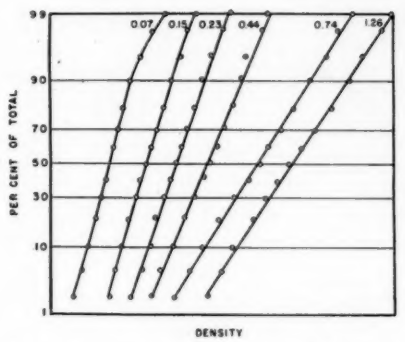

FIG. 15. Cumulative frequency curves, for different densities on FG Neg., made with a scanning aperture of 39.9μ in diameter.

of grains in this photographic material that during the scanning operation areas were encountered where the aperture was either completely covered or completely free of any silver deposit.

The cumulative frequency data shown as ogives in Fig. 17 are plotted on probability paper in Figs. 21 and 22. The resultant curves are not straight lines throughout their entire length, as required if the frequency distribution function were Gaussian. With the smallest aperture there is little, if any, of the curve that can be considered as a straight line. As the scanning aperture increases in size, the proportion of the curve which can be considered as straight increases. However, for the largest aperture ($\phi = 156.9\mu$), the straight-line portion of the curve is shorter than for the one next smaller ($\phi = 79.8\mu$). While from the strictly mathematical point of view no distribution which has finite limits can be Gaussian, the length of the straight-line portion of the cumulative frequency curves as plotted on probability paper is an indication of the range of densities which can be represented by a Gaussian distribution function. The standard deviation, σ_{dc}, was computed (Eq. 5) from the individual density readings and σ_{dg} was read from the slope of the curves in Figs. 21 and 22. The value for the smallest aperture was calculated by disregarding the 3.1 percent of the deviation larger than 1.3 in density. These values, together with those of $\sigma_{dc} \cdot (2a)^{\frac{1}{2}}$, are given in Table V. The values of standard deviation, σ_{dg}, as obtained from the slopes of the cumulative frequency curves (in Figs. 21 and 22) are in good agreement with the calculated values, σ_{dc}, for those curves which have long straight-line portions (for diameters of 20.2, 39.9, and 79.8μ); that is, the agreement is good when the frequency of occurrence of the density fluctuations is nearly Gaussian. However, for the two smaller apertures (having diameters of 5.3 and 10.7μ) and for the largest aperture (having a diameter of 156.9μ), the values of standard deviation obtained by the graphic method are larger than the calculated values.

The value of $\sigma_{dc} \cdot (2a)^{\frac{1}{2}}$ is plotted against the $a^{\frac{1}{2}}$ in Fig. 23. As in the case of the previous measurements shown graphically in Figs. 12 and 13, this curve is not a straight line, as demanded by theory. Except for the smallest aperture, this product increases with increase in the size of the scanning area. While for the smallest aperture used the value of this product is greater than that for the next larger scanning spot, its value is really an indeterminate because the 3.1 percent of the fluctuations which were too large to read have been neglected. However, if all of the higher densities (greater than 1.3) could have been measured and had been included in the computation, σ_{dc} would have been even higher than that given in the table. This indicates that under some conditions at least $\sigma_{dc} \cdot (2a)^{\frac{1}{2}}$ may increase for small scanning apertures.

Comparison of Granularity Measurements in Terms of Transmittance and Density Fluctuations

In a previous section it was pointed out that relative transmittance fluctuations, $\Delta T/T_m$, are

an approximation to density fluctuations, ΔD (Eq. (8)), and that the accuracy of this approximation depends upon the higher powers of $\Delta T/T_m$ being so small that they can be neglected. As an experimental check on this approximation, repeated granularity measurements in terms of transmittance, *GG*, and density, *S*, were made on different areas of the same sample of Super-XX Aero Film. This sample, which had a density of 0.43, was 3.5 cm long and 1 cm wide. Using a scanning aperture 39.9μ in diameter, microphotometer records were made on a transmittance basis by scanning across the sample at each end, in the middle, and from end to end. Using the same optical system and aperture, similar records were made on a density basis. While these two sets of measurements were made on the same sample and over the same general areas, they were not made over the same identical areas. These records were then cut into sections representing the measurements over a length on the sample equivalent to at least 35 times the diameter of the scanning circle. Each section was integrated to obtain the value of the standard deviation of relative transmittance or density. These values, together with the values of granularity, *GG* and *S*, are given in Table VI. The variations in the values of granularity as obtained by each of these two methods over different areas on the same sample are many times larger than the instrumental errors and must represent real differences in granular structure among the several small areas, each 39.9μ wide by (35×39.9)μ long, to which the individual values of granularity in Table VI apply. These may be termed sampling variations.

The product of the mean value of σ_{tg} and $\log_{10} e$ (0.4343) which, according to Eq. (8), should be an approximation to σ_{dg} is 0.019±0.002, while the value of σ_{dg} is 0.022±0.002. These values are equal within the limits of the probable error which is approximately 10 percent. Thus, with a scanning spot having a diameter of 39.9μ and the sample (Super-XX Aero, $D=0.43$) used in obtaining the data shown in Table VI, it is evident that ΔD is equal to $0.4343\cdot(\Delta T/T_m)$, within the limits of the probable error. Hence, for this particular set of conditions, all but the first term in the second member of Eq. (8) may be neglected. That this is not true for other conditions is shown by the curve in Fig. 24. Curve *A* shows the relationship between the Selwyn granularity, *S* (which is based upon σ_{dg}), and the size of the scanning aperture. Curve *B* shows the same relationship for the Goetz-Gould granularity, *GG* (which is based upon σ_{tg}). These curves are for the sample of Super-XX having a density of 0.43. Since the data in Table VI indicate that ΔD is equal to $0.4343\cdot(\Delta T/T_m)$ when a scanning aperture having a diameter of 39.9μ is used, the two curves in Fig. 24 are drawn to coincide at that value of scanning aperture. These curves are in fair agreement, within the limits of the probable error, when scanning apertures equal to or greater than 39.9μ in diameter are used. However, for smaller diameters of scanning apertures, the values of *GG* are definitely lower than those of *S*. It also appears that for the

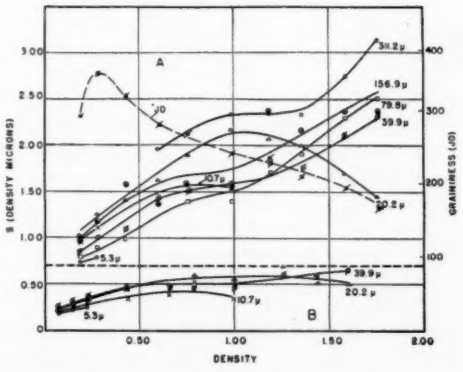

FIG. 16. Variation of granularity, *S*, with density as measured with scanning apertures of various diameters. The curves in part *A* are for Super-XX and those in part *B* for FG Neg.

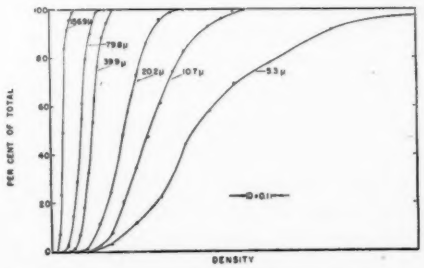

FIG. 17. Cumulative frequency curves for a density of 0.42 on Tri-X, obtained with scanning apertures of various diameters.

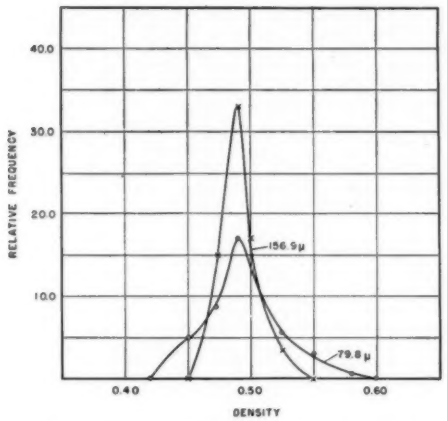

FIG. 18. Frequency distribution curves for a density of 0.42 on Tri-X, obtained with circular scanning apertures of various diameters.

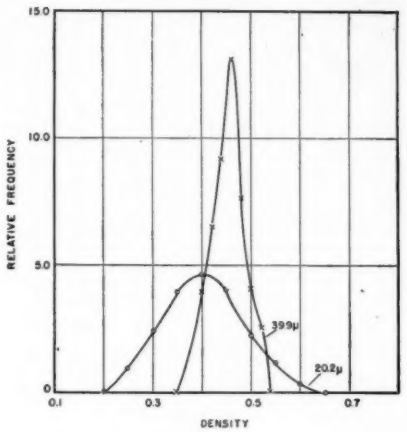

FIG. 19. Frequency distribution curves for a density of 0.42 on Tri-X, obtained with scanning apertures of various diameters.

largest apertures the values in terms of σ_{tg} tend to be smaller than those expressed in terms of σ_{dg}.

As an additional check, the values of the individual density fluctuations on the sample of Tri-X obtained, as described in the previous section, were reduced to transmittance and the value of σ_{te} was computed. For measurements made with the scanning aperture having a diameter of 39.9μ, a value of 0.39 was obtained for both σ_{dc} and $0.4343 \cdot \sigma_{te}$. However, for the measurements made with the scanning aperture having a diameter of 5.3, $\sigma_{dc}=0.313$, while $0.4343 \cdot \sigma_{te}=0.238$. This result is in agreement with the results shown graphically in Fig. 24. It must be concluded therefore that only under certain restricted conditions with respect to the characteristics of the photographic deposit and size of scanning aperture is it safe to assume that ΔD is equal to $0.4343 \cdot \Delta T/T_m$. The magnitude of the difference may be sufficiently great to impair seriously the usefulness of such an assumption.

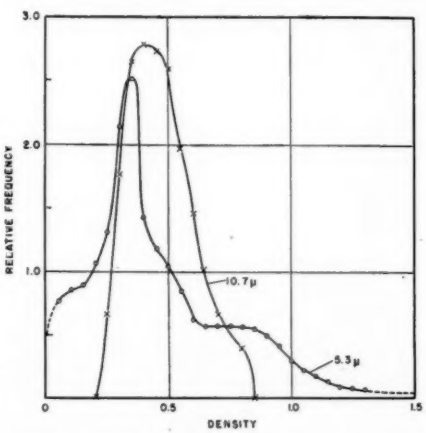

FIG. 20. Frequency distribution curves for a density of 0.42 on Tri-X, obtained with scanning apertures of various diameters.

VII. INTERPOLATED RÉSUMÉ

Before proceeding with suggestions for changes in the instrumental or analytical techniques for obtaining granularity values which will correlate more closely with those of graininess, a summary of the experimental results obtained thus far and conclusions drawn therefrom will be given. This will serve to clarify the situation and to emphasize the necessity of making certain changes in the methods of making the objective measurements or in the analytical treatment of the basic data derived therefrom or perhaps in the modification of both.

σ_{tg} *Versus* Size of Scanning Aperture

It is apparent from the data in Table II (Column 3) that granularity as defined by Goetz and Gould decreases rapidly and continuously as the size (area a) of the scanning aperture is increased. These authors state that theoretical considerations require that the relation betwee n

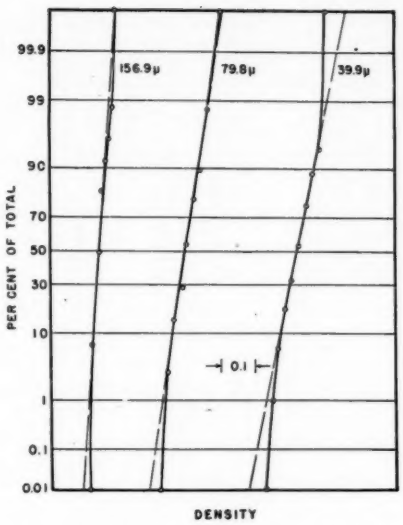

FIG. 21. Cumulative frequency curves for a density of 0.42 on Tri-X, obtained with scanning apertures of various diameters.

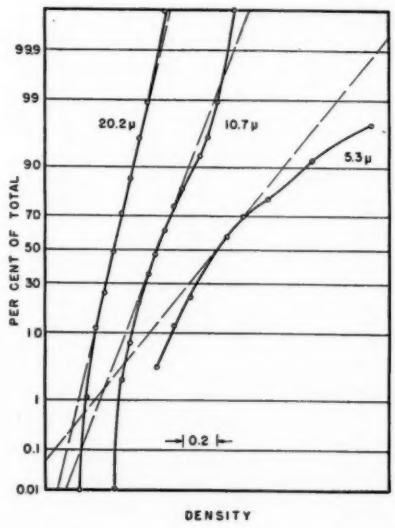

FIG. 22. Cumulative frequency curves for a density of 0.42 on Tri-X, obtained with scanning apertures of various diameters.

granularity and the area of the scanning aperture is such that the product of granularity, GG, by $a^{\frac{1}{2}}$ is constant. That this is not the case for the three photographic materials represented in Table II is shown by the values in the last column

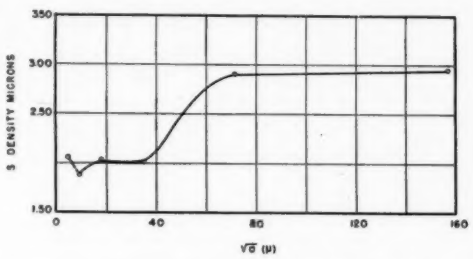

FIG. 23. The variation of granularity, S, with $\sqrt{a}$ for a density of 0.42 on Tri-X.

TABLE V. Effect on standard deviation of the non-Gaussian frequency distribution.

Scanning aperture ϕ (in μ)	Standard deviation σ_{dg}	σ_{dc}	Granularity $\sigma_{dc}\cdot(2a)^{\frac{1}{2}}$
5.3	0.313	0.304	2.08
10.7	.141	.134	1.89
20.2	.080	.081	2.03
39.9	.040	.039	2.00
79.8	.029	.028	2.90
156.9	.015	.013	2.95

and by the curves in Fig. 8. The theoretical treatment involves the assumption of a Gaussian distribution of the relative transmittance variations, $\Delta T/T_m$. The curves in Figs. 9–11 show definite departures from the Gaussian distribution, hence the constancy of $GG\cdot a^{\frac{1}{2}}$ cannot be expected to persist and is no longer a necessary condition.

As noted previously, the values of σ_{tg} (Column 2, Table II) decrease rapidly as ϕ increases. For diameters greater than 79.8μ using Pan-X and FG Neg., they are so small as to be of doubtful significance, the probable error being of the same order as the values themselves. Since granularity as defined by Goetz and Gould is evaluated in terms of the variations in relative transmittances, one would expect to obtain curves of the shape shown in Fig. 8. As the scanning aperture becomes smaller, the transmittance variations must become correspondingly larger if the product of σ_{tg} and $a^{\frac{1}{2}}$ is to remain constant. Since the maximum possible transmittance fluctuation is limited by the fact that the minimum and maximum transmittance cannot be less than 0 nor greater than 100 percent, it follows that the product, $\sigma_{tg}\cdot a^{\frac{1}{2}}$ must decrease when the size of the scanning aperture is made sufficiently small.

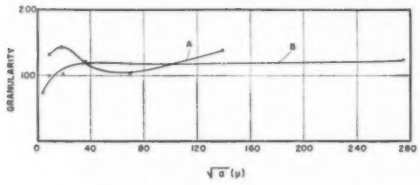

FIG. 24. Variation of Selwyn granularity (Curve *A*) and Goetz-Gould granularity (Curve *B*) with the diameter of the scanning aperture for the same sample of Super-XX (density = 0.42).

$\sigma_{dg} \cdot (2a)^{\frac{1}{2}}$ *Versus* Size of Scanning Aperture

In the case of the granularity values obtained by Selwyn's method, $S = \sigma_{dg} \cdot (2a)^{\frac{1}{2}}$, the data in the last column of Table III and the curves in Figs. 12 and 13 show definitely that S (for a particular sample) is not independent of the size ($a^{\frac{1}{2}}$ or ϕ^*) of the scanning aperture. However, our results agree at least qualitatively with those reported by Selwyn within the range of scanning aperture sizes used by him ($\phi = 32\mu$ to $\phi = 198\mu$). He has, in fact, reported some departures from the constancy of S within this region. The most pronounced departures from constancy of S for scanning apertures of various sizes (as required by the assumption of Gaussian distribution of density values) occur when scanning apertures are used which yield cumulative frequency functions which (when plotted on probability paper) are not straight lines (see Fig. 14).

The causes which determine the shapes of the curves shown in Figs. 12 and 13 are not entirely clear. It should be noted, however, that density may rise to very high values when small scanning apertures are used. For instance, we have measured the densities of individual developed silver grains of at least 3.0. Hence, $\sigma_{dg} \cdot (2a)^{\frac{1}{2}}$ could remain constant down to very small scanning apertures. On the other hand, the data in Fig. 23 show a definite drop in granularity, $\sigma_{dg} \cdot (2a)^{\frac{1}{2}}$, with decreasing scanning areas and then a sudden rise when the aperture becomes so small that the density values approach those of the silver grains themselves. These data indicate that flare is not reducing the values of the density fluctuations appreciably, at least within the range of densities to which the curves in Figs. 12 and 13 apply.

* For scanning apertures which are circular in shape, ϕ is directly proportional to $a^{\frac{1}{2}}$. Hence, $S = f(a^{\frac{1}{2}})$ must have the same shape as $S = f(\phi)$. $a^{\frac{1}{2}} = 0.886\phi$.

In making measurements with small scanning apertures, the most obvious source of error would seem to be that introduced by flare light in the optical system. To reduce the flare light to a minimum the glass-air surfaces of the microscope objective were treated with low reflectance coatings and the auxiliary aperture in the condenser system was adjusted at all times so that only the necessary area on the sample was illuminated. An experimental indication that flare light has been reduced to a minimum is given by Fig. 6, since the presence of any appreciable flare light would tend to produce a difference between the experimental and computed curves. For the particular photographic materials investigated, the distribution of density as measured with small scanning apertures is not Gaussian, and granularity as measured with small apertures is not independent of the scanning area. However, it should be noted that even though the materials studied cover a wide range of coarseness of the granular structure, the exact curve shapes, as shown for these materials, are not necessarily representative of those that would be obtained with other materials.

The Dependence of $\sigma_{dg} \cdot (2a)^{\frac{1}{2}} = f(D)$ upon Size of Scanning Aperture

In Fig. 16 the granularity-*versus*-density curves for Super-XX are plotted for the series of scanning aperture sizes which we have used. Curve *JD* shows the relation between graininess and density for the same photographic material. It will be seen that the granularity values obtained for scanning spots having diameters of 39.9μ and greater increase almost continuously, and at a relatively constant rate, with increasing density. The curve obtained with the 20.2μ scanning aperture increases to a maximum at a density slightly greater than 1.0 and then decreases continuously throughout the density range studied. The curve for the 10.7μ scanning spot rises to a maximum at a density of about 0.80 and then decreases slightly at a density of 1 which, unfortunately, is the highest density on which a satisfactory reading can be obtained with our present equipment. It seems probable that granularity values will continue to decrease for densities greater than 1. Using a 5.3μ scanning

spot, we were unable to obtain (by mechanical integration) satisfactory readings for densities above 0.28. There is a slight increase in granularity from a density of 0.19 up to 0.28, but the increase is small and it is improbable that the shape of the granularity-density curve for this aperture would resemble at all closely the shape of the graininess-density curve.

This evidence indicates that, for scanning apertures of 20μ and less, the shape of the granularity-density function begins to resemble somewhat that of the graininess-density curve. We are forced to conclude, however, that even if the size of the scanning spot is decreased to a very small value the shape of this granularity-density function will not match that of the graininess-density relationship.

Density-Frequency Distribution, σ_{dc} *Versus a*

The curves in Fig. 14 show that for the smaller scanning apertures the density-frequency functions are not Gaussian in form. It seems desirable, therefore, to abandon this assumption and the attempt to characterize completely the form of the density-frequency function by σ_{dg}.

There still remains the possibility that some different method of interpreting the measurements made by this technique would yield the desired relationship between granularity and density. One such possibility is suggested by the data represented by the curves in Figs. 18–20. These show clearly that the frequency of occurrence of density values departs markedly from a Gaussian distribution when scanning spots having diameters less than 40μ are used. The values of σ_{dg} used in plotting Fig. 16 are based on the assumption of a Gaussian distribution and are determined by measuring the slope of the straight-line portion of the cumulative frequency curves as shown in Figs. 14 and 15. A value of σ_{dg} determined in this way does not constitute a significant characteristic of the whole frequency distribution when the Gaussian relationship is not fulfilled. We can, however, by using all of the density determinations compute values of σ_{dc} for each of these distribution functions by formula (5). This has been done for the curves in Figs. 18–20, and the results obtained, shown in Table IV, are compared with those derived from the graphic method. While there are differences, especially for the small scanning spots, these differences are relatively small and it does not appear likely that the use of the computed values, σ_{dc}, will materially change the shape of the granularity-density function. Under these circumstances it hardly seems worth while to follow this lead further.

We consider that a completely satisfactory solution of this problem demands that the granularity-density function derived from objective measurements shall be identical in shape to that of the graininess function. The word "derived" used in the preceding sentence includes not only the technique of making the physical measurements, but also the interpretative methods applied to the data. The "interpretative" process may include, in addition to various mathematical operations, the application of a predetermined psychophysical function or relationship. This must be the same for different photographic materials and possibly may be of the general type (a luminance or acuity discrimination function) used by Goetz and Gould in an attempt to convert their objective measurements into "visual graininess" values.

We wish to reiterate that at the present time we are concerned only with the evaluation of the granularity and graininess of these photographic deposits *per se*, and while we recognize the desirability, and, in fact, the necessity of obtaining granularity measurements which can be

TABLE VI. Comparison of granularity measurements in terms of transmittance and density fluctuations. Super-XX, $D=0.43$, $\phi=39.9\mu$.

	Standard deviation σ_{tg}	Standard deviation σ_{dg}	Granularity *GG*	Granularity *S*
	0.041	0.018	57	0.90
	.044	.022	62	1.10
	.049	.022	69	1.10
	.044	.020	62	1.00
	.036	.022	51	1.10
	.044	.022	62	1.10
	.051	.025	72	1.25
	.044	.022	62	1.10
	.039	.023	55	1.15
	.051	.022	72	1.10
	.039	.018	55	0.90
	.037	.022	53	1.10
	.044	.025	62	1.25
	.042	.020	60	1.00
	.036	.023	51	1.15
	.044	.023	62	1.15
	.046		65	
Mean	0.043±0.005	0.022±0.002	61	1.10

used eventually in the prediction of the graininess of positives made from negatives, this problem is not being considered by us in this communication.

As pointed out in our previous paper, a method of evaluating granularity may fail to give the completely satisfactory solution just defined, but may still be of considerable value, at least from a pragmatic point of view, provided it yields numbers which place various photographic materials in the same proportional order relative to each other as their graininess values. In the communication referred to, it was shown that none of the objective methods examined meet this latter criterion or merit. We have not examined as yet a large group of photographic materials by using the variable size of scanning spot, hence we are not in a position to say that the use of a scanning spot smaller than that which was used in obtaining the data published in our previous communication, together with σ_{dg} or σ_{dc}, will or will not result in the proportional placing, relative to their graininess values, of a group of photographic materials differing widely in granular structure.

VIII. ALTERNATIVE METHODS OF ANALYZING THE BASIC DATA

The appearance of a granular structure is then conditioned largely by the luminance* differences which exist between the various elements of the visual field. From this point of view, therefore, it is likely that the data contained in the density-frequency curves in Figs. 18–20 are not presented in their most significant form. The frequency of occurrence of density differences, ΔD, can be derived directly from these curves, and if plotted in the conventional manner, the negative and positive ΔD's appear on the opposite sides of the arithmetic mean. As far as the visual mechanism is concerned, there seems to be no necessity for distinguishing between positive and negative values of ΔD since both are equally effective in contributing to the appearance of brightness inhomogeneity within the visual field. It may be of value, therefore, to replot these data in such a way as to show the frequency of occurrence of ΔD, disregarding the positive and negative signs. The curve in Fig. 25 illustrates the form which such a frequency relationship assumes. This is for the scanning aperture having a diameter of 10.7μ. As shown by this curve, there are a large number of ΔD's having values less than 0.20 but there are an appreciable number of ΔD's having values between 0.20 and 0.37. It is possible that the final judgment of blending distance may be determined to a considerable extent by the occurrence of a relatively few large ΔD's. Hence, a profitable course to follow may be an attempt to determine the magnitude of the role which these relatively few large ΔD's play in the determination of graininess. Thinking in terms of the visual appearance of these granular deposits it begins to seem improbable that any average of all of the ΔD's, such as an arithmetic mean or a root mean square average, σ_{dc}, can be a significant criterion of the lack of homogeneity in the appearance of the visual field.

We cannot at this time follow this lead very far simply because we have been unable, with our present equipment, to accumulate a sufficiently large volume of experimental data similar to that shown in Figs. 18–20 on various types of materials to serve effectively for the establishment of useful relationships. Moreover, there are some considerations that cannot be discussed profitably at this time which raise doubts as to the utility, for the purpose of evaluating graininess, of the ΔD evaluated by the technique used in obtaining those data from which Figs. 18–20 and 25 are

* In this paper, and more particularly in subsequent members of the series which we propose to publish under the general title, "Photographic Granularity and Graininess," it will frequently be necessary to distinguish clearly between the physical, psychophysical, and psychological aspects of visual phenomena. For this purpose we shall follow the recommendations of the Colorimetry Committee of the Optical Society of America ["The concept of color," J. Opt. Soc. Am. **33**, 552 (1943); "The pyschophysics of color," J. Opt. Soc. Am. **34**, 246 (1944)]. The new terms of greatest importance for our purposes are:

(1) *Luminance.* This replaces the current term *brightness.* It is denoted by the symbol, B, and its numerical magnitude will be expressed in terms of foot-lamberts, ft.-l.

(2) *Illuminance.* This replaces the current term *illumination* which is reserved as a designation of the process involved. Values of illuminance will be given in terms of the unit, foot-candle, ft.-c.

(3) *Brightness.* This term, having been released from its present usage by the adoption of luminance as noted above, will be used as the name of one of the three attributes of visual sensation, *brightness, hue,* and *saturation.* Brightness is that attribute of visual sensation which correlates most closely with the intensity or quantity aspect of the physical stimulus, that is, radiant energy. The reader who is not familiar with the systematic nomenclature proposed by the Colorimetry Committee of the Optical Society is urged to consult the references given in order to familiarize himself with these terms and symbols and with the units in which they may be expressed.

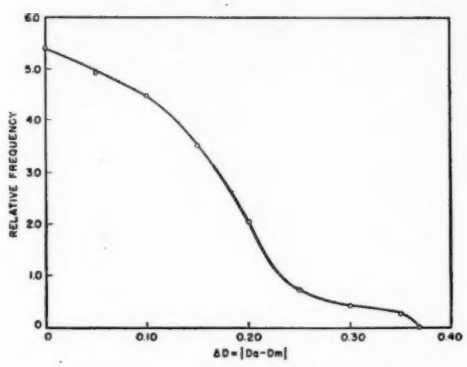

FIG. 25. Frequency of occurrence of density differences as measured with a 10.7-μ-diameter scanning aperture on a sample of Tri-X having a density of 0.42

plotted. We admit quite frankly that we have not yet explored fully the potentialities of the ΔD-frequency curves shown in Fig. 25. Equipment is being constructed which will make it possible to obtain rapidly a large volume of data of this type. When this is available we propose to make a careful appraisal of these ΔD-frequency distributions.

IX. SOME SIGNIFICANT VISUAL ASPECTS

We are now faced with the possible necessity of modifying the technique of making the objective measurements. In choosing a different method, a careful analysis of the characteristics of the human visual mechanism and its mode of functioning should enhance the possibility of making a choice which will lead to fruitful results.

A great amount of work has been done during the past few decades in an effort to determine with relatively high precision the various characteristics of the human visual system. These characteristics include the dioptrical dimensions of the eye, retinal structure, neural responses, and various visual sensitivities, such as visual acuity, luminance discrimination, etc. A lengthy discussion of these factors does not seem to be appropriate at this time. We propose to publish soon a detailed discussion of some of these visual characteristics, especially of those which bear most directly on the problem of evaluating the graininess of developed silver images. We do, however, wish to draw attention to a few facts which we believe are of importance in deciding upon the future course to be followed in seeking more significant relations between granularity and graininess

The perception of graininess in a visual field is dependent on the existence of suprathreshold differences in luminance between small elements of the visual field. The angular subtenses of these small visual field elements must also be somewhat above that visual acuity threshold which is valid for the existing conditions. Since the visual sensory response to an objective stimulus is proportional to the logarithm of the stimulus intensity, log I,** the direct objective correlate of a difference in luminance, ΔB, is a difference between the logarithms of two stimulus intensities, $\Delta \log I$. When the stimulus is provided by a granular deposit of developed silver, the difference in the log of the stimulus intensity, $\Delta \log I$, is provided by a density difference, ΔD. It seems safe to assume, therefore, that the measurement of density, D, or of density difference, ΔD, should provide the most direct and most significant data for the evaluation of

** This logarithmic relation is valid only for a limited range of stimulus intensities. The stimulus intensities met with in viewing the granular structures and in the making of graininess measurements generally fall within the range over which the logarithmic relationship is approximately valid. The logarithmic relation between visual stimulus and visual sensory response is generally designated as the *Weber-Fechner law*. Since its enunciation almost a century ago, controversy has raged as to its validity. By its most violent critics it has been ruthlessly condemned as a snare and a delusion. We agree that the usage of the word "law" in this connection is inappropriate and that the term *psychophysical relationship* would be more suitable. The particular psychophysical relationship commonly called the Weber-Fechner law is actually a representation of the sensitivity of the human visual mechanism to luminance differences. In common with all such psychophysical relationships, it is valid only under those boundary conditions used in its determination. As pointed out in the report of the Colorimetry Committee previously referred to, "for all practical purposes psychophysical relationships are definitions in physical terms of concepts derived from the objective aspects of the response of the human organism to physical stimuli."

The literature of this subject has been well summarized by Hecht ["A theory of visual intensity discrimination," J. Gen. Physiol. **18**, 767 (1934–35)]. The evidence is conclusive that the logarithmic relationship does not hold if the entire range of luminance values, 0 to 5000 or 10,000 foot-lamberts, is considered. However, for values of luminance lying between the approximate limits 1 to 5000 or 10,000 foot-lamberts, and under certain specified conditions of adaptation, the logarithmic relationship is sufficiently valid for many practical purposes so that it has a definite usefulness and supports our conclusion that the measurement of D or ΔD is more promising for our purposes than that of T or ΔT.

graininess. In this respect we conclude that the technique used by Selwyn is to be preferred to that proposed by Goetz and Gould.

In setting up an instrumental method of measuring the D or ΔD for small elements of the granular structure, a decision must be made concerning the size of the field elements to be measured. This follows since we have shown in this communication that the magnitude and frequency of occurrence of D and ΔD are not independent of the size of the scanning aperture. A careful study of just what part of the granular structure is included by apertures of various sizes should be instructive. The number of silver grains or of grain clumps isolated by an aperture of a given size will depend on the coarseness of the granular structure and hence on the photographic material being considered.

The photomicrographs reproduced in Fig. 26 show the situation for four photographic materials differing widely in granular structure. At the top of the figure the brightness distribution within seven areas varying from 5 to 320μ in diameter is shown for the Tri-X material. The three pictures at the top (320, 160, and 80μ) were obtained by using a magnification of 150 diameters. All of the other photomicrographs in Fig. 26 were made with a magnification of 600 diameters. The diameters of the areas illustrated in the four lower rows are 5, 10, 20, 40, and 80μ, respectively, as indicated by the numbers appearing just below the five members of the second row from the top.

It should be remembered that in making granularity measurements the value of density obtained is that of the integrated density of that part of the silver image isolated by the scanning aperture. There seems to be little reason to expect that the density differences between areas of 320μ in diameter can give any significant information concerning the graininess of this material which must be determined by the brightness distribution *within* a small fraction of this area. The same is almost certainly true of the areas having diameters of 160, 80, and 40μ. The complexity and the relatively large number of surface elements in the area having a diameter of 20μ leads us to doubt that even for this small aperture the D's or the ΔD's derived from the measurements with a scanning aperture of this size will be found of very great significance in the evaluation of the graininess of this material or of those having similar granular structures. We cannot predict from the meager data now available the exact size of the scanning aperture which will yield the most useful results, but we do venture the opinion that for materials having granular structures similar to that of Tri-X it will prove to be at least not greater and probably less than 20μ in diameter.

An inspection of the photomicrographs for the Super-XX and the Pan-X materials leads us to believe that the areas of 20μ and greater all consist of configurations made up of such numerous visual field elements that the integrated D's or ΔD's of areas of these sizes cannot have much meaning with respect to graininess. It is even doubtful that the 10-μ aperture is sufficiently small for the Pan-X material.

The 5-μ aperture on the Fine Grain Negative material still contains a goodly number of visual field elements differing in brightness. It seems likely that this may be found too large to give the desired information concerning D's and ΔD's useful for the evaluation of graininess of this material.

We have already expressed the conviction that in an objective method of measuring granularity which will give results from which the graininess of the granular structure can be computed or predicted, the size of the scanning aperture must be related in some unique and relevant manner to that of the "effective scanning area" of the human eye. This necessity seems to be recognized implicitly by Selwyn[5] who speculates as to the size of the "effective scanning spot" of the eye and bases his estimation of that size upon the commonly accepted resolving power of the eye as one minute of arc.

At present we have no definite evidence as to what constitutes this effective visual scanning area. We know that the retina consists of a mosaic of closely packed rods and cones, also that at the center of the fovea there are no rods. Here the packing of the cones is so close that they tend to assume a hexagonal cross-sectional shape. Moreover, at this point the cones are smaller in diameter than in any other part of the retina. It seems likely that the judgment of the presence or

[5] See reference 3, page 523.

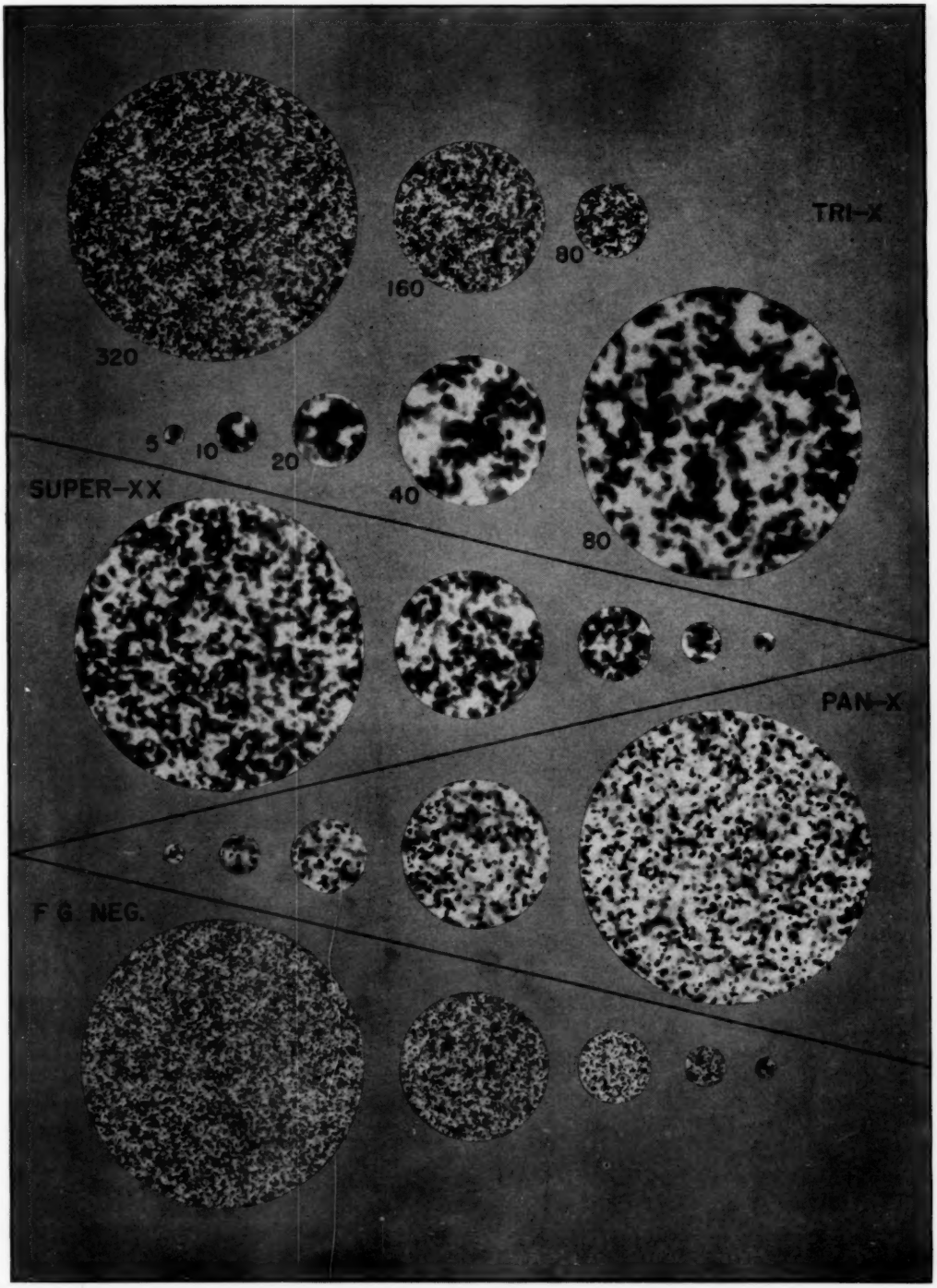

FIG. 26. Photomicrographs representing the areas covered by scanning apertures of different diameters.

absence of graininess in the visual field is dependent upon the neural responses arising from the stimulated cones in a very small area immediately around the point on the retina where it is intersected by the visual axis. This is the point at which is formed the image of a visual field element on which attention is fixed. The experimental evidence[6] indicates that at the exact center of the fovea the diameter (or more properly the distance between the centers of adjacent cones) of the cones is only about 1.0μ, the average distance between centers for a small area of approximately 30μ in diameter being about 1.5μ.

TABLE VII. Dimensional relationship between the retinal mosaic and the retinal image of a granular structure at the blending distance.

D	D_b (cm)	$\angle°$	$CD_{vf}(\mu)$	$CD_p(\mu)$
Kodak Aerographic Tri-X Panchromatic Film				
0.26	485	0.6	422	13.2
0.32	524	0.5	455	14.2
0.45	548	0.5	477	14.9
0.77	519	0.5	452	14.1
1.12	470	0.6	410	12.8
1.32	450	0.6	391	12.2
1.54	391	0.7	339	10.6
1.70	339	0.8	294	9.2
Kodak Aeromap Super-XX Film				
0.19	294	1.0	256	8.0
0.28	350	0.8	304	9.5
0.43	322	0.8	278	8.7
0.60	280	1.0	243	7.6
0.76	270	1.1	237	7.4
0.99	242	1.2	211	6.6
1.19	234	1.2	202	6.3
1.36	208	1.2	179	5.6
1.59	194	1.4	169	5.3
1.76	168	1.7	147	4.6
Kodak Panatomic-X Panchromatic Film				
0.09	174	1.6	150	4.7
0.15	188	1.4	163	5.1
0.24	186	1.4	160	5.0
0.37	178	1.6	157	4.9
0.45	174	1.6	150	4.7
0.53	168	1.7	147	4.6
0.68	166	1.7	144	4.5
0.86	162	1.7	141	4.4
Eastman Fine Grain Panchromatic Duplicating Negative Film				
0.07	106	2.6	93	2.9
0.15	122	2.3	106	3.3
0.23	120	2.3	102	3.2
0.44	118	2.3	102	3.2
0.66	116	2.4	99	3.1
0.79	114	2.4	96	3.0
1.00	108	2.5	93	2.9

[6] S. L. Polyak, *The Retina* (University of Chicago Press, Chicago, 1941).

The front focal length of the average human eye is approximately 17.2 mm. By using this value, it is possible to compute the angular subtense of a single cone and from this the diameters of that part of a granular structure which is imaged on a single cone when the structure is at the blending distance as determined in the measurement of graininess. It does not seem permissible to assume, without further evidence than we now have, that the effective scanning area is identical in size to that of a single retinal receptor. But it is at least interesting and perhaps instructive to determine the size of that part of the visual field which is covered by the image of a single cone when projected forward, by the refracting elements of the eye, onto the granular structure at the blending distance.

In the first column of Table VII will be found the density values for groups of developed silver deposits made on four photographic materials varying widely in granular structure. In the second column are shown the blending distances, D_b, determined by using the Jones-Deisch instrument, the magnification on the screen of this instrument being in all cases 32 diameters. The field luminance with no sample in position was in all cases 19 foot-lamberts. In the third column are given the values of angular subtense of the graininess field at the blending distance, and in the next column are shown the distances, CD_{vf} (in microns), between the centers of adjacent retinal receptors (foveal cones) when projected by the dioptrical elements of the eye onto the graininess field at the blending distance. Since the magnification in the graininess instrument is 32, the distance between centers of the cones referred back to the photographic deposit itself is obtained by dividing the values in Column 4 by 32. These, CD_p, are shown in the last column of the table. As is to be expected, these center distance values depend upon the density of the deposit on any given material and they depend also very profoundly upon the photographic material itself, being relatively large for those materials of coarser granular structure and smaller for the finer-grained materials.

By using the data in Table VII, it is possible to make up photomicrographs which represent the distribution of illuminance on the retina when an observer is looking at a granular pattern at the

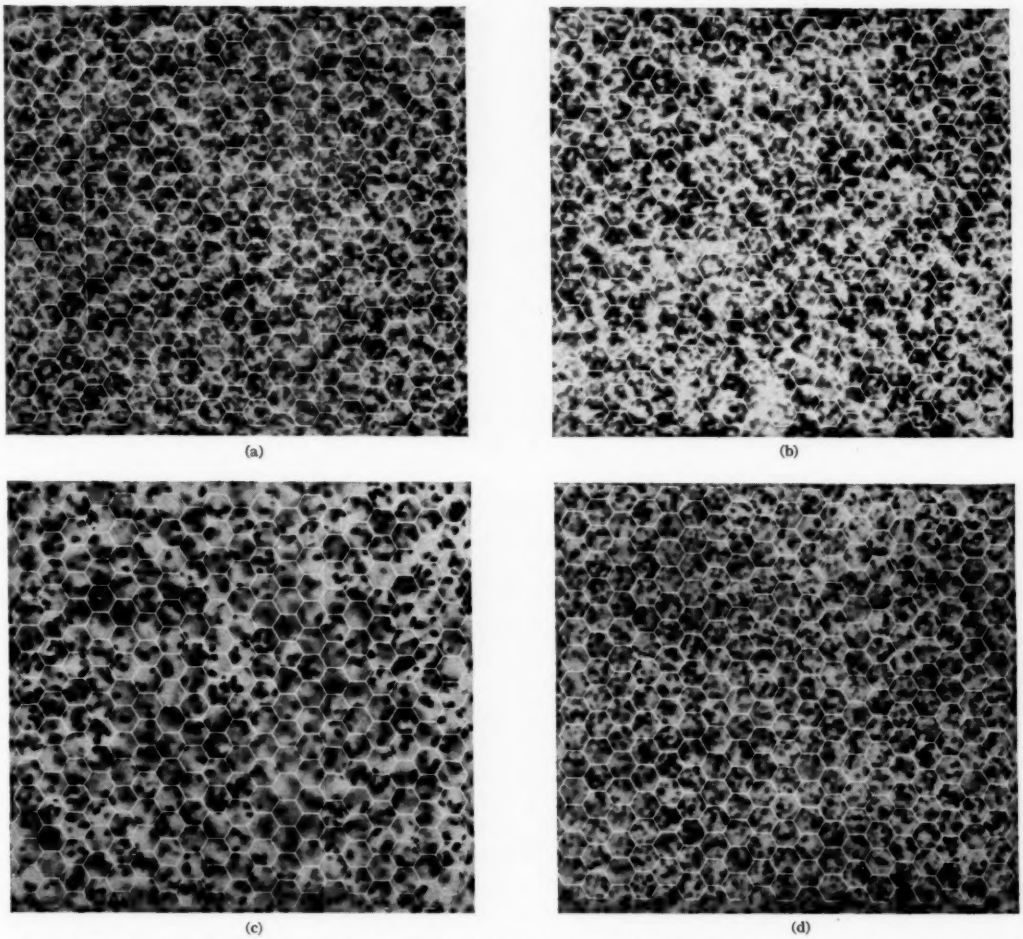

FIG. 27. Composite photomicrographs representing the distribution of illuminance on the retinal mosaic when the sample is at the blending distance. (a) Tri-X, $D=0.45$; (b) Super-XX, $D=0.43$; (c) Pan-X, $D=0.45$; (d) FG Neg., $D=0.44$.

blending distance. Four such pictures are shown in Fig. 27. The hexagonal grid of white lines represents a conventionalized retinal mosaic of closely packed hexagonal cones. The white lines represent the sheaths of neuroglial tissue separating the cones from each other. The white lines as drawn are somewhat too narrow to show the thickness of this neuroglial tissue with respect to the dimensions of the cones themselves. In the central region of the fovea this neuroglial tissue has a thickness of about 0.2μ where the average center distance between adjacent cones is approximately 1.5μ. The magnification of the grain pattern is adjusted in each case to such a value, determined by the blending distances shown in Table VII, that these photomicrographs represent the distribution of illuminance in the image of the granular structure on the retinal mosaic when the granular structure is at the blending distance.

We realize that the image-forming characteristics of the dioptrical elements of the eye may not be identical with those of the optical system used in making the photomicrographs of these granular structures. Both, however, are subject to generally similar diffraction effects, possibly to

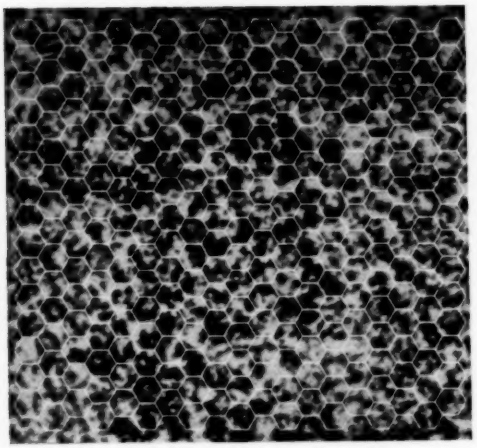

FIG. 28(a)

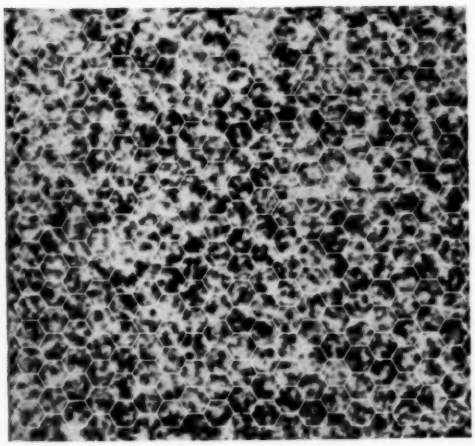

FIG. 28(b)

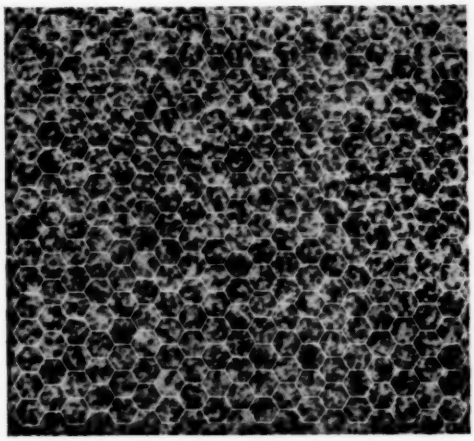

FIG. 28(c)

FIG. 28. Composite photomicrographs representing the distribution of illuminance on the retinal mosaic (Super-XX, $D=0.43$). The photomicrograph (a) is for a viewing distance 25 percent less than the blending distance; (c) is for the viewing distance 25 percent greater than the blending distance; and (b) is for a viewing distance equal to the blending distance.

some chromatic aberration and to degradation of contrast by flare light. The configuration of the luminance pattern, with respect to the number, size, and distribution of its elements within each hexagonal element, is surprisingly similar for these four photographic materials, especially when the wide variation in graininess (as evidenced by the D_b values in Table VII) and the large differences in the coarseness of the granular structure, as indicated by the photomicrographs in Fig. 26, are considered. It is particularly interesting and significant to note that the number of visual field elements within the areas representing single visual receptors is small—seldom, if ever, in excess of 8 or 10.

The change in the distribution of illuminance on the retinal mosaic when the viewing distance is made other than the blending distance can also be shown graphically in this manner. The photomicrograph (b) in Fig. 28 shows the distribution of illuminance on the retinal mosaic when the granular structure is viewed at its blending distance, D_b. The photomicrograph, Fig. 28(a), shows the character of the retinal image when the viewing distance is 25 percent less than D_b, and the Fig. 28(c) illustrates the condition when the viewing distance is 25 percent greater than D_b. It will be seen that the change in the configuration of the illuminance distribution within each hexagonal element is very noticeably changed. There are appreciably more field elements per cone in Fig. 28(c) and distinctly fewer in Fig. 28(a) than in Fig. 28(b). It has been found that an observer with normal vision, after some experience in using the graininess instrument, can perceive, on the average, changes in D_b of approximately ± 5 percent.

Admittedly the evidence presented in the last section concerning the characteristics and the

mode of functioning of the human visual mechanism has provided no quantitative information about the size of the scanning area of the retina which is effective in the judgment of graininess. A more careful analysis of the existing information concerning the visual acuity, resolving power, brightness, and contrast sensitivities, neural responses, etc., must be made. Perhaps it will be necessary to make some additional studies of these and other visual characteristics designed specifically to throw light on the visual factors involved in the judgment of graininess. In fact, it may be found that this method of approach will be futile and that we shall have to resort to a more direct and empirical method involving the making of objective measurements in a variety of ways and comparing these results with the direct psychophysical determinations of graininess. Even if this course must be followed eventually, a thorough understanding of visual processes will aid in formulating new and fruitful experimental procedures and such knowledge will at least throw some additional light on the present dimly discerned picture. In the next paper of this series a discussion of those visual characteristics and modes of functioning which seem to have the most direct bearing on the granularity-graininess problem will be given.

JOURNAL OF THE OPTICAL SOCIETY OF AMERICA VOLUME 36, NUMBER 4 APRIL, 1946

Transmittance and Reflectance of Germicidal (λ2537) Energy

MATTHEW LUCKIESH* AND A. H. TAYLOR**
Lighting Research Laboratory, General Electric Company, Nela Park, Cleveland, Ohio
(Received February 25, 1946)

BACTERIA can be destroyed by radiant energy throughout a wide range of wavelengths, provided the intensity and duration of exposure are adequate.[1] The energy of maximal effectiveness is in the spectral region of approximately λ2500 to λ2700. This is indicated in Fig. 1, for B. coli, based on the work of L. L. Holladay and the authors. It is probable that this curve approximately represents the spectral germicidal effectiveness of energy for a wide range of organisms that can be killed by ultraviolet energy. However, the dosage—product of time and intensity—differs considerably for various organisms.

For many years quartz mercury-arcs have been the most important available sources of germicidal energy. At a distance of about 2 feet from a quartz mercury-arc, consuming 300 to 400 watts, the germicidal effectiveness is many times that of midsummer noon sunlight on a clear day. The new so-called "germicidal lamps," consisting of a low pressure mercury-arc in a special ultraviolet-transmitting glass, have a germicidal efficiency 5 to 10 times that of the quartz mercury-arc. These germicidal lamps are relatively powerful sources of ultraviolet energy in the region of λ2537, which fortuitously is near the region of maximal germicidal effectiveness as seen in Fig. 1.

These new and relatively efficient sources of germicidal energy have greatly extended the practical application of ultraviolet energy. Airborne bacteria can be effectively killed,[2] as air of reasonable depths is quite transparent to energy of λ2537. However, it is desirable to control this energy effectively, which means that materials which efficiently reflect and transmit it are needed. In many cases it is equally desirable to have materials which effectively absorb this energy in order to confine it as desired, and to prevent it from reaching the eyes and skin of persons in the area.

---

* Director, Lighting Research Laboratory, General Electric Company.
** Physicist, Lighting Research Laboratory, General Electric Company.

[1] Matthew Luckiesh, "Disinfection with germicidal lamps," Elec. World, Part I—**124**, 72 (Sept. 29, 1945); Part II—**124**, 109 (Oct. 13, 1945); Part III—**124**, 90 (Oct. 27, 1945).

[2] Matthew Luckiesh and L. L. Holladay, "Tests and data on disinfection of air with germicidal lamps," Gen. Elec. Rev. **45**, 223 (April 1942).

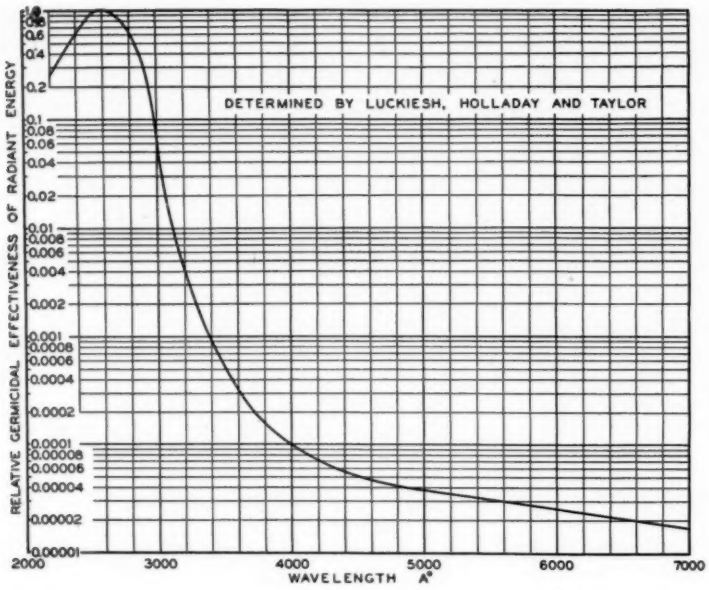

FIG. 1. Relative germicidal effectiveness of equal amounts of radiant energy of various wave-lengths as determined for B. coli.

Although air is quite transparent to energy at λ2537 for the depths met with in practice, potable waters vary greatly in their transmittance.[3,4] Inasmuch as the germicidal energy must be transmitted to a reasonable depth if it is to be a practicable agency of disinfection or sterilization, it is essential to determine the transmittance of water from various sources and of many other liquids. For liquids which have a transmittance of at least two or three percent in thicknesses of $\frac{1}{4}$ inch or more, the apparatus illustrated in Fig. 2 has proved to be quite satisfactory. The vertical cylindrical tube with a transparent quartz bottom is shown in place over a glass disk coated with zinc silicate, below which is a light-sensitive photo-tube connected to an amplifier. A small source of germicidal energy placed in the upper compartment irradiates the zinc silicate phosphor through the water cell. The spectral sensitivity of the zinc silicate to ultraviolet energy is shown in Fig. 3. The spectral distribution of energy from the lamp is such that less than one percent of the green fluorescence of the phosphor is due to energy of wave-lengths other than λ2537. A differential shutter consisting of quartz and pyrex is used to compensate further for radiant

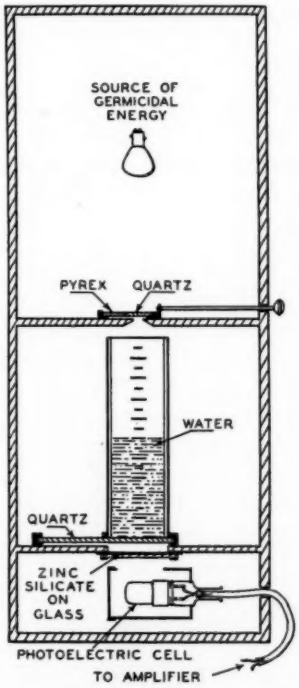

FIG. 2. Apparatus for measuring the transmission of liquids at λ2537.

[3] Matthew Luckiesh and L. L. Holladay, "Disinfecting water by means of germicidal lamps," Gen. Elec. Rev. **47**, 45 (April 1944).

[4] Matthew Luckiesh, A. H. Taylor, and G. P. Kerr, "Germicidal energy," Gen. Elec. Rev. **47**, 7 (September 1944).

energy longer than λ3000. By moving the cell to the right it is replaced by the quartz plate extension of its base to obtain a reading for zero thickness of the liquid.

Figure 4 and Table I illustrate the variation in transmittance of waters from various cities.[4] A sample of water from a cold-water spigot in each city was shipped in a glass-stoppered bottle to our laboratory for measurement. The wide variation in the transmittance of the different waters is due to minute quantities of materials suspended or dissolved in the water. They may be present in the water when it leaves the filtration plant, or they may be acquired in the process of distribution. A small amount of iron from rusty water pipes very appreciably decreases its transmittance. In fact, considerable investigation of the effect of various compounds ordinarily present in drinking waters reveals iron compounds as being generally responsible for much of the absorption of energy of λ2537.

The absorption of λ2537 energy by ordinary tap water can be greatly reduced, at least in some cases, by intense irradiation with this energy, with an ultimate absorption approximately the same as that of double-distilled water. At present we have no complete explanation for this finding. Many other factors such as heating the water to the boiling point, immersing rubber jar rings in it, filtering through ordinary filter paper, etc., greatly alter its transmittance. Its extreme sensitivity to such operations suggests some applications of measurements of transmittance in water analysis.

TABLE I. The transmission of germicidal energy (λ2537) by water from various cities of the United States. The transmission varies exponentially with the depth d of clear water. The transmission $t=(1-r)e^{-ad}$ where r is the fraction reflected at the surface and a is the absorption coefficient of the water. Since r is approximately equal to 0.02, $t=0.98e^{-ad}$.

City	Absorption coefficient a per cm	per in.	Percent transmitted by 3 in.	6 in.	12 in.	Depth in inches for 90-percent absorption
Atlanta	.0258	.0656	80	66	45	34.8
Cleveland	.0471	.120	68	48	23	19.1
Philadelphia	.0514	.131	66	45	20	17.5
Buffalo	.0546	.139	65	43	19	16.5
Detroit	.0562	.143	64	42	18	16.0
Chicago	.0611	.155	62	39	15	14.7
Pittsburgh	.0782	.199	54	30	9	11.5
LaGrange, Illinois	.0782	.199	54	30	9	11.5
New York	.0804	.204	53	29	8.5	11.2
Dallas	.0804	.204	53	29	8.5	11.2
Portland, Oregon	.0827	.210	52	28	7.9	10.9
Denver	.0896	.228	49	25	6.4	10.0
Oakland, California	.102	.258	45	21	4.4	8.85
Minneapolis	.142	.360	33	11	1.3	6.34
Kansas City	.166	.422	28	7.8	0.62	5.41
Akron, Ohio	.177	.449	26	6.6	0.45	5.09
Los Angeles	.178	.452	25	6.5	0.43	5.04
St. Louis	.184	.468	24	6.0	0.36	4.88
Boston	.184	.468	24	6.0	0.36	4.88

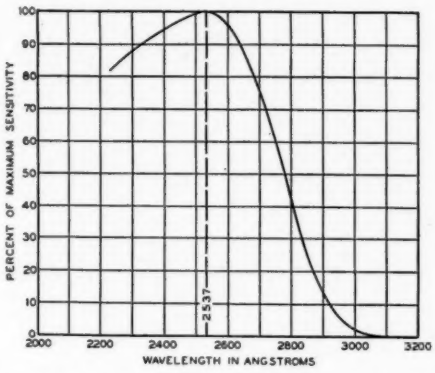

FIG. 3. Relative effectiveness of energy of different wavelengths in producing fluorescence of zinc-silicate phosphor. (Data furnished by Dr. B. T. Barnes.)

In addition to measuring many samples of water from different sources, we have measured the absorption-coefficients of many liquids such as alcohols, beers, wines, soft drinks, vinegar, milk, and many commercial solvents. With the exception of methyl alcohol and ether, they generally have high absorption-coefficients at λ2537. If the disinfection of a liquid is under consideration, a measurement of its transmittance is the first essential step. By comparing with work done on water disinfection, the practicability of disinfecting the given liquid can be appraised.

Aside from results previously reported by one of the present authors[5-7] we are unaware of any published ultraviolet reflectance data obtained by methods which completely integrate the reflected flux. We have used two types of integrating spheres, shown diagrammatically in Figs. 5 and 6. The reflectometer of Fig. 5 is used to measure[8] the reflectance of energy of λ2537. Energy from a special (RP-12) source enters the sphere through an aperture ¾ inch in

[5] A. H. Taylor, "Reflection-factors of various materials for visible and ultraviolet radiation," J. Opt. Soc. Am. **24**, 192 (1934).

[6] A. H. Taylor, "Light and ultraviolet reflection by various materials," Trans. Illum. Eng. Soc. **30**, 563 (1935).

[7] A. H. Taylor, "Ultraviolet reflectance characteristics of various materials," Illum. Eng. **36**, 927 (1941).

[8] A. H. Taylor, "Measuring germicidal energy," Gen. Elec. Rev. **47**, 53 (October 1944).

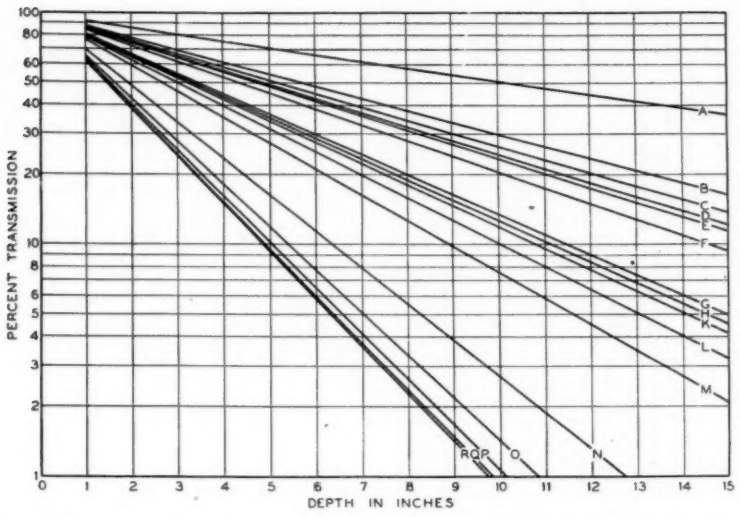

FIG. 4. The transmission-factors for germicidal (λ2537) energy for various thicknesses of water from public water systems of the following cities:

(A) Atlanta, Georgia
(B) Cleveland, Ohio
(C) Philadelphia, Pennsylvania
(D) Buffalo, New York
(E) Detroit, Michigan
(F) Chicago, Illinois
(G) Pittsburgh, Pennsylvania
LaGrange, Illinois
(H) New York, New York
Dallas, Texas
(K) Portland, Oregon
(L) Denver, Colorado
(M) Oakland, California
(N) Minneapolis, Minnesota
(O) Kansas City, Missouri
(P) Los Angeles, California
Akron, Ohio
(Q) St. Louis, Missouri
(R) Boston, Massachusetts

diameter at one side of the sphere and falls on the specimen mounted over a larger hole at the opposite side of the sphere. The inner surface of the sphere is smoked with magnesium oxide which has high reflectance throughout the ultraviolet region. An opaque shield, also coated with magnesium oxide, prevents any first-reflected flux from the specimen from reaching the photo-tube directly. Hence all the flux reflected by the specimen must be reflected once by it and once by the sphere wall before any of it reaches the photo-tube. Next the sphere is rotated 90 degrees about its vertical axis, bringing into position another $\frac{3}{4}$-inch aperture through which the flux enters the sphere and falls on the sphere wall at a point not screened from the photo-tube. The amount of energy reaching the photo-tube in the first case is less than that in the second case by the amount absorbed by the specimen under test. Thus the ratio of the photo-tube current in the first and second sphere positions gives a direct measure of the reflectance of the specimen. The differential shutter of Pyrex and quartz limits the measurement to the spectral region below λ3000. Since the source used radiates nearly all its ultraviolet energy in the region of λ2537, the reflectance value determined is for that wave-length. The photo-tube has a cadmium-magnesium alloy cathode, sensitive in that spectral region. The photo-tube surface may not properly integrate energy from all directions, hence we have substituted for it a glass plate coated with zinc silicate phosphor, like that used in Fig. 2, and use an RCA-929 photo-tube to measure its brightness due to fluorescence.

The reflectometer of Fig. 6 is used with a Bausch and Lomb No. 2800 quartz monochromator for spectral measurements throughout the ultraviolet region and up to the middle of the visible spectrum. By means of quartz lenses the arc of a Type *S*-1 lamp (a tungsten-mercury-arc) in a clear quartz bulb is focused on the test specimen through a hole in the sphere wall. The sphere is coated with smoked magnesium oxide. The quartz monochromator views a small spot on the wall on the axis of rotation. The operation, photometrically, is the same as for the sphere shown in Fig. 4, the monochromator

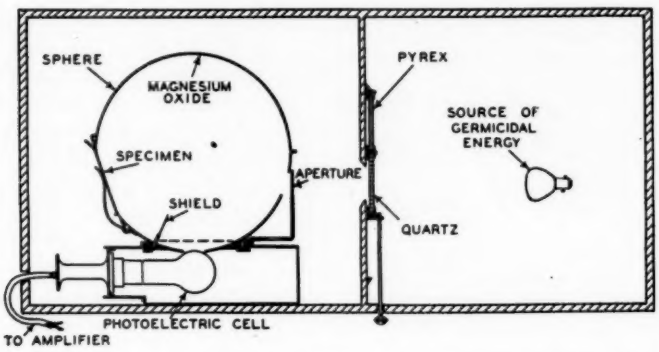

FIG. 5. Absolute reflectometer for the measurement of total reflectance of various materials at λ2537.

being substituted for the phototube. Energy measurements are made by means of a phototube and amplifier.

A great many measurements have been made with these two reflectometers, and some of the results of practical value are presented in Tables II–IV. The two reflectometers give excellent agreement for energy of λ2537.

In the construction of germicidal equipment, efficient reflecting materials are necessary. Among the metals, aluminum is outstanding. Its reflectance can be varied over a wide range by the methods of processing, hence one objective of our researches has been to find the best method of treatment to obtain and maintain high reflectance. This work is still in progress.

The "Alzak" process[9] has attained wide commercial use in the treatment of aluminum reflectors. In this process the first part of the treatment, known as "electrolytic brightening," removes impurities from the surface. The second treatment applies a thin oxide coating. This coating protects the surface from weathering effects, but reduces the initial reflectance somewhat. The reduction is greater in the ultraviolet region than in the visible spectrum. Figure 7 shows the effect of the Alzak treatment with oxide thicknesses of 0.00015 inch and 0.00022 inch for diffusely etched aluminum. These coatings are within the range used commercially. Similarly, Fig. 8 shows the results for specularly finished Alzak. The reduction of reflectance in the ultraviolet region is less with specular than with diffuse finish when the oxide coating is applied. The same is true for the visible spectrum.[9] The specimens of Figs. 7 and 8 were prepared by the Research Laboratories of the Aluminum Company of America through the courtesy of Dr. J. D. Edwards.

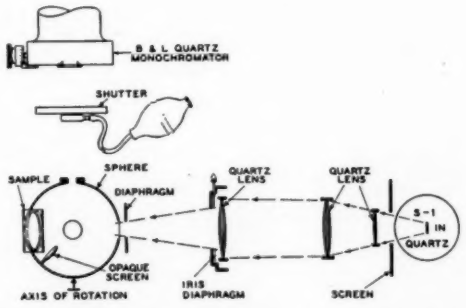

FIG. 6. Absolute reflectometer used with Bausch and Lomb No. 2800 quartz monochromator in the measurement of spectral reflectance.

[9] Junius D. Edwards, "Aluminum reflectors," Trans. Illum. Eng. Soc. **34**, 427 (1939).

It will be noted in Figs. 7 and 8 that three specimens exceed 90 percent reflectance at some spectral regions. These values appear somewhat high, but, as previously mentioned, the two reflectometers shown in Figs. 5 and 6 were in good agreement for reflectance at λ2537. As a matter of fact, however, individual specimens of treated aluminum will vary in reflectance and consequently the important fact is that aluminum is by far the best material for use as a reflecting medium for germicidal energy.

Figure 9 indicates the spectral reflectance of

TABLE II. Ultraviolet and light reflectance of some pigments, powders, etc.

Material	Percent reflectance λ2537	λ2967	λ3650	*Light
Pressed zinc oxide	2.5	2.5	4	88
Barytes	65	70	77	86
Titanium oxide	6	6	31	94
Pressed magnesium oxide	77	86	87	93–95
Smoked magnesium oxide	93	93	94	95–97
Pressed calcium carbonate	78	83	86	96

* Measured with integrating sphere reflectometer.

aluminum deposited by evaporation in a vacuum, also aluminum foil, silver, chromium, nickel, and stainless steel. The dotted part of the reflectance curve of silver is a region of partial transmission, as indicated by Fig. 10. No reflectance measurements were made in the dotted region, because of the lack of spectral lines in the source used, hence this part of the curve is estimated.

In Table III are shown some of the results of exposing aluminum paints to energy of λ2537. It will be noted that this generally increased the reflectance.

When the new germicidal sources are used in occupied areas indoors for the destruction of air-borne bacteria, they are usually installed so that they irradiate the upper air of the area and so that no germicidal energy can reach the eyes of the occupants directly from the sources or equipment. This is necessary since the germicidal energy produces erythema and conjunctivitis. If the occupants are in the area continuously for long periods of time, the ceiling and upper walls should have low reflectance for the germicidal energy to avoid conjunctivitis of the personnel.

Most paints, with the exception of water-soluble paints, are poor reflectors of energy of λ2537. Many have been tested in our laboratory and most of them have reflectance values of only 4 to 6 percent at λ2537. This probably represents surface reflection principally, as most vehicles used in paints have high absorption for this energy. Three water paints tested have reflectance values of 11, 15, and 35 percent at λ2537. White wall plaster has reflectance values of the order of 45 to 60 percent for germicidal energy. Such reflectances are probably too high for safety in interiors where germicidal lamps are used.

In Table IV reflectance data for some important materials are presented. Some other materials are included as a matter of interest.

Most of the data presented above represent only one or two specimens of each type of material, hence the values given are only indicative for those materials, but not necessarily strictly applicable to any other specimen of the same material. The authors know of no *absolute* standards of reflectance, and this includes smoked magnesium oxide. One of the authors recently found that a layer of smoked magnesium oxide approximately $\frac{1}{8}$ inch thick, deposited on clear quartz, was still not opaque to light from a tungsten-filament lamp. In order to achieve the maximum possible reflectance with *any* material, it is necessary to make the thickness such that it is opaque to the radiant energy under consideration.[10]

TABLE III. Ultraviolet and light reflectance of several aluminum paints before and after intensive irradiation with λ2537 energy.

Paint No.	Percent reflectance λ2652 Before	λ2652 After	λ2967 Before	λ2967 After	λ3650 Before	λ3650 After	Light Before	Light After
1	63	74	67	77	72	79	80	82
2	68	72	69	74	72	74	80	80
3	56	71	60	72	67	73	70	78
4	66	68	67	69	69	70	76	75
5	66	66	69	66	71	70	75	75
6	62	64	68	69	68	70	74	73
7	48	64	49	67	56	69	60	71
8	57	63	59	64	64	65	67	68
9	51	55	55	56	63	58	66	67

TABLE IV. Ultraviolet and light reflectance of miscellaneous materials.

Material	Percent reflectance at λ2537	λ2967	λ3650	Light
White wall plaster	46	65	76	90
S.W. white Decotint paint	33	41	58	79
Kalsomine white water paint	12	20	40	70
Alabastine white water paint	10	14	45	78
White porcelain enamel	4.7	5.4	63	80
Flat black Egyptian lacquer	5	5	5	5
Lantern slide glass	4	4	4	4
Photographic paper (AZO, gloss)				
Exposed, black	6	6	6	6
Unexposed, white	24	43	72	81
White back	39	47	70	82
Seven samples of wallpaper				
Ceiling papers				
Ivory	31	40	49	64
White	23	33	49	72
White	21	26	48	75
White	21	30	45	69
Side-wall papers				
Pink figured	31	40	49	64
Ivory figured	26	35	50	75
Brownish figured	18	21	33	55

[10] A. H. Taylor, "The nature and causes of small color differences in industry; lighting for their detection," J. Opt. Soc. Am. **32**, 651 (1942).

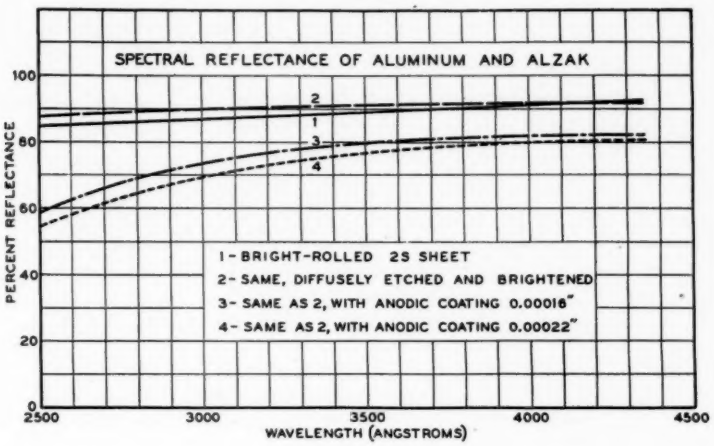
SPECTRAL REFLECTANCE OF ALUMINUM AND ALZAK
PERCENT REFLECTANCE
WAVELENGTH (ANGSTROMS)
1 - BRIGHT-ROLLED 2S SHEET
2 - SAME, DIFFUSELY ETCHED AND BRIGHTENED
3 - SAME AS 2, WITH ANODIC COATING 0.00016"
4 - SAME AS 2, WITH ANODIC COATING 0.00022"

FIG. 7. Spectral reflectance of aluminum and diffusely finished Alzak (specimens prepared by Aluminum Research Laboratories, Aluminum Company of America, New Kensington, Pennsylvania).

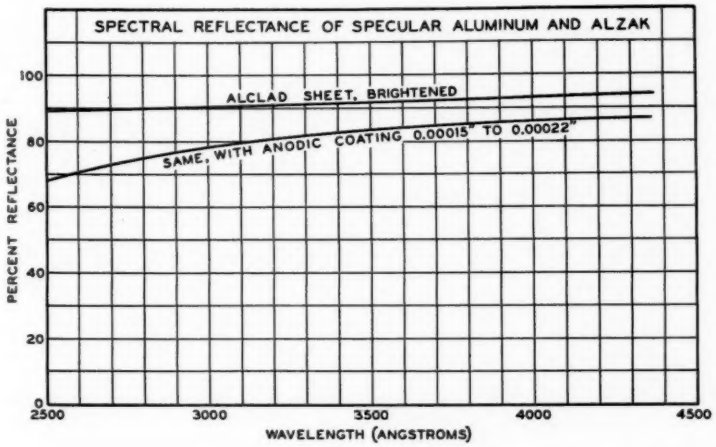
SPECTRAL REFLECTANCE OF SPECULAR ALUMINUM AND ALZAK
ALCLAD SHEET, BRIGHTENED
SAME, WITH ANODIC COATING 0.00015" TO 0.00022"
PERCENT REFLECTANCE
WAVELENGTH (ANGSTROMS)

FIG. 8. Spectral reflectance of specularly finished Alzak.

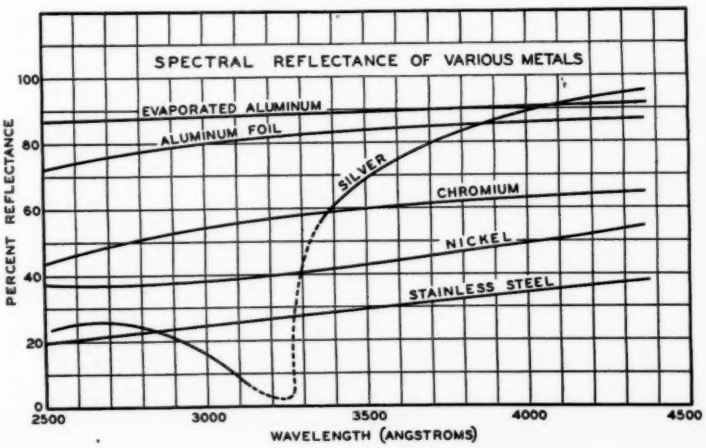

FIG. 9. Spectral reflectance of several metals. Note inferiority of chromium as compared with aluminum and Alzak.

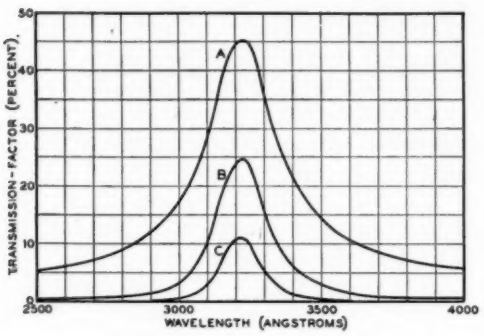

FIG. 10. Spectral transmission of three thicknesses of vaporized silver on clear quartz.

In the preparation of standard reflecting surfaces for use with the recording spectrophotometer, it is our practice to compress a high grade of magnesium oxide powder into a metal ring under high pressure, making the surface over $\frac{1}{16}$ inch below the edge of the ring, then using magnesium ribbon to smoke a layer of oxide approximately $\frac{1}{16}$ inch thick on the surface. The compressed magnesium oxide has a reflectance only a little below that of the final smoked surface, so in effect we are substantially achieving "infinite thickness."

The authors wish to express their appreciation to Mr. George P. Kerr who made most of the measurements upon which the data are based.

JOURNAL OF THE OPTICAL SOCIETY OF AMERICA VOLUME 36, NUMBER 4 APRIL, 1946

A Device to Facilitate the Reading of Spectrophotometric Curves†

GENEVIEVE REIMANN*
Textile Color Card Association of the United States, National Bureau of Standards, Washington, D. C.

AND

EARL J. CARMINE**
Davis Instrument Manufacturing Company, Baltimore, Maryland

A device which reduces eyestrain, caused by the many transverse and vertical movements of the eyes in the reading of spectrophotometric curves, is described. The spectrophotometric curve, the wave-length scale, and the reflectance scale are brought into controlled juxtaposition for reading. Means for magnifying the curve and related scales, setting the wave-length accurately and progressing quickly from point to point along the curve, are provided. The apparatus may be used with or without a wave-length correction and is applicable to either the selected or weighted ordinate method of reading. Its use is considerably less tiring than any other method tried and increases notably the speed of reading, particularly when there are several curves to a sheet.

INTRODUCTION

THE careful reading of spectrophotometric curves, such as those obtained from a spectrophotometer of the recording type, is tedious, time-consuming, and often the cause of eyestrain.

The reading for a single wave-length on a spectrophotometric curve requires a concentrated visual inspection of the point where the curve and the wave-length ordinate cross each other, the referring of this point to the reflectance scale, usually found at the left-hand side of the graph sheet, and the recording of the value. In reading the values for a single spectrophotometric curve, using the weighted-ordinate method of reading, the eye must travel in both horizontal and vertical directions and fixate on given, specific points at least 120 times; if a wave-length correction is used, this is increased to 160 times. If the 30-selected-ordinate method of reading is used, the eye must travel in both transverse and vertical directions and fixate on given, specific points from 180 to 270 times for each curve.

The smallest division on a conventional (General Electric) graph sheet from which spectrophotometric data are read is but one millimeter wide. When making a reading and applying a wave-length correction, this division is further subdivided into ten or twenty parts. This subdividing is done by visual estimate and, when the weighted-ordinate method is used, must be done at each of the forty nominal wave-lengths of the visible spectrum. If, as is often done, a transparent celluloid (in which a single hair-line is cut) and a magnifying lens are used as aids in estimating and applying the wave-length correction, the wave-length scale and the reflectance scale are usually out of the line of sight and the eyes must continually re-accommodate and re-focus, when making the readings and recording them. When there is much of this work to be done and it continues from day to day, the eyestrain is considerable and the work at best is tedious and requires undue concentration.

DESCRIPTION

A device has been developed which, to a considerable extent, overcomes the drawbacks outlined above. The instrument was designed so that most of the movements ordinarily made by the eyes in reading spectrophotometric curves would be eliminated or greatly reduced by mechanical means. This was done by bringing into controlled juxtaposition the spectrophotometric curve, the wave-length scale, and the reflectance scale.

The equipment is illustrated in Fig. 1. In this photograph a graph sheet is shown mounted in place for reading. The following essential features may be noted.

† Paper presented at the Thirtieth Annual Meeting of the Optical Society of America, New York, New York, October 18–20, 1945.

* Research associate.

** Mechanical engineer.

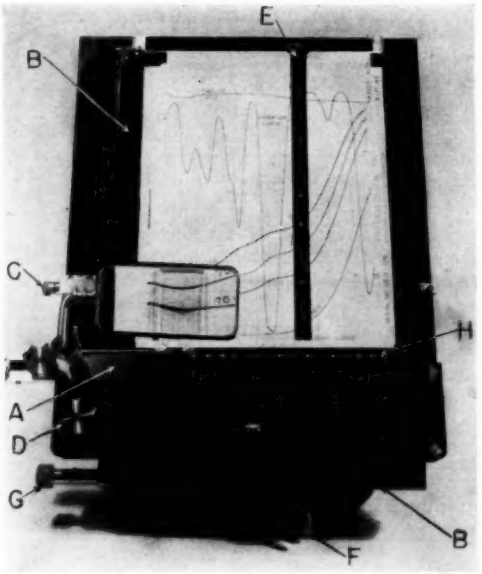

FIG. 1. Photograph of device, showing graph sheet in position for reading.

1. A mechanism *A* for horizontal motion, carrying a rectangular adjustable lens and a smaller rectangular plastic plate on which a horizontal and a vertical hair-line are ruled. This plastic plate may be seen through the lens in the photograph. It rests directly on the graph sheet. This mechanism may be moved rapidly back and forth by pressing on the standard supporting the lens, or may be moved by minute amounts by rotating the knob at the left of the standard. By this device the vertical hairline on the indicator may be moved rapidly from wave-length to wave-length and then set precisely (to 0.1 or 0.05 mμ) at the corrected wave-length. The lens can, of course, be removed if it is not desired to use it.

2. A mechanism for moving the platform *B* carrying the graph sheet, this movement being lengthwise of the sheet and at right angles to the horizontal movement of the lens and indicator. Rapid motion may be obtained by release of the knurled screw at *C*, slow motion by turning the knob at *D*. Any part of the graph sheet may thus be brought readily under the lens and indicator for reading.

3. A movable reflectance or transmittance scale *E*. This may rapidly be moved back and forth in a horizontal direction by grasping two knobs at *F*, or slowly by turning the knob *G*. This scale is not to be read from, but serves as a guide so that the eye does not have to look back and forth to the scale at the edge of the sheet. All values are read from the fine scale on the graph sheet itself.

4. A removable wave-length scale *H*. This consists of two parts. The black part on which the scale is engraved serves as a guide to the eye, making unnecessary any motion of the eyes to the wave-length scale at the bottom of the graph sheet. The scale extends from 380 to 770 mμ. The white part is used for recording the wave-length corrections, if they are to be made. When these corrections have served their purpose, they are erased. A new set of correction values may thus be written on the white part of the scale for each sheet.

The apparatus is portable. The platform carrying the graph sheet can be tilted to any angle convenient for reading and locked in place. All movements can be made with the left hand, leaving the right hand free to record data. Contemplated improvements in design include a more rapid means of lining up the paper and equipping the device with a mechanical counter.

ACKNOWLEDGMENTS

The encouragement and cooperation of members of the Photometry and Colorimetry Section of the National Bureau of Standards, particularly Dr. K. S. Gibson and Dr. D. B. Judd; of Mr. R. T. Mease, formerly of the Bureau staff; Miss Dorothy Nickerson of the Department of Agriculture; and Mr. Alfred U. Davis of the Davis Instrument Manufacturing Company, Baltimore, in the development of the curve reader, are gratefully acknowledged.

Correcting the Spherical and Chromatic Aberrations of the Eye

A. C. S. VAN HEEL
Laboratory for Technical Physics of the Technical University, Delft, Holland
(Received December 7, 1945)

THE chromatical and spherical aberrations of the eye being well established, it seemed worth while to design systems for correcting them. The influence of this correction upon vision cannot be predicted. We therefore thought it interesting to study the effect in some special cases. The practical application of one of these systems will be given.

1. Several years ago the result of the correction of the spherical aberration was published.[1] Systems have been calculated and executed, whose power for small incident heights is small and which have a spherical aberration of the same order of magnitude as that of the eye but with reverse sign. These consist of a plano-concave crown lens and a plano-convex flint lens, cemented at their plane surfaces (see Fig. 1). The glass types are:

	n_D	ν
crown	1.51284	61.4
flint	1.71917	29.3.

As a matter of course the radii are of the same order of magnitude as those occurring in the eye. The systems can be used with either the crown lens or the flint lens on the side of the incident light. The aberration alters its value when the system is used in a reverse position.

As it is required that the power for paraxial rays be very nearly zero, some difficulty arises in giving the radii the prescribed values with the necessary exactness. This can be avoided by the following procedure, which yielded rapid results. The radii are made within a reasonable approximation, while the thicknesses are made too great. After an exact measurement of the curvatures, the appropriate thicknesses for obtaining zero power for paraxial rays are calculated and the thicknesses then are adjusted by grinding the plane surfaces. The aberrations of the finished system then follow from the calculations.

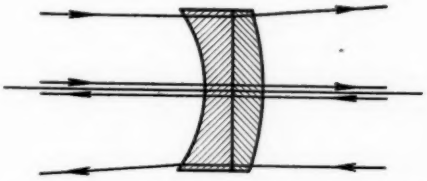

FIG. 1. Lens for correcting spherical aberration of the eye.

It must be mentioned that the systems are not corrected for color. Observations had to be made in monochromatic light, for which sodium light was chosen.

We will give now a somewhat more detailed description of one of the systems.

The diameter is 8.0 mm, the radii of the concave and convex surfaces are, respectively, 5.797 and 8.936 mm; the thickness of the concave crown lens is 0.595 mm, that of the convex flint lens 1.155 mm.

In Table I the vertex powers T in m^{-1} are given together with the corresponding exit heights h in mm of the image rays, the object point supposedly being at infinity. I relates to the position of Fig. 1 with the light coming from left, II to the same with the light coming from right.

The residual power for paraxial rays can be and indeed was annihilated by a suitable weak lens. The then remaining vertex power at an exit height of 2 mm amounts to -0.9 diopter for case I and to -1.5 dptr for case II.

With our series of systems, vertex powers for the rim rays can be realized up to $+13$ dptr for 2-mm exit height. The effect of a system can furthermore be influenced by its distance from the eye, increase of the distance of the system from the eye resulting in the diminution of the aberration.

The spherical aberrations of all eyes fall within this range. The right eye of the author, for

TABLE I.

	I			II		
h	parax.	1.65	2.21	parax.	1.81	2.17
T	−0.39	−0.94	−1.43	−0.44	−1.53	−2.08

[1] "Influencing the spherical aberration of the eye," Dioptric Rev. (London) **37**, 496 (1935).

example, is emmetropic and has a spherical aberration of 0.9 dptr for a pupil diameter of 2×2 mm.[2] This tallies with the results of Ames and Proctor.[3]

Observations were made with a transparent plate with squares filled with equidistant, alternately black and transparent lines. Each square consisted of four parts whose lines made an angle of 0°, 45°, 90°, and 135° with the vertical, respectively. The inter-space of the lines had values from 1.3 to 2.5 mm. This plate had been supplied by *Éditions de la Revue d'Optique*, Paris ("mires Foucault"). It was illuminated by a sodium lamp of 100 watts. A slab of opal glass was placed between lamp and plate. The distance from the eye of the observer was several meters. If necessary the observer was furnished with his usual correction glass. The system, whose diameter was stopped down to 4 mm, was placed before one of the eyes in such a position that it was exactly centered with the eye, as the extra-axial images are bad. The lines that could just be resolved were noted. The observations were checked by observations outside the system.

The observers all agreed that with the weaker systems, by which the spherical aberration of the eye is partly or wholly compensated or even somewhat overcompensated, there is no easily observable amelioration of the visual acuity when any of these systems in any position was applied to the eye. Nor was the contrast raised in an appreciable degree.

It was noted that the observers had to wait a certain time in order to be able to see clearly with any of the systems. Evidently the interpretation of the retinal images has to be adapted to the new light distribution. The same difficulties of seeing clearly occur when the system is removed; the interpretation now has to be re-adapted.

Thus it appears that partial or complete correction, and even a certain amount of overcorrection, of the spherical aberration of the eye does not influence visual acuity or contrast appreciably.

With the more powerful systems, giving a strong overcorrection, a deterioration of the image plainly ensued.

In the light of these results it may be questioned to what degree the complete correction for spherical aberration of the pencils leaving an instrument for subjective observation (telescope, simple and compound microscope) is necessary. Only further experiments in this direction may enable us to elucidate this point. It has been found for example, that a low power microscope which has exit pupil of 4 mm and is used with monochromatic light (in order to exclude chromatic effects) has practically the same resolving power when spherically corrected or when spherically overcorrected to a large amount.

TABLE II.

mm	mm		n_C	n_D	n_F
$r_1=+75.85$	$d_1'=1.5$	fluor crown	1.46333	1.46550	1.47057
$r_2=-54.95$	$d_2'=1.5$	extra dense flint	1.79248	1.80122	1.82383
$r_3=+54.95$	$d_3'=1.5$	fluor crown	1.46333	1.46550	1.47057
$r_4=-75.85$					

TABLE III.

	C	D	F
corrector	+0.31	+0.13	−0.37
eye	+0.32	+0.10	−0.34

2. These old and presumably not generally known observations have been supplemented with those of a new system, correcting the chromatic aberration of the eye. The data for the eye were taken from the cited article of Ames and Proctor. The data of this system are given in Table II.

The power in diopters for the C, D, and F lines are given in Table III together with the required correction of the emmetropic eye as deduced from the observations of Ames and Proctor.

The spherical aberration and coma for points not far from the axis ($w=1°$) are at incident heights up to 2 mm well under 0.1 dptr; therefore, they are of no consequence. The chromatic aberration of magnification however is so great that the system only can be used for a field of 2 or 3 degrees.

With common white light this system, provided it is well centered with respect to the eye, gives a sharp image, which shows somewhat better contrast than the naked eye, as could have been expected.

It is noteworthy that the corrector has a practical application and indeed has been used

[2] Handelingen 22d Ned. Natuur- en Geneesk. Congres, Rotterdam (1929), p. 109.
[3] Ames and Proctor, J. Opt. Soc. Am. **5**, 22 (1921).

or several years in a trichromatic colorimeter.[4] In this apparatus a color is matched by a mixture of three standard colors—red, green, and blue—whose intensities can be regulated by continuously variable square diaphragms, whose aperture after reduction of the standards to the primary standards is a measure of the color. The setting with this colorimeter sometimes was hampered by the fact that the boundary between the two halves of the field of view could not be made to disappear. This was explained by the difference of constitution of the light of the contiguous fields.

When, for example, we want to match the light from a sodium lamp with a mixture of red and green, it is very well feasible to equalize the brilliancy and the hue of the two fields. The boundary, however, delimits at the side of the sodium lamp a field with light of wave-length 0.589μ, while at the other side this wave-length hardly occurs. The observer in these conditions could not obtain a sharp image for the yellow and for the red and for the green wave-lengths simultaneously; thus the boundary always remained visible in some way.

By placing the described corrector before the eye this trouble has been completely overcome. It therefore has been attached permanently to the colorimeter. The variation of the chromatic aberration for different observers is too small to be taken into account.

[4] H. P. J. Verbeek, "A Trichromatic Colorimeter," Physica **1**, 1082 (1934).

JOURNAL OF THE OPTICAL SOCIETY OF AMERICA VOLUME 36, NUMBER 4 APRIL, 1946

Resonance Spectrum of Iodine

D. H. RANK
The Pennsylvania State College, State College, Pennsylvania
(Received February 25, 1946)

THE resonance spectrum of iodine first observed by R. W. Wood[1] has received the attention of a great many investigators. A rather complete treatment of the work on this spectrum has been given by Jevons.[2]

Previous to the war when the author was engaged in developing technique for the photography of Raman spectra with high resolving power,[3] plates were taken on the iodine resonance spectrum. The technique of excitation of the fluorescence spectrum is identical with that used for the Raman effect. The fact is that "Wood's light furnace" technique is probably the most powerful method of exciting Raman spectra when high resolution is demanded. A description of the light source and its spectral characteristics is given in the previous paper by the author in this Journal. The only difference in the excitation method from that used in the above mentioned paper is that the "scattering tube" was evacuated for the production of the resonance spectrum.

[1] R. W.Wood, Physik. Zeits. **11**, 1195 (1910).
[2] W. Jevons, *Band Spectra of Diatomic Molecules* (The Physical Society, London, 1932).
[3] J. A. Van Horn and D. H. Rank, Phys. Rev. **62**, 294 (1942).

SPECTRAL APPARATUS

Two different spectroscopic methods were used in this investigation. The resonance spectrum was photographed in the near infra-red, the measurements covering the 29 to 39 doublets of the series. Wood's[4] original measurements covered the resonance series from the origin to the 27th member. Oldenberg[5] has extended the series to the 37th member. However Oldenberg's measurements were made with a very fast low dispersion prism spectrograph and have little quantitative value. The near infra-red region was covered by the author using a concave grating. The region from the 1st to 13th doublets inclusive was photographed by means of a Fabry and Perot etalon in combination with a grating.

GRATING MEASUREMENTS

The spectrograph used in the near infra-red was a one-meter radius, 4-inch, 15,000 lines per inch concave grating in a Paschen mounting. The grating was ruled by Wood and had its maximum in the 8000A region. The normal to

[4] R. W. Wood and M. Kimura, Phil. Mag. **35**, 252 (1918).
[5] O. Oldenberg, Zeits. f. Physik **45**, 451 (1927).

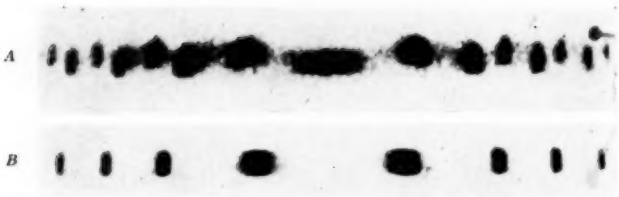

FIG. 1. *A*, enlargement of interference pattern of $P=8$ resonance doublet. *B*, enlargement of interference pattern of one of the standard neon lines.

the grating was at approximately 9000A. Plates were obtained with and without the second-order mercury lines on them. By means of the mercury lines it was possible to note any shifts in the iron comparison spectrum because of improper comparison source positioning. Measurements were made against the second-order iron standards. The plates used were Eastman type I-P. Exposures varied from 10 to 20 hours in length.

INTERFEROMETER MEASUREMENTS

Light from the resonance tube was focused on a coarse slit by means of an achromatic lens. The light from the auxiliary slit was rendered parallel by means of a second achromatic lens. Parallel light from the second lens was allowed to fall on the etalon. The interference fringes formed by the etalon were focused on the slit of the analyzing spectrograph. Second and third lenses were taken from the collimator and telescope assemblies of a Hilger constant deviation spectroscope. Use was made of the focusing adjustment of the above mentioned telescope in bringing the fringes into sharp focus on the spectrograph slit. The focal length of the telescope objective was about 30 cm.

The analyzing spectrograph made use of the same grating as mentioned above. This grating was mounted in a Wadsworth mounting to render the spectra stigmatic on the normal. Collimation was achieved by means of a spherical mirror of about 60-inch focal length. The quartz plates of the etalon were coated with gold by evaporation. Reflectivity of the films was such that about six "effective" beams were produced by the etalon in the yellow red region of the spectrum.

Upon inspection of Wood's[4] data on the "fundamental" doublets it was found that it was possible to throw the fringes produced by the second member of the doublet approximately half-way between the fringes produced by the first member of the doublet by a suitable choice of spacer for the etalon. This condition applies to all the members of the series which were investigated, to a good enough approximation so that a single spacer was used. The spacer plugs were made of invar and had a length of 6.537 mm. Overlapping of the orders of interference was of course necessitated by the small dispersion of the fast analyzing spectrograph. With a slit width wide enough so that measurable fringes were obtained resolution of the doublets by the spectrograph was not possible. It can be seen by reference to Fig. 1 that the fringes formed by the two members of the doublet are displaced with respect to each other so that the red and violet components of the fundamental doublet can be easily recognized.

Neon comparison spectra were used as wavelength standards. The neon geissler tube was mounted immediately in front of the window of the resonance tube in such a position that the light from this tube or the light from the resonance tube could be brought to a focus on the auxiliary slit of the interferometer optical system. Exposures for the neon standards required 2 seconds. The resonance spectrum required ex-

TABLE I.

p	$P(J_r+1)$	$R(J_r-1)$	Eq. (2) residuals	Eq. (1) residuals	Eq. (1) Wood's data
1	18089.17	18094.30	+.02	+ .13	−.07
3	17666.54	17671.66	.00*F*	+ .22	−.02
4	457.09	462.20	.00	+ .24	+.04
6	041.98	047.03	+.01	+ .23	+.36
8	16631.95	16636.95	+.02	+ .16	+.01
10	227.05	232.03	+.02	+ .07	.00
11	026.59	031.55	+.01	.00	−.05
13	15629.58	15634.49	.00*F*	− .07	−.18
15	*W* 237.7	*W* 242.6	+.18	+ .08	+.08
16	*W* 044.3	*W* 048.9	+.07	− .04	−.04
17	*W*14851.6	*W*14856.4	+.14	+ .02	+.02
18	*W* 660.8	*W* 665.7	−.21	− .32	−.32
20	*W* 282.8	*W* 287.8	−.19	− .28	−.28
22	*W*13910.7	*W*13915.5	−.06	− .11	−.11
23	*W* 727.0	*W* 731.8	−.26	− .29	−.29
25	*W* 363.8	*W* 368.2	.00*F*	− .03	−.03
27	*W* 006.0	*W* 011.0	−.14	− .20	−.20
29	12655.7	12659.9	−.19	− .39	
30	481.7	486.5	−.01	− .32	
32	140.3	144.6	+.26	− .41	
34	11805.1	11809.5	+.28	− .97	
35	640.0	644.2	+.55	−1.09	
36	476.9	481.4	.00*F*	−2.1	
37	315.4	319.6	+.19	−2.5	
39	10997.4	001.4	+.40	−3.7	

posures of from 10 to 20 minutes. Reduction of the interferometer plates was accomplished by making use of the method of exact fractions to determine the etalon thickness. The method followed in measuring and calculating the fractional orders was that described by C. V. Jackson.[6] Mean of the residuals of the measured neon lines from their standard values was .003A. It was noted that the iodine fringes were definitely broader than the neon fringes. However the resolving power of the etalon was not sufficient to show the fine structure observed by Wood.[7] The interferometer measurements made on these resonance doublets are probably accurate to $\pm.02$ cm^{-1}.

Results of all the measurements are given in Table I. Column one lists the order number of the doublet. Columns two and three list the wave numbers in a vacuum. The measurements which are due to Wood are marked with a *W*.

R. Mecke[8] has fitted Wood's "fundamental doublet" series to an empirical formula which holds within experimental error for the first 27 members of the series. The residuals of Wood's measurements from Mecke's formula are given in the last column of the table. When the author attempted to use Mecke's formula to calculate the higher members of the series, it was found that both the higher members of the series and the interferometer measurements did not agree with calculated values within experimental error. The residuals from the values calculated from Mecke's formula are given in column 5 of the table. Mecke's empirical equation for the violet component of the doublet series is

$$\tilde{\nu}=18307.50-213.667p+0.592p^2+.00207p^3, \quad (1)$$

where p is the order number of the doublet. Attempts were made by the author to fit his and Wood's data for the series to a cubic equation. These attempts were unsuccessful in that the higher members of the series gave rise to residuals beyond experimental error of the measurements. The measurements were then fitted to a quartic equation in the following fashion. The points $p=3$, $p=13$, and $p=36$ were chosen for their accuracy and position. $p=25$ was chosen from Wood's data for its position in the series. The empirical equation obtained was,

$$\tilde{\nu}=18307.50-213.7977p+.614045p^2 +.000931961p^3+.00001866p^4. \quad (2)$$

Enough figures are carried in the equation so that the sum is accurate to .01 cm^{-1} for the whole series. The residuals from this formula, calculated minus observed, are given in column 4. The letter *F* after a residual in this column means that this point was used for fitting the curve. Inspection of the table of residuals shows that Eq. (2) fits the data within the limits of experimental error for the whole series measured. The interferometer measurements of the $p=1$ doublet were found to agree within experimental error with the lines assigned to this transition in the analysis of the iodine absorption spectrum by Wood and Loomis.[9]

Doublet separations measured by the interferometer were fitted to least squares. The resulting empirical equation is

$$\Delta\tilde{\nu}=5.168-.0194p. \quad (3)$$

The molecular constants for the ground state of the iodine molecule as derived from Eqs. (2) and (3) are in cm^{-1}

$$\begin{aligned} \omega_e &= 214.57, \\ x_e\omega_e &= 0.6127, \\ y_e\omega_e &= 0.000895, \\ z_e\omega_e &= 0.0000187, \\ B_e'' &= 0.0375, \\ \alpha'' &= 0.000141. \end{aligned}$$

The value of B_e'' will be found to be in substantial agreement with B_e'' as determined by Loomis[10] from an analysis of the iodine adsorption bands e.g., $B_e''=.037300$.

The author wishes to thank Mr. J. A. Van Horn for his assistance in the experimental work with the interferometer.

Note added in proof: Using the value of B_e given by Loomis[10] to compute the intercept of Eq. (3) a value of 5.139 cm^{-1} was obtained. The $d\Delta\tilde{\nu}$'s were then calculated using the data obtained from the interferometer measurements of the resonance doublets. A least-squares reduction of the data yielded

$$d\Delta\tilde{\nu}=.0161p. \quad (4)$$

The value obtained for α'' from Eq. (4) is $\alpha''=.000117$ which is probably considerably more reliable than the value calculated from Eq. (3) directly.

[6] C. V. Jackson, Proc. Roy. Soc. **130**, 395 (1931).
[7] R. W. Wood, Phil. Mag. **35**, 236 (1918).
[8] R. Mecke, Zeits. f. Physik **7**, 73 (1921).
[9] R. W. Wood and F. W. Loomis, Phil. Mag. **6**, 231 (1928).
[10] F. W. Loomis, Phys. Rev. **29**, 112 (1927).

JOURNAL OF THE OPTICAL SOCIETY OF AMERICA VOLUME 36, NUMBER 4 APRIL, 1946

A Method for Precision Alignments

A. C. S. VAN HEEL
Laboratory for Technical Physics of the Technical University, Delft, Holland
(Received December 7, 1945)

THE difficulties of the alignment of three material points need not be dwelled upon, as they are amply discussed by J. Bonnaffé.[1] This author also describes a method to obtain a higher precision than can be attained by the unaided eye. For the last he gives a precision of 2 mm for the position of the middle point, when the outer points are 25 or 30 m apart. By observing the diffraction image with a telescope, whose object glass has been covered by a screen with a small aperture of 1-mm diameter, he reached a precision of between 0.2 and 0.5 mm with a distance of 30 to 50 m between the outer points.

In trying to reproduce these results we soon looked for other methods, as the experiments had to be performed in the dark, which seemed to us a disadvantage for applications on shipbuilding yards, barrage dams, etc. Further we were not satisfied that the utmost precision obtainable had been reached.

First an attempt was made to make use of the maxima and minima appearing as a result of diffraction on the outside of the geometrical shadow of a straight edge. By pointing on the maxima and the minima with cross wires first with the screen on the left side and afterwards on the right side, and by combining the results, a precision at least three times higher ensued. Besides, the pointings could be made with the room light on.

Finally, instead of a straight edge, a double slit was used as in the usual modification of Young's classical experiment. The screen with the double slit was displaced until the first minimum on the left-hand side coincided with the cross wires, and then the right-hand minimum was brought into coincidence with the cross wires. As the light source (a pointolight lamp) gave white light, the colors within the minima could be made use of. In this way a very high precision could be attained, even without any special training of the observer and again with the room lights on.

This high precision was obtained by the refinement of setting the cross wires on the transition of reddish to bluish colors within the first minimum. The setting indeed was so delicate that a slide with micrometric screw reading to 1/200 mm had to be used.

In order that the observer should be able to make the settings himself without the aid of an assistant, the light path had been folded up by means of a mirror. The arrangement consisted of the pointolight lamp, the screen with double slit at a distance of 35 m, a plane mirror at a distance of 17.5 m from the screen, and the cross wires with observing system (magnifying glass or short distance telescope), the last at the same distance from the mirror as the screen and placed next to it. Thus the observer could displace the screen while observing the interference pattern. The effective distances between source and screen and between screen and cross wires being equal, *viz.* 35 m, the effective distance between the outer points amounted to 70 m.

Experiments with more than two slits did not give better results. The most appropriate form appeared to be two slits of 2 mm wide each and 2 mm from each other. The distance between the minima in our experiments amounted to 5 mm.

The mean error of the mean of a series of fifteen settings appeared to be 0.01 mm, the maximum deviation from the mean being 0.08 mm. This precision of 0.01 mm corresponds to 0.02 in the plane of the cross wires, i.e., 1/250 of the distance between the minima.

The position of the screen in the middle between the two outer points being ascertained to 0.01 mm, the alignment is secured with this most simple apparatus to $0.01/3.5\times10^4$ radians or 0.06 second of arc.

A little consideration shows that the same method presumably could be applied to ascertain the deviations of machine parts, lathe beds, etc., from a true plane to within some microns or perhaps even better. It seems advantageous for these cases to make use of a collimator with a slit parallel to the plane to be investigated.

[1] J. Bonnaffé, Revue d'Optique 9, 17 (1930).

At the same distances of 35 and 35 m settings were made by the method of Bonnaffé, giving a mean error of 0.06 mm for the mean of fifteen settings from one side with a maximum deviation of 1.0 mm. The position of the screen thus was ascertained to about 0.1 mm from the settings from right and left, which precision corresponds with the data given by Bonnaffé. The straight edge method given above yielded under the same circumstances a mean error of 0.03 mm for the mean of fifteen settings from one side with a maximum deviation of 0.3 mm.

I am indebted to Messrs. H. Mondria and M. L. Kasteleyn for the execution of most of the experiments. These were performed in 1941 and 1942.

Letters to the Editor

Simultaneous Linear Equations in Absorption Spectrophotometry and Mass Spectrometry

J. L. Saunderson and H. H. Grossman
The Dow Chemical Company, Midland, Michigan
February 25, 1946

It was pointed out by Comrie[1] that the solution to the set of n simultaneous linear equations in n unknowns of the form

$$\begin{aligned} a_{11}x_1+a_{12}x_2+a_{13}x_3+\cdots+a_{1n}x_n&=k_1\\ a_{21}x_1+a_{22}x_2+a_{23}x_3+\cdots+a_{2n}x_n&=k_2\\ a_{31}x_1+a_{32}x_2+a_{33}x_3+\cdots+a_{3n}x_n&=k_3\\ \cdots\cdots\cdots\cdots\cdots&\\ a_{n1}x_1+a_{n2}x_2+a_{n3}x_3+\cdots+a_{nn}x_n&=k_n \end{aligned} \qquad (1)$$

can be expressed as

$$x_j=\alpha_{j1}k_1+\alpha_{j2}k_2+\alpha_{j3}k_3+\cdots+\alpha_{jn}k_n=\sum_{i=1}^{n}\alpha_{ji}k_i, \qquad (2)$$

where the α's are the solutions to the n sets of n equations formed by setting one k in the Eqs. (1) equal to unity and the remaining k's equal to zero. For example, when $k=1$ and $k_2=k_3=\cdots=k_n=0$, the solutions are $x_1=\alpha_{11}$, $x_2=\alpha_{21}$, $\cdots$ and $x_n=\alpha_{n1}$.

This method of solution was suggested by Comrie when the Eqs. (1) are encountered frequently having the a's always the same but different values for the k's. Such is the case for the routine solution to the problem of a multicomponent analysis by the methods of absorption spectrophotometry or mass spectrometry. The sum of products indicated by Eq. (2) can be done rapidly in one continuous machine operation on a modern calculating machine, such as the Friden model ST.

Recently an electrical computer for solving the Eqs. (1) by the method of successive approximations has been described by Morgan and Crawford.[2] One model of this computer[3] has eleven x dials and eleven k dials on the front panel for the solution of eleven simultaneous linear equations. The a's are set internally in the instrument for one specific set of equations. When n is of the order of four, direct calculation of the unknowns by Eq. (2) can be accomplished in about the same length of time as is required for the solution by the electrical computer, assuming in the first case that the α's are known and in the second case that the a's are already set in the computer. For large n, say eleven, the electrical computer is appreciably faster. On the other hand, if several different problems are encountered having different sets of a's, the a dials would have to be changed for each different case so that it might be more convenient to use the direct calculation method with previously calculated α's.

It is the purpose of this note to point out that the two methods can be combined to give an appreciable gain in speed and convenience. It is evident that Eq. 2 can be solved on the electrical computer without going through successive approximations. The α's can be substituted for the a's, the dials formerly associated with the unknowns can be set for the k's, and each former k dial can be balanced independently to give the values of the x's. This method is three or four times faster than the previous method of successive approximations. The α's may of course be found from Eqs. (1) with the electrical computer by successively setting each k equal to unity with the others at zero. The Eqs. (1) must therefore be solved n times by the usual method of successive approximations.

In solving the Eqs. (1) by the method of successive approximations in the general case (k's not equal to zero), the following method for greatly increasing the accuracy is useful. Let the solutions found with the electrical computer be x_1', x_2', x_3', $\cdots$, x_n'. The equations can then be "checked" by summing the products on a calculator. Let the result so found for each equation be k_j', that is,

$$k_j'=\sum_{i=1}^{n}a_{ji}x_i'. \qquad (3)$$

If $x_j=x_j'+\delta x_j$ and $k_j=k_j'+\delta k_j$, Eqs. (1) can be solved again for the δx's by substituting the δk's for the k's. This method is convenient since the a's are already set into the electrical computer. The original x_j''s can then be corrected by the amount δx_j giving the solutions x_j with considerable accuracy. The α's, of course, can also be found by this method from the Eqs. (1). Once determined, then, the α's may be substituted for the a's in the computer making possible the use of Eq. (2) for the direct determination of the unknowns.

[1] L. J. Comrie, J. Sci. Inst. **21**, 129 (1944).
[2] T. D. Morgan and F. W. Crawford, Oil and Gas J. (Aug. 26, 1944); also J. Opt. Soc. Am. **12**, 801 (1945).
[3] The commercial instrument is manufactured by Engineering Laboratories, Inc., and is called the Spectro-computer.

An Illuminator for Use in Metallographic Microscopy

ERNEST E. FAIRBANKS
Southern Experiment Station, Bureau of Mines, Tuscaloosa, Alabama
January 29, 1946

JEWELL[1] mentions the fact that the metal mirror of his illuminator was just slightly dulled by use of an extremely fine abrasive. If this surface is ground too much, he points out, it will produce an excessive scattering of light so that the detail under examination will become indistinct and lacking in contrast. However, in the description of relief illumination[2] no mention is made of the light scattering effect of the dull reflecting mirror surface. It is this light scattering that accounts for uniformity of the microscopic field as shown in the photomicrographs accompanying the article. Without the scattering, polished metallic surfaces would appear dark in the center of the microscopic field (area of oblique illumination) and bright in the outer portions (area of vertical illumination).

The advantages of oblique illumination in dealing with etched surfaces or those polished in relief are well known. Jewell succeeded in obtaining excellent photomicrographs by his lighting arrangement. The role of light scattering suggested to the writer that a carefully prepared specimen surface might be employed so that the illuminator could be completely eliminated. If this arrangement were possible an objective could be used to its full advantage. Illuminators reduce the effectiveness of the microscope objective in much the same manner as is the case when an f 2 photographic lens has its diaphragm closed to f 4.5.

In the proposed method the specimen surface should be non-specular to the extent of producing a certain amount of light scattering. In common with Jewell's mirror surface it is a fine ground surface rather than a highly polished surface. The photomicrographs of such surfaces obtained without the use of an illuminator proved more satisfactory than the best obtained from highly polished surfaces by conventional methods. The limit of magnification was about 100×.[3] A somewhat novel arrangement is believed capable of extending this range to nearly 600×.

The method was found useful in the photography of opaque and non-opaque materials occurring together in thin sections, by means of a single plate or film. The interrelationships of the dissimilar materials are brought out in the same photomicrograph. A special preparation known as a "polished thin section" has been considered necessary for this type of photography. It is difficult to prepare; thus rarely used. Ordinary thin sections are relatively abundant. Their fine ground surfaces were considered to have the proper characteristics to permit their use as substitutes for the more difficultly prepared sections.

A trial series of 13 photos of ordinary glass covered thin sections were prepared by combined illumination consisting of non-polarized light from two sources without the use of an illuminator attached to the microscope. All of the trial photomicrographs proved excellent in every respect. Their application to mineral surfaces should not exhaust the possibilities for this type of relief illumination.

[1] Lewis E. Jewell, J. Opt. Soc. Am. **14**, 165 (1927).
[2] Reference 1, pp. 162–165.
[3] Ernest E. Fairbanks, "Photomicrography by combined transmitted and reflected light," Econ. Geol. **39**, 591 (1944).

On Testing the Angles of Reflecting Prisms

W. F. C. FERGUSON
New York University, Washington Square, New York City, New York
February 11, 1946

DIFFICULTIES encountered because of errors in the angles of reflecting prisms are principally of two kinds: (1) difficulty in fitting the prisms in their mountings, and (2) injury to the optical definition. The first of these can ordinarily be overcome in the design of the mounting. Definition is injured only to the extent of the dispersion introduced by incorrect angles. The effect is the same as if a thin dispersing prism were added to the reflecting prism. For measuring the resultant chromatic defect caused by such an error, whether in axial or pyramidal angles of a prism, the Twyman interferometer has been found ideal.

With a source of mercury light with a green filter (Wratten No. 62) the prism is arranged for testing on the interferometer as usual and the instrument adjusted to give no fringes, or as few as possible. Then the green filter is replaced with a blue filter (Wratten No. 47). If there is dispersion produced by the prism the blue wave fronts are not parallel to the green wave fronts and blue interference fringes now appear.

The angular dispersion is readily calculated from the observed fringes, remembering that the light passes twice through the prism as it is tested. If no fringes are observed in green light (λ5461), then blue fringes (λ4358) 45 mm apart indicate that the green-blue dispersion for one passage through the prism is 1″. This dispersion is found to be almost identical with that of the C-F wave-lengths from hydrogen for usual prism glass. Any tolerance on prism angles can best be expressed as resultant dispersion, primarily, and this can be tested directly.

The deviation produced by a thin prism which would give the observed dispersion is, therefore, to a close approximation: angular dispersion multiplied by the ν-value of dispersion of the glass. Thus a thin crown glass prism ($\nu=60$) which gives 1″ dispersion produces 1′ deviation, and has an angle of about 2′. This is the resultant error in angles of the reflecting prism insofar as it affects the optical definition.

Variations of the above procedure are sometimes found useful: making the measurements with λ5461; or, first introducing several straight fringes of one color and then observing the difference in the spacing of the fringes observed in the second color.

In passing, it may be mentioned that an H-2 mercury lamp without the transformer, but with two cone heating coils, 50 ohms, in series, is a satisfactory source for interferometry. Fringes remain highly visible for a path difference of several centimeters.

The above method of testing prisms was developed at the Mergenthaler Linotype Company of Brooklyn, New York.